TECHNISCHE UNIVERSITÄT MÜNCHEN

Lehrstuhl für Tierhygiene

Evaluation of an active immunoprophylaxis against prion diseases

Gunnar Kaiser-Schulz

Vollständiger Abdruck der von der Fakultät Wissenschaftszentrum Weihenstephan für Ernährung, Landnutzung und Umwelt der Technischen Universität München zur Erlangung des akademischen Grades eines

Doktors der Naturwissenschaften

genehmigten Dissertation.

Vorsitzender: Univ.-Prof. Dr. H. R. Fries

Prüfer der Dissertation:

1. Univ.-Prof. Dr. Dr. h.c. J. Bauer
2. Univ.-Prof. Dr. H. Schätzl
3. Univ.-Prof. Dr. H. H. D. Meyer

Die Dissertation wurde am 22.10.2008 bei der Technischen Universität München eingereicht und durch die Fakultät Wissenschaftszentrum Weihenstephan für Ernährung, Landnutzung und Umwelt am 30.01.2009 angenommen.

Meiner Mutter

Table of contents

Summary

Prion diseases like Creutzfeldt-Jakob disease (CJD) in man and bovine spongiform encephalopathy (BSE) in cattle are fatal neurodegenerative diseases characterized by the conformational conversion of the normal, mainly α-helical cellular prion protein (PrP^{C}) into the abnormal β-sheet rich infectious isoform PrP^{Sc}. So far no therapeutic or prophylactic approach is known. Immunisation against prions failed until now most likely due to the very pronounced self-tolerance to PrP^{C}.

Previous studies of this group showed that it is possible to overcome self-tolerance using recombinantly expressed dimeric PrP (tandem-PrP; tPrP), in association with different adjuvants. Anti-prion efficacy was obtained *in vitro* by demonstrating the capability of sera to prevent PrP^{Sc} *de novo* synthesis. This work was performed to gain more insight into tPrP features and to enhance the immune response in PrP wild type mice. Biochemical examination revealed differences in the structure of tPrP depending on refolding conditions after purification from *E.coli*. Interestingly, direct physical contact of tPrP with adjuvant CpG-ODN led to high molecular aggregates. As expected at present immunisation studies confirmed previous results. Humoral response was induced after subcutaneous injection of tPrP and CpG-ODN. Antibody features such as titer, epitope reactivity and specificities were mapped in detail. Furthermore, activation of T lymphocytes was measured of individual mice by cytokine assays. To improve delivery of the antigen subcutaneous immunization with tPrP and CpG-ODN co-encapsulated in biodegradable polylactide-co-glycolide microspheres (PLGA-MS) were performed. Results showed enhanced CD4 T cell responses and more prominent the induction of CD8 T cells compared to administration of pure protein and adjuvant. In this vaccination protocol PLGA-MS function as endosomal delivery device of antigen plus CpG-ODN to macrophages and dendritic cells. Moreover, PLGA-MS have an immunological long term effect as only small sized particles can be taken up by cells. Bigger ones deposit at the place of entry and slowly degrade thus leading to a constant stimulation of the immune system. Unfortunately, PLGA-MS based DNA vaccination approaches with a tPrP construct generated only poor humoral and T cell responses. Finally, a long term immunisation trial including prion inocculation was performed to examine protective effect of immunisation. Most animals immunized did not show a prolongation of incubation time compared to untreated control mice. Three mice treated with co-encapsulated tPrP+CpG-

ODN did not develop any signs of prion disease leading to the assumption that protective effect for these animals was achieved.

Zusammenfassung

Prionen-Erkrankungen, wie beispielsweise die Creutzfeldt-Jakob Krankheit bei Menschen und Bovine spongiforme Enzephalopathie in Kühen, sind durch die Umwandlung der Konformation von überwiegend α-helikalem, zellulären Prion Protein PrP^C in die abnorme β-Faltblatt reiche, infektiöse Isoform charakterisiert. Bisher ist weder eine Therapie, noch ein prophylaktischer Schutz gegen diese Krankheiten bekannt. Immunisierungen blieben bisher ohne Erfolg wahrscheinlich aufgrund der ausgeprägten Selbst-Toleranz gegen PrP^C.

Frühere Studien dieser Gruppe zeigten eine partielle Überwindung der Selbst-Toleranz mit Hilfe von rekombinant exprimiertem, dimeren PrP (tandem-PrP, tPrP) in Kombination mit verschieden Adjuvantien. Die Wirksamkeit gegen Prionen wurde *in vitro* durch die Fähigkeit der Seren die PrP^{Sc} Neusynthese zu verhindern nachgewiesen. Diese Arbeit wurde mit dem Ziel durchgeführt genaueren Einblick in die Eigenschaften von tPrP zu gewinnen und eine Verbesserung der Immunantwort in PrP Wildtyp Mäusen zu erreichen. Biochemische Untersuchungen deckten Strukturunterschiede von tPrP, die auf die Rückfaltungsbedingungen nach der Aufreinigung aus *E.coli* basieren. Darüber hinaus führte der direkter Kontakt zwischen tPrP und dem verwendeten Adjuvant CpG-ODN zur Ausbildung hoch molekularen Aggregaten. Die neuen Immunisierungen bestätigten erwartungsgemäß vorangegangene Ergebnisse. Nach subkutaner Injektioin von tPrP und CpG-ODN wurde eine humorale Immunantwort ausgelöst und die Eigenschaften (Titer, Epitope und Spezifität) entsprechender Antikörper im Detail untersucht. Des Weiteren wurde die Aktivierung von T Lymphozyten mittels Zytokin-Assays gemessen. Um die Effizienz der Antigen Darreichung zu verbessern, wurden subkutane Immunisierungen mit in biodegradierbare Microspheres (PLGA-MS) eingekapselte tPrP und CpG-ODN durchgeführt. Als Ergebnis zeigte sich eine erhöhte CD4 T Zell Antwort und eine noch stärker ausgeprägte CD8 T Zell Antwort, im Vergleich zur Gabe von reinem Protein mit Adjuvant. In diesem Vakzinierungsansatz fungieren die PLGA-MS als endosomale Transporteinheiten für Antigen und CpG-ODN an Makrophagen und Dendritische Zellen. Darüber hinaus haben PLGA-MS eine immunologische Langzeitwirkung. Die Zellen können nur kleinere Partikel aufnehmen, größere bleiben als lokale Ablagerungen erhalten, die durch nach und nach durch Degradierung abgegeben werden und somit eine gleichbleibende Stimulation des Immunsystems bewirken. Leider hat

die tPrP basierte DNA Vakzinierung mit Applikation über PLGA-MS nur zu sehr geringer humoraler und T Zell vermittelter Immunantwort geführt.

Abschließend wurde ein Langzeitexperiment mit anschließender Prionen Inokulation durchgeführt, um die schützenden Eigenschaften der Immunisierung zu untersuchen. Die meisten der immunisierten Mäuse zeigten keine Verlängerung der Inkubationsdauer im Vergleich zu nicht immunisierten Kontrolltieren. Drei der mit eingekapselten tPrP CpG-ODN PLGA-MS behandelten Tiere entwickelten keinerlei Krankheitssymptome. Dieses Ergebnis lässt darauf schließen, dass zumindest bei diesen Tieren ein Impfschutz erfolgreich aufgebaut werden konnte.

1 Introduction

1.1 Historical background

Transmissible spongiform encephalopathies (TSEs) or prion diseases are neurodegenerative illnesses affecting both animals and humans and are invariably fatal. Public interest and investigation of the underlying causes highly increased with the epidemic occurrence of BSE (bovine spongiform encephalopathy) with more than 180.000 confirmed cases in Great Britain and numerous cases in other European countries. Since 1996 a direct linkage to a new variant of human Creutzfeldt-Jakob disease caused by consumption of contaminated meat was discussed and raised the fear of a threat to public health (Collinge et al., 1996a;Will et al., 1996;Will, 1998). The nature of causative agent has been a controversial issue for many years since not all prion diseases are infectious at least via natural routes. On the other hand they can also occur spontaneously or on a familial genetic background.

The first known literature report about the naturally occurring disease of sheep and goat in U.K, France and Germany is dated to 1732 and was published later in Great Britain (McGowan, 1922). Affected animals rub their coat hence the disease was named scrapie. In 1936 experimental transmission of scrapie to healthy goat and sheep by inoculation of diseased sheep brain homogenates was demonstrated (Cuille, 1939). Thus, infection of a virus was assumed as the causative agent of disease and 1954 the term "slow virus" was defined due to the long natural incubation times of many years (Sigurdson, 1954).

Vincent Zigas discovered kuru in 1956, a very rare degenerative brain disorder that occurred primarily among the Fore natives in Papua New Guinea (ZIGAS, 1981). One year later he was joined by Carleton Gajdusek who initiated systematic investigation of kuru (GAJDUSEK et al., 1957;ZIGAS et al., 1957) and received the Nobel prize of Physiology or Medicine for his work in 1976. William Hadlow noticed similarities between kuru and scrapie at a neuropathological and clinical level. He recommended transmission experiments to apes in 1959. Gajdusek succeeded in the transmission of kuru via intracerebral inoculation of chimpanzees with kuru infected brain homogenates a few years later (GAJDUSEK et al., 1966). Another rare human degenerative disease had already been described 1920 independently by Hans Creutzfeldt and Alfons Jakob (Creutzfeldt, 1920;Jakob, 1921). The pathological alterations of the CNS in patience affected by Creuzfeldt-Jakob disease (CJD) were comparable to those of kuru infected (KLATZO et al., 1959). Transmission of CJD to

chimpanzees via intracerebral inoculation (Gibbs, Jr. et al., 1968) and several reports of iatrogenic infections due to contaminated neurological electrodes and infected transplants (e.g. dura mater, cornea) from human to human showed the infectivity of the disease.

Contrary to the assumption of a causative virus infection neither a virus, nor an immune response could be detected upon prion infections. Furthermore extensive treatment of the scrapie agent with UV-light and ionising radiation could not lower infectivity even thought under these conditions DNA and RNA are known to be destroyed. Instead of this protein denaturation with urea or sodium hydroxid reduced infectivity (Alper et al., 1966;Alper et al., 1967). These findings led to the conclusion of a pure protein infective agent devoid of any nucleic acid. The mathematician JS Griffith proposed the first hypothetic model of an autocatalytic protein self-replication responsible for scrapie infection (Griffith, 1967). In 1982 isolating of a glycoprotein as the major component of the infectious fraction from brain was obtained. This partially protease resistant protein was found to form filaments called scrapie-associated-fibrils (SAF) or prion rods that often accumulate as amyloid deposits (Hilmert et al., 1984;Prusiner et al., 1981;Prusiner, 1982). Stanley Prusiner who received the Nobel prize of medicine for his discovery in 1997 invented the term prion (proteinaceous infectious particle) for the new biological principle of infection (Prusiner, 1982). The proteinase-K resistant part of protein isolated from enriched infected hamster brain homogenates showed a molecular weight of 27-30 kDa whereas non treated protein was bigger (33-35 kDa). The term PrP^{Sc} (prion protein **sc**rapie) was defined implicating the infective character of the prion protein. The N-terminal sequence of PrP^{Sc} was elucidated using Edman degradation (Prusiner et al., 1984) and allowed identification and cloning of the PrP coding gene denoted *Prnp* (Oesch et al., 1985). Antibodies obtained from sera of immunized mice where also reactive against non infected tissue and together with the finding that PrP mRNAs levels where similar in infected and non infected tissue gave rise to the definition of a non infectious cellular prion protein termed PrP^{C} (Basler et al., 1986;Oesch et al., 1985). The two PrP isoforms shared the identical amino acid sequence but severely differed in their biochemical properties (Prusiner, 1991).

1.2 Prion diseases

The degenerative tissue damages caused by prion infections are very similar in both animal and humans. They are characterized by spongiform degeneration of the grey matter which can strongly vary from case to case. The massive loss of neurons is correlated to increased astrocytic proliferation and occurs late in disease progression, corresponding to onset of behavioral symptoms. Characteristic amyloid deposits found in prion affected brains are based on misfolded, β-sheet rich protein accumulation (Clinton et al., 1992).
Incubation time from infection to onset of symptoms is variable but mostly takes from years to decades, at least in case of cattle and human diseases. All prion diseases are irreversibly fatal.

1.2.1 Animal prion diseases

Scrapie was the first prion disease described as early as 1732 (McGowan, 1922). The disease affecting sheep and goat was named after one of its symptoms, the compulsive scraping of their fleece against rocks, trees or fences. Further symptoms are loss of coordination causing unsteady gait and convulsive collapse (Foster et al., 2001). Transmission of scrapie was found to happen naturally both from mother to lamp and to other animals of the flock (Brotherston et al., 1968;Dickinson et al., 1974). Scrapie is apparently not transmissible to humans.

Table 1 Animal prion diseases

Natural host	Disease	Mechanism of transmission/infection
Sheep/Goat	Scrapie	Vertical and horizontal infection in genetically susceptible sheep; oral transmission, sporadic
Cattle	BSE (bovine spongiform encephalopathy)	Infection with prion contaminated food, sporadic
Mink	TME (transmissible mink encephalopathy)	Oral infection with prion contaminated tissue (sheep and cattle), sporadic (?)
Deer, Elk	CWD (chronic wasting disease)	Direct transmission possible, similar to scrapie (?)
Cats	FSE (feline spongiform encephalopathy)	Infection with prion contaminated food

Chronic wasting disease (CWD) is a TSE affecting captive and free ranging deer and elk mainly located in areas of North America and is known since more than 30 years (Williams et al., 1980). CWD has many features in common with scrapie, including the apparent efficiency of horizontal transmission. Although CWD can be transmitted by intracerebral inoculation to cattle, sheep, and goats, ongoing studies have not demonstrated that domestic livestock are

susceptible via oral exposure. It seems very likely that this disease in non domestic animals will continue to spread (Williams, 2005).

Bovine spongiform encephalitis (BSE) or more commonly termed "mad cow disease" was first confirmed in cattle by British veterinarians in 1986 (Wells et al., 1987). Diseased animals initially started to react very nervous on light or acoustic stimuli. They lost weight and milk production decreased. During the progress of illness animals developed ataxia until they lost their ability to stand and their mental status degraded to the point of madness (Wilesmith et al., 1988). The primary source of BSE infections in cattle are most likely commercial protein rich nutritional supplements like MBM (meat and bone meal) containing the infectious agent. MBM is mainly produced from carcasses of sheep and cattle by a standard rendering process that does not completely inactivate the infectious agent. It was discussed that changes in the rendering process in U.K. in late 1970s (lowering production temperature and omitting hydrocarbon organic solvents) might have led to reduction in inactivation of the agent in MBM. Primary infection might either have been scrapie infected sheep or cattle which had developed BSE spontaneously. In any case, each new cycle was followed by more extensive contamination of MBM (Horn, 2001). To date almost 190.000 confirmed BSE cases are known worldwide (Table 2), whereas estimations assume about one million cases (Anderson et al., 1996). The 1988 ban on the use of ruminant MBM in cattle feed and 1990 Specified Bovine offal (SBO) controls markedly reduced the risk of infection. The feeding of MBM to all farmed animals was banned in 1996 and an EU-wide ban has been in place since 2001. Nevertheless, the number of infected cattle steadily decreases. In 2007 only more than 150 animals where tested positive (Table 2).

Table 2
Confirmed cases of BSE worldwide up to 31 December 2007 including countries with 100 or more total cases (http://www.food.gov.uk/ - May 2008)

Country	2007	2006	2005	Total since 1986
UK (GB & Northern Ireland)	67	124	224	**183.256**
Ireland	25	41	69	**1.622**
Portugal	10	32	51	**1.036**
France	7	8	31	**993**
Spain	36	64	98	**717**
Switzerland	0	5	3	**467**
Germany	4	16	32	**415**
Italy	2	6	8	**143**
Belgium	0	2	2	**133**

Some other animal prion diseases have been recognized in farmed mink (transmissible mink encephalopathy) as well as in domestic and captive cats (feline spongiform encephalopathy) (Table 2) (Aldhous, 1990;Marsh et al., 1992). FSE is supposed to be linked with BSE because it is thought to be caused by contaminated food and its spread followed the appearance of BSE. Other domestic animals like birds, dogs or pigs seem to be resistant to oral BSE infection.

1.2.2 Human prion diseases

Human prion diseases can be classified into three groups depending on their etiology: sporadic, inherited and acquired (Table **3**)**.**

Table 3
Summary of human prion diseases

Disease name	**Mechanism of infection**
CJD familial (fCJD) sporadic (sCJD) iatrogenic (iCJD) variant (vCJD)	 Inherited (mutation of *Prnp*) Spontaneous conversion Acquired by contaminated instruments on tissue Acquired by infection with BSE
Kuru	Acquired via oral infection, ritual cannibalism
GSS (Gerstmann-Sträussler-Scheinker disease)	Inherited (mutation of *Prnp*)
FFI (fatal familial insomnia)	Inherited (mutation of *Prnp*)

Sporadic CJD was the first TSE described in humans and has an evenly distribution with world wide incidence of about one per million inhabitants (Creutzfeldt, 1920;Jakob, 1921). It is a rapidly progressing multifocal dementia with the onset of symptoms at the age of 45-75 and is fatal 3-6 months later. Depression, lost of weight, tiredness, insomnia and general pain sensation are characteristic symptoms. In later stage rapidly progressive dementia, loss of ability to speak and neurological failures such as ataxia and partial blindness occur.

About 80-90% of all human prion diseases are sporadic and only 10-15% are associated with autosomal dominant mutations of the prion protein gene. More than 20 pathogenic changes of *Prnp* are known so far. They can be divided into point mutations, either causing amino acid exchange or a stop codon, and insertions into the octarepeat region, adding up to 9 further repeats to the 5 usually present tandem repeats (Figure 1). These mutations are believed to

destabilize the prion protein and might lead to spontaneous conformational changes (Owen et al., 1989).

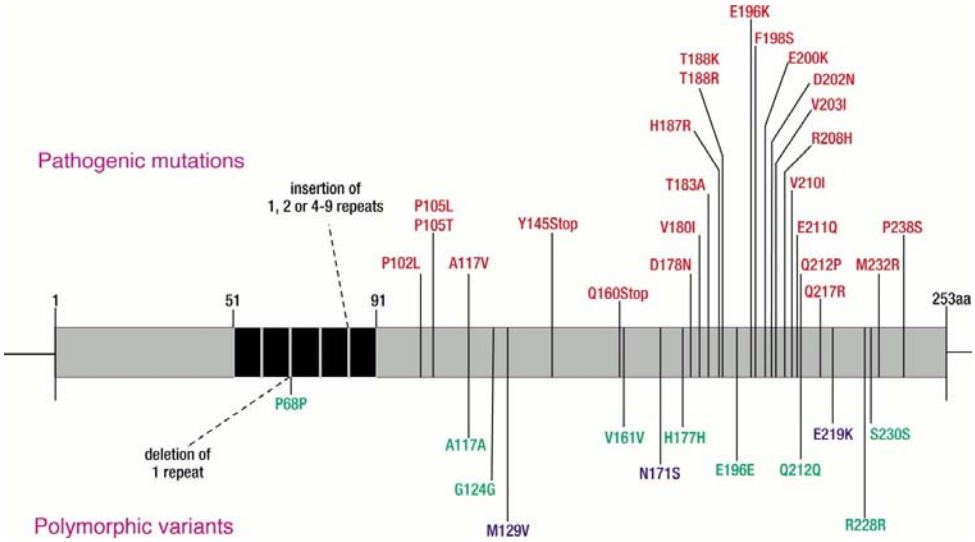

Figure 1
Pathogenic mutations and polymorphic variants of the human prion protein. In red: mutations that correlate with inherited prion diseases. In green & blue: polymorphisms, that might influence susceptibility for prion infections and the disease phenotype (taken from Collinge, 2001)

Progress of inherited or familial CJD (fCJD) is similar to sCJD with a prolonged progression and mainly affects patience of advanced age. Gerstmann-Sträussler-Scheinker syndrome (GSS) is another disorder caused by mutations of *Prnp* (Gerstmann, 1936). P102L is the most common change and was associated with the occurrence of GSS first (Hsiao et al., 1989). By now links to mutations of seven different PrP codons were found. The average age of symptomatic onset is 45 years but can strongly vary (25-59 years) just as the course of disease has an average of 6-7 years but might range from 2-17 years. Since 1981 GSS was defined as TSE as non-human primates were could be infected experimentally (Masters et al., 1981).
The most recent inherited TSE was discovered in 1986 in Italy. The very rare FFI (fatal familial insomnia) is caused by a mutation D178N in combination with methionine at codon 129 of the prion protein gene. Course of illness is very heterogeneous but in most cases comes along with pronounced insomnia and other neurological deficits. FFI was classified as TSE when experimental transmission had succeeded (Tateishi et al., 1995).
Several polymorphisms of Prnp were found in humans, whereas the most important one is located at position 129, coding either for methionine or valin. Even thought 50% of the European population are homozygous at codon position 129 virtually all sporadic and

acquired cases of the disease affected heterozygous individuals, probably as result of a genetic predisposition (Collinge et al., 1991;Palmer et al., 1991).

Prions are not infectious via natural routes between humans, e.g. via family or sexual contact. Accidentally transmission from human to human happened in some rare iatrogenic cases either by direct transfer of infection caused by inadequately decontaminated intracerebral electrodes or grafting of dura mater and cornea of infected donators. Most iCJD infections were caused by aplication of human growth hormones produced from pituitary gland contaminated with CJD of infected individuals.

The by far the most investigated form of acquired human prion diseases is kuru which occurred among the Fore people in the highlands of eastern Papua New Guinea (GAJDUSEK et al., 1957;ZIGAS et al., 1957). The spread of disease was based on ritual cannibalism of deceased members of the community and reached epidemic proportions. Mainly women and children of both sexes were affected and it was the prevalent cause of death amongst women of the Fore people. The reason for this uneven sexual distribution of infection was based on the attendance at the rituals mainly by women and children consuming brain and internal organs. Furthermore, they got in close contact with contaminated tissues and may therefore have been infected by lesions of skin and via their conjunctiva. This would explain very rare infections of children with incubation times as short as 4.5 years, on the other hand more than 40 years of incubation were monitored (Alpers M., 1987). Average incubation time via oral transmission was estimated to take about 12 years (Collinge, 2001). The epidemic was dated back to beginning of 20th century and presumably was brought into the fatal circle by a spontaneous CJD case of a community member. Since mid of 1950th cannibalism was banned which stopped further spread of kuru although between 1996 and 2004 11 Fore people died of the disease who all were born before the ban (Collinge et al., 2006).

Since 1993 epidemiological monitoring of CJD was intensified in several European countries due to concerns BSE might transmit to human via the food chain. Indeed some cases of particular young infected people occurred in the following years. So far more than 210 people were affected by this new variant of CJD (Table 4).

Table 4
Current data of vCJD cases worldwide until April 2008 (http://www.cjd.ed.ac.uk/ - May 2008)

Country	Number of vCJD cases (alive)
UK	163 (3)
France	23 (2)
Republic of Ireland	4 (0)
USA	3 (0)
Spain	3 (0)
Portugal	2 (1)
Netherlands	2 (0)
Saudi Arabia	1 (1)
Italy	1 (0)
Canada	1 (0)

There are some differences in the progression of vCJD compared to classic CJD from which the most important is the early onset of disease in average at 29 years (range from 16-51). Furthermore duration of the course is prolonged to 14 month in average (9-35 months). The phase of psychiatric symptoms takes longer and is followed by similar progression to sCJD but additionally about 50 % of patients develop painful sensory symptoms. Finally all affected people get ataxia followed by progressive dementia ending up in conditions of helplessness. Pathologically vCJD and classic CJD share features like spongiform changes, astrocytic gliosis and neuronal loss but additionally the variant shows very characteristic amyloid plaques surrounded by Kuru like spongiform vacuoles (florid plaques) spread all over the cerebrum, cerebellum and thalamus (Will et al., 1996). A unique attribute of vCJD compared to all other human prion diseases is the finding of PrP^{Sc} in tonsils and other lymphoreticular tissue (Collinge, 1997;Hill et al., 1999).

Correlation between the occurrence of a new variant of CJD and BSE initially was assumed because of the geographic and chronological co-localization in U.K. In the meantime experimental data confirmed this assumption. It is possible to discriminate different prion strains by examination of characteristic glycosylation pattern of PrP^{Sc}. In case of BSE and vCJD they are the same but different from classical CJD and scrapie (Collinge et al., 1996b). Experimental infection of macaques revealed vCJD characteristic plaques in brains of infected animals (Lasmezas et al., 1996).

Most importantly food production of tissue from cattle bearing a possible risk of prion infection was stopped in 1989. Even thought with all steps taken the number of *de novo* infections should be small or hindered it is very difficult to predict the expected number of vCJD cases in the future. They might range from a few hundred to couple of thousands (Donnelly et al., 2002;Ghani et al., 2002).

1.3 The prion protein

According to the protein only hypothesis postulated by Stanley Prusiner the prion protein in its pathogenic isoform PrP^{Sc} displays the sole infectious element of prion diseases (Prusiner, 1982). Several data support the conception of prions mainly or even entirely consisting of an abnormal isoform of cellular PrP^{C}. The pathogenic form PrP^{Sc} acts as template for a conformational change of PrP^{C} during postranslational contact (Caughey et al., 1991;Cohen et al., 1994;Prusiner, 1997). In vitro conversion of PrP^{C} into PrP^{Sc} was demonstrated some time ago (Kocisko et al., 1994). More recently infectivity of recombinantly expressed and in vitro converted PrP was shown in transgenic mice and strongly supports the protein only hypothesis (Legname et al., 2004).

1.3.1 Features of PrP

The prion protein gene is highly conserved in evolution suggesting the importance of protein function (Schatzl et al., 1995;Wopfner et al., 1999). It is located on chromosome 2 in mice, corresponding to the short arm of chromosome 20 in humans. All known PrP genes contain the complete open reading (ORF) frame in a single exon (Robakis et al., 1986;Sparkes et al., 1986;Wopfner et al., 1999), thus no PrP isoforms based on alternative splicing are possible (Basler et al., 1986). Genes of mouse, sheep, cattle and rat consist of 3 exons with the ORF located on exon 3 accompanied by a 3' untranslated region (3'UTR). The PrP promotors contain several G+C rich repeats for binding of transcription factors SP1 and AP1 and lack a TATA box (McKnight et al., 1986).

The size of mRNA is 2.1-2.5 kb and codes for 254 amino acids (aa) in mice. Figure 2 shows the primary structure of mouse PrP flanked by short signal peptides that are removed during maturation resulting in a 209 aa protein. The N-terminal signal peptide leads to expression of PrP into the rough ER (Oesch et al., 1985), whereas the C-terminal signal results in the attachment of a GPI anchor at serine position 231 and is mandatory for fixation of PrP into the outer membrane of the cell (Stahl et al., 1987). Furthermore asparagines at position 180 and 196 can be glycosylated during maturation resulting in PrP of 3 different molecular weights (non-, mono- and di-glycosylation) (Bolton et al., 1985;Manuelidis, 1985). Two cysteines at position 178 and 213 stabilise conformation of PrP by formation of a disulfide bridge (Hope et al., 1986). Defined NMR structures could only be found of PrP C-terminus but not for the N-terminus until aa 120 (Figure 2B) (Peretz et al., 2001).

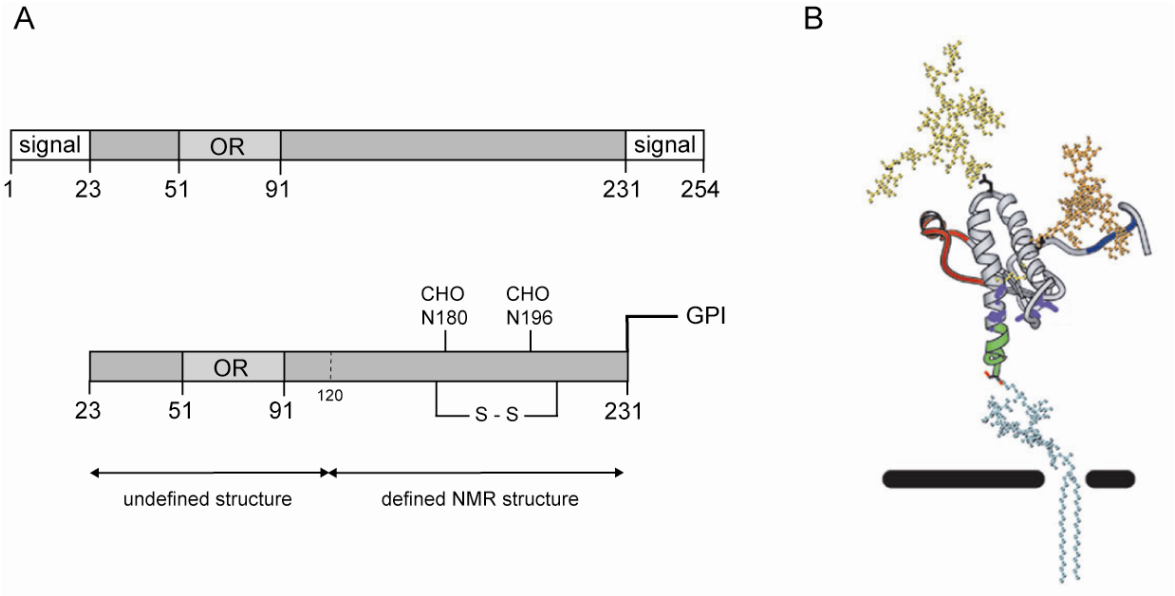

Figure 2
Primary and mature structure of mouse PrP **(A)**.The N- and C terminal signal peptides are cleaved during maturation, a GPI anchor is attached to the C-terminal end and can be N-glycosylated twice at positions 180 and 196. A disulfide bond (S-S) is built. **(B)** Structure of PrP^{C} as it is attached to the outer leaflet of the plasma membrane via its GPI anchor. Carbohydrate molecules are shown in yellow (Peretz, 2001)

Figure 3 shows the cellular trafficking of PrP in the cell. Accurately folded PrP will pass though Golgi compartments and reach the outer membrane via the secretory pathway (Borchelt et al., 1990;Caughey et al., 1991;Taraboulos et al., 1990). Internalisation appears to happen through rafts, caveolae-like domains (CLD) or in membrane regions rich in cholesterol and glycosphingolipids by invagination (Taraboulos et al., 1995). Since reports showed that the conversion of PrP^{C} to PrP^{Sc} happens close to the plasma membrane probably in raft or CLD along the endocytic pathway, cell surface localisation of PrP^{C} seems to have major importance. Internalised PrP is transported to endosomes and can either be recycled back to cell surface or finally be degraded in acidic compartments (Vey et al., 1996). Lysosomes or late endosomes might be further compartments of conversion as low pH enables un- and re-folding of PrP (Arnold et al., 1995;Taraboulos et al., 1992). In infected cells PrP^{Sc} will accumulate in lysosomes and be degraded only at very slow rate.

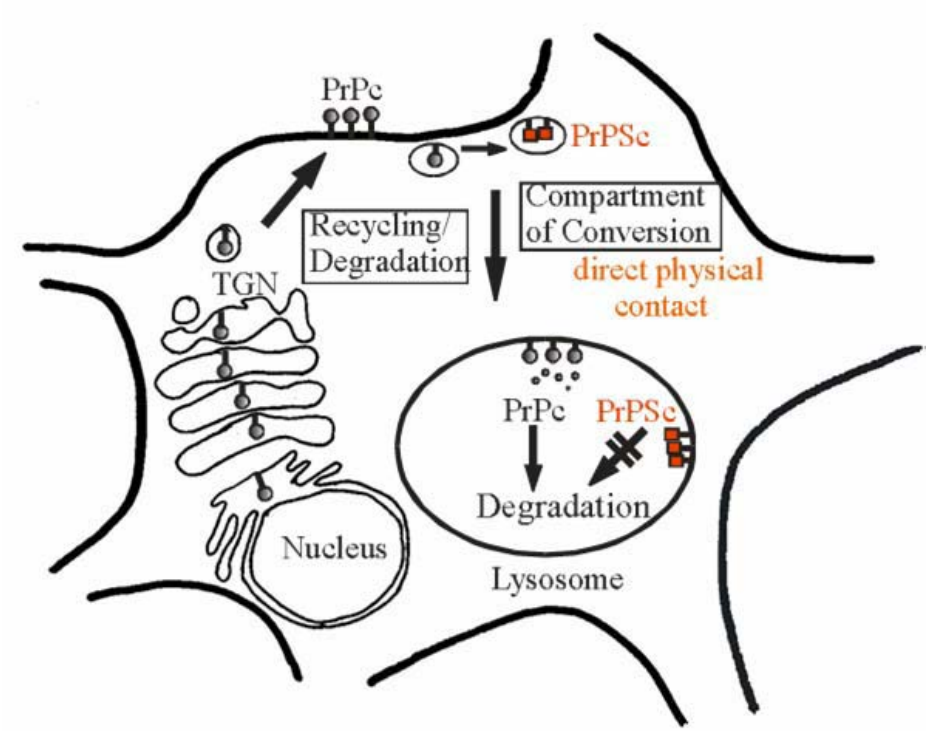

Figure 3
Cellular trafficking of PrP^{C}. After translation into the ER, PrP^{C} is transported to the outer membrane via trans-Golgi network and the secretory pathway. Degradation happens in lysosomes after internalisation. Conversion of PrP^{C} to PrP^{Sc} presumably happens directly at the membrane or in early endosomal compartments. PrP^{Sc} can not be degraded in the lysosomes or at least very slowly.

1.3.2 Physiological function of PrP

The prion protein gene was identified in many mammalians, birds (Harris et al., 1993;Wopfner et al., 1999), marsupials (Windl et al., 1995), amphibians (Strumbo et al., 2001) and fish (Oidtmann et al., 2003). Highest concentration of PrP^{C} was found in neurons (Kretzschmar et al., 1986), more precisely at the synaptic and pre-synaptic ends (Borchelt et al., 1994;Fournier et al., 1995;Herms et al., 1999). Regardless of the predominant occurrence in the central nervous system PrP is also expressed in many other tissues particularly in cells of the immune system (Dodelet et al., 1998).

Knowledge of the physiological function of PrP still remains elusive. PrP deficient knockout mice ($PrP^{0/0}$ mice) showed complete resistance to prion infection (Bueler et al., 1993) and did not develop a distinctive phenotype concerning lack of PrP^{C} (Bueler et al., 1992). Animals revealed some minor changes of their synaptic physiology (Collinge et al., 1994) and in circadian rhythm (Tobler et al., 1996). Later a reduction of slow after-hyperpolarisations were found in some knockout mice which were based on abnormal intracellular Calcium levels. Furthermore some of $PrP^{0/0}$ mice showed higher sensitivity to copper toxicity during oxidative

stress (Brown et al., 1998;Pauly et al., 1998). Membrane preparations of respective animals showed a 50 % reduction of Cu^{2+} content compared to wild type mice (Brown et al., 1997). Hence a role as carrier protein for metal ions into the cell and a superoxide dismutase activity has been discussed (Brown et al., 1997;Brown et al., 1999). Indeed synthetic peptides arround the octarepeat region of PrP (aa 50-90) were shown to bind Cu^{2+} ions (Hornshaw et al., 1995;Jackson et al., 2001;Pauly et al., 1998) and a pH dependent affinity was demonstrated with CD, NMR and mass spectrometry (Viles et al., 1999;Whittal et al., 2000).

Another possible function of PrP might be that of a receptor for binding of extracellular ligands. Several potential binding partners were identified such as the laminin receptor precursor (LRP) binds PrP at the cell surface (Gauczynski et al., 2001;Rieger et al., 1997). Other factors found to interact with PrP are Bcl-2 (Kurschner et al., 1996), HSP 60 (Edenhofer et al., 1996) or synapsin Ib, Grb2 and non characterized partners like prion interacting protein 1 (pint1) (Spielhaupter et al., 2001). As some of these interaction partners play a major role in signal transduction pathways there are estimations of a respective function for PrP.

1.3.3 Conformation of PrP^C and PrP^{Sc}

The protein only hypothesis seemingly is contradictory to the long accepted idea of protein science that the amino acid sequence defines only one single biologically active confirmation of a protein (Anfinsen, 1973). Nevertheless it could be shown that isolated PrP^C and PrP^{Sc} molecules, examined by optical spectroscopy, had different secondary structures despite they consisted of identical amino acid sequences (Pan et al., 1993). Fourier transform infrared spectroscopy (FTIR), mass spectrometry and circular dichroism (CD) studies revealed that PrP^C consists of about 42 % α-sheet and only 3 % β-sheet, whereas PrP^{Sc} has 30 % α-sheet and 45 % β-sheet (Gasset et al., 1993;Pergami et al., 1996;Stahl et al., 1993). So far it was not possible to obtain the three dimensional structure via crystallographic measurements as it has been impossible to produce crystals of PrP. Nevertheless N-terminally truncated PrP was expressed in *E.coli* and the structure measured with nuclear magnetic resonance (NMR) after purification and refolding (Riek et al., 1996). The results confirmed a short anitparallel β-sheet and 3 of four α-helices previously predicted by computer modeling (Cohen et al., 1994). In the following the globular structure of the C-terminus was confirmed also for full length PrP whereas the N-terminal segment 23-120 was found flexibly disordered (Riek et al., 1997). Other NMR studies showed comparable conformations for hamster, human and bovine PrP

(Hosszu et al., 1999;James et al., 1997). The N-terminus of PrP of most species is known to contain a region with 5 repeats of 8 aa (mainly proline, glycine and histidine). This "octarepeats" can bind metal ions or other ligands thus the N-terminus of PrP might obtain a defined globular structure *in vivo*. There is some experimental evidence in this respect as the existence of a poly-L-proline type II helix structure of *in vivo* conformation of PrP was shown (Gill et al., 2000).

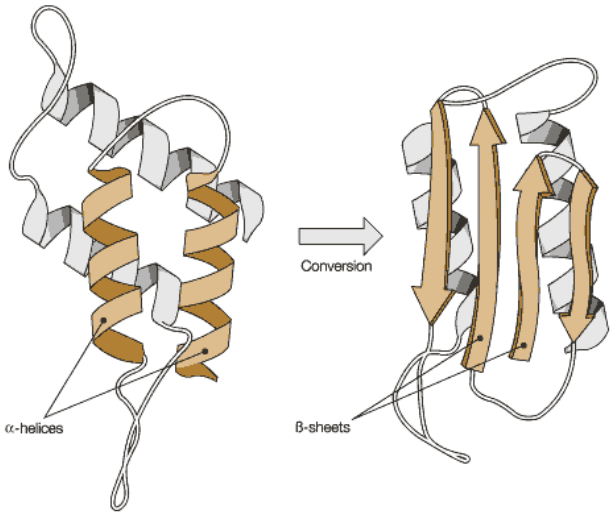

Characteristics	**PrP^C**	**PrP^{Sc}**
Infectivity	No	Yes
Secondary structure	mainly α-helical	mainly β-sheet
Half life time	2-6 hours	16-24 hours and longer
Proteinase-K digestion	sensitive	partially resistant
Ultracentrifugation in detergent	soluble	insoluble

Figure 4
Features of PrP^C und PrP^{Sc} are summarized. Structure prediciton model of (Prusiner, 1999).

Insolubility of the PrP^{Sc} isoform has prevented studies of its three dimensional structure at atomic level so far thus only computer models are available (

Figure 4). Recently crystallographic analysis of 2D crystals consisting of N-terminally truncated PrP^{Sc} (PrP 27-30) provided the first insight at intermediate resolution on the molecular architecture of prions (Wille et al., 2002;Wille et al., 2007). It was argued that left-handed β-helices of the C-terminus readily form the core of a trimer disc surrounded by α-helically formed N-terminus. Figure 5 shows a model completing the little knowledge of

measurements with computer simulation. Hence trimers discs may further aggregate to form SAF or prion rod like structures (Govaerts et al., 2004).

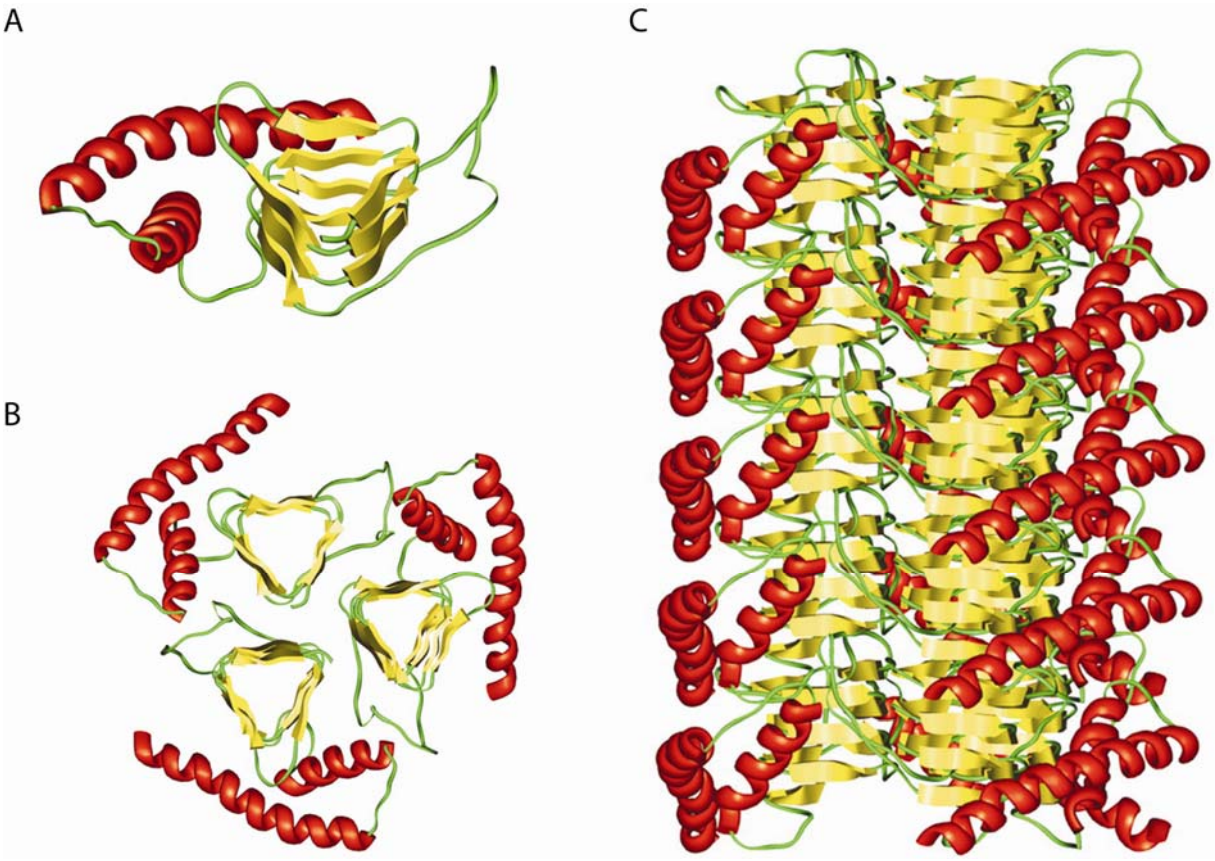

Figure 5
Model of PrP^{Sc} structure and predicted formation of pion rods. **(A)** model of a possible PrP^{Sc} conformation based on NMR measurements. **(B)** Trimer model with three PrP^{Sc} left handed β-sheet structures building the core. **(C)** Model of prion rod formation is based of trimer plated lying on top of each other. (Govaerts et al., 2004)

According to the prion only hypothesis direct contact between PrP^{C} of the host and exogenous scrapie prions is mandatory for the conversion into PrP^{Sc}. The major conformational change should involve refolding of the region between residues 90-120 and lead to conversion of the first α-helix and two short β-sheets into a large β-sheet structure. The remaining two C-terminal α-helices and the disulphide bonds are needed to be preserved for infectivity of PrP^{Sc} (Hornemann et al., 1997;Prusiner, 1998;Wille et al., 2002).

There are two basic models for the conversion of PrP^{C} into its pathogenic form. Corresponding to the heterodimer hypothesis suggested by Prusiner PrP^{C} partially unfolds to an intermediate state named PrP^{*} which then forms a heterodimeric complex with PrP^{Sc}

(Cohen et al., 1994;Prusiner et al., 1990). Refolding of PrP^{*} under the influence of PrP^{Sc} leads to a PrP^{Sc} homodimer complex in an autocatalytic process, perhaps under the influence of a molecular chaperon. The newly built PrP^{Sc} can now form further heterodimers with PrP^{*}. The energy barrier for conversion, especially regarding transfer of PrP^{C} to PrP^{*} might be very high (Cohen et al., 1994). Hence PrP^{*} is very unstable and falls back into PrP^{C} conformation very rapidly if no PrP^{Sc} is around to form a heterodimer. This feature would also explain the small likelihood of spontaneous prion diseases and the increased age of occurrence. Mutation of PrP might have a destabilizing effect on its structure thus lowering the energy barrier of PrP^{*} formation. Hence the chance of disease for individuals inherited the mutation is increased.

The second model was initially proposed by Gajdusek and further developed by Landsbury and Caughey (Brown et al., 1990;Caughey et al., 1995;Come et al., 1993). According to the nucleation dependent polymerisation model PrP^{C} of the host can directly deposit at a polymerisation seed consisting of PrP^{Sc} oligomers. A transition state like PrP^{*} is not necessary as PrP^{C} directly adopts the conformation of the seed and leads to high molecular aggregates of PrP^{Sc}. Bigger aggregates might disrupt and form new seeds.

Both models are appropriate to explain familial and infectious manifestations of prion diseases and are not contradictory. They are both based on the existence of a pathogenic isoform whereas either formation of PrP^{*} or a PrP^{Sc} seed is favoured.

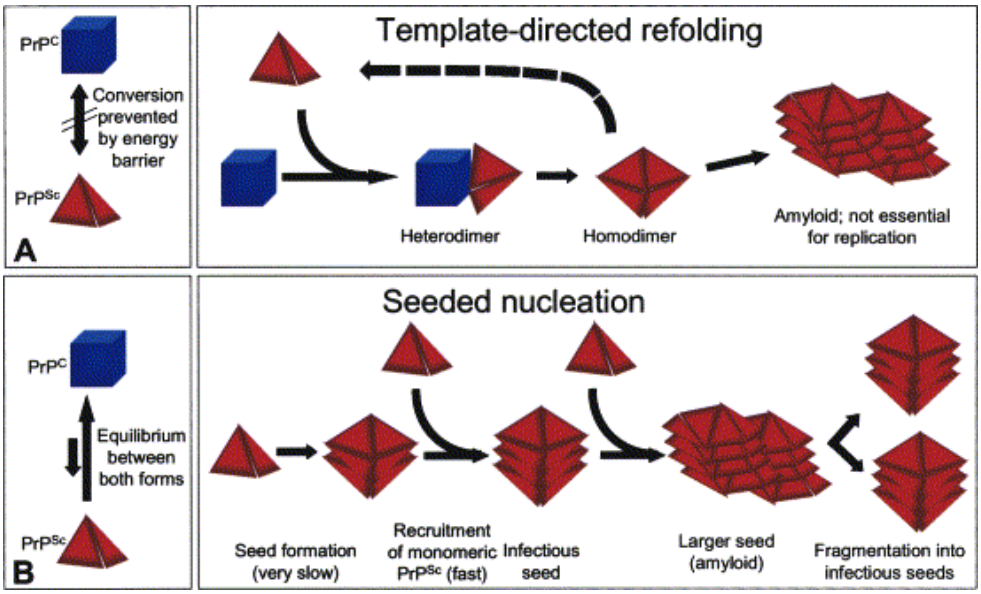

Figure 6
Prion conversion and replication models **(A)** Heterodimer model **(B)** Nucleation dependent polymerisation model (Aguzzi & Polymenidou, 2004).

1.3.4 Species barrier and prion strains

Infection with prions between species almost always showed a prolonged incubation time during the first passage compared to transmission within the same species. After several passages in a homologous host incubation time shortens and adapts to the approximate duration of the previous host. Hence the existence of a species barrier has been postulated some time ago (Pattison et al., 1968). As reasons for the occurrence of the species barrier differences of PrP amino acid sequence between donor and recipient were discussed (Prusiner, 1997;Schatzl et al., 1995;Scott et al., 1989). This means species with similar PrP like sheep and cattle exhibit a low species barrier, whereas diverse species (e.g. syrian hamster/mouse) show a pronounced barrier. Experimental results of infection trials using chimeric proteins confirmed this hypothesis (Scott et al., 1989;Telling et al., 1994;Telling et al., 1995). Other reasons might be the species specific binding of factor X, a so far undefined host factor that might be involved in the conversion to PrP^{Sc} by binding to the C-terminus of PrP^{C} (Kaneko et al., 1997;Telling et al., 1995) and the prion strains.

Several prion strains have been isolated and showed individually biological and biochemical properties. They differ in incubation time and neuropathological changes (lesion profile). In addition strains revealed different fragment sizes in Western Blot analysis following proteinase K treatment as well as differences in the ratio of glycosylated isoform (banding pattern of un-, mono- and di-glycosylated PrP) (Collinge et al., 1996b). These features are not changed during transmission across species and strains could actually be re-isolation from mice after intermediate passage within other species bearing a different PrP primary structure (Bruce et al., 1994). This led to the conclusion for the incidence of different PrP^{Sc} conformations causative for the appearance of prion stains (Telling et al., 1996). To date at least three different sporadic/iatrogenic CJD strains and a single vCJD strain were found in humans (Collinge et al., 1996b;Parchi et al., 1996;Parchi et al., 1999). Strain-specific protein conformation can also be influenced by metal ion binding to PrP^{Sc} (Wadsworth et al., 1999)). This and other methodological differences may lead to discrepancies in strain definition (Hill et al., 2003).

1.3.5 Spread of prions after peripheral infection

Peripheral exposure is the most common way of natural TSE transmission. Consumption of infected feed most likely is involved in the spread of BSE in cattle (Wilesmith et al., 1991). Furthermore consumption of BSE infected tissue is widely accepted to cause vCJD (Bruce et

al., 1997;Hill et al., 1997). Experimental peripheral transmissions of scrapie showed that accumulation of PrP^{Sc} and infectivity was found in lymphoid tissue long before either was discoverd in the CNS (Beekes et al., 2000;Brown et al., 1999;Farquhar et al., 1994;Kimberlin et al., 1979). CWD was first detected in draining lymphnodes of the gastrointestinal tract after oral exposure in mule deer (Sigurdson et al., 1999). In addition natural scrapie was found in Peyer´s patch and gut associated lymphoid tissue at first (Heggebo et al., 2000;van Keulen et al., 1999). Splenectomy shortly before or directly followed peripheral prion challenge significantly prolonged incubation time (Fraser et al., 1978). Hence the lymphoid tissue plays an important role in the spread of prion diseases. Membranous epithelial cells (M-cells) have been identified as major port of entry for pathogens in the gut (Neutra et al., 1996). Differentiated M-cells were shown to be sufficient for active transepithelial prion transport *in vitro* (Heppner et al., 2001a). Therefore, prions may gain access to the immune system by M-cell dependent transcytosis (Figure 7). Dendritic cells were discussed as second cell type able to acquire PrP^{Sc} from the intestinal lumen and deliver it to mesenteric lymph nodes (Huang et al., 2004).

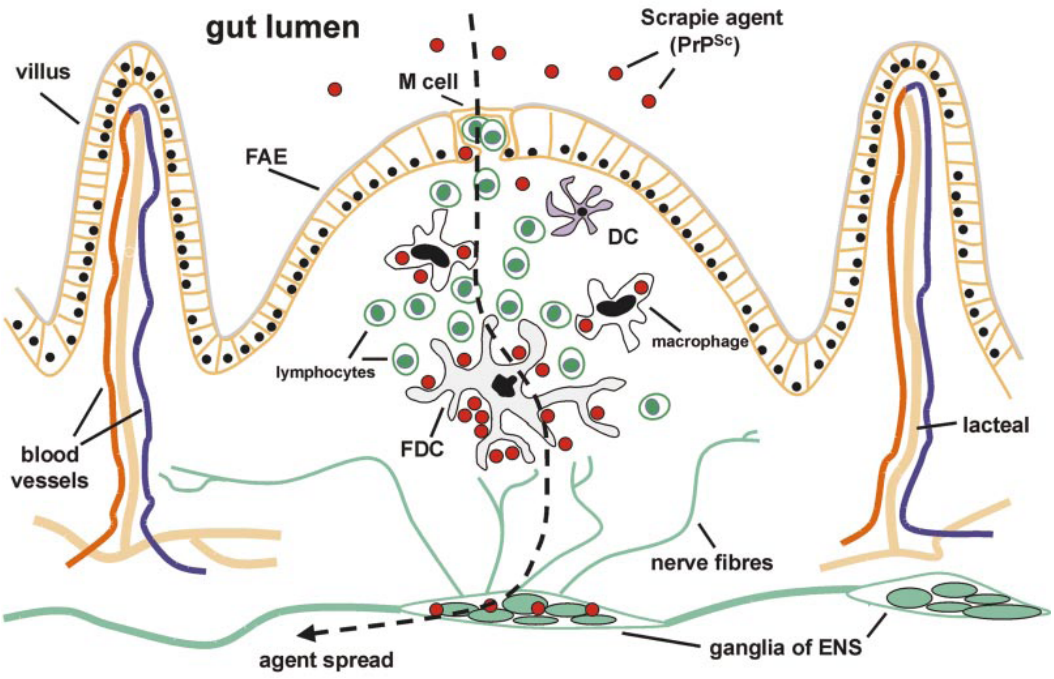

Figure 7
Possible spread of PrP^{Sc} from the gut lumen to the nervous system after oral infection. PrP^{Sc} is detected within Peyer's patches upon FDCs, macrophages and cells with morphology consistent with that of M cells very soon after ingestion. (Mabbott et al., 2006)

Macrophages have been shown to contain lysosomal PrP accumulations in spleen of scrapie infected mice (Jeffrey et al., 2000). Depletion of macrophages increased the accumulation of PrP^{Sc} in spleen and shortened incubation time (Beringue et al., 2000). Likewise in vitro cultivation of macrophages decreased infectivity of scrapie (Carp et al., 1982). These data suggest that macrophages impair in early scrapie agent replication. T lymphocytes apparently are not involved in scrapie pathogenesis as neither thymectomy nor transgenic mice deficient in T lymphocyte compartment had an effect on the susceptibility or accumulation of infectivity in spleen (Fraser et al., 1978;Klein et al., 1998;McFarlin et al., 1971). In contrast in B lymphocyte deficient mice infectivity and spread of prions was significantly impaired (Klein et al., 1997). Although B lymphocytes are crucial for neuro-invation and trafficking of prions within lymphoid organs several experimental data ruled out that the bulk of infectivity is contained in lymphocytes (Frigg et al., 1999;Raeber et al., 1999). There is no evidence for the spread of infectivity to CNS via the blood stream. B lymphocytes might rather act indirectly as they provide important signals for the maturation of other cell types (Chaplin et al., 1998;Kosco-Vilbois et al., 1997). In this context mice deficient in mature B lymphocytes are indirectly deficient in functional FDCs and M-cells as both require stimulation to maintain their differentiated state. Follicular dendritic cells are discussed as to be the main candidate for prion accumulation in lymphoid tissue because they express large amounts of cellular PrP (Jeffrey et al., 2000). Infection most likely spreads to the CNS via enteric nervous system (Beekes et al., 1996;Kimberlin et al., 1989;McBride et al., 1999). However, as the germinal centers of lymphoid tissue are poorly innervated it is not known how infectivity reaches the nerves from FDCs. Recently contact between nerve fibers and PrP^{Sc} propagation dendritic cells was detected and might indicate DCs have a direct impact in prion neuroinvasion (Dorban et al., 2007).

1.4 Therapy and prophylaxis

In the past years much effort was made to find a therapy or prophylaxis against prion diseases. As already the early clinical signs of the diseases are accompanied with neuronal loss and unrecoverable damage of the central nervous system development of prophylactic approaches appear promising as therapeutic treatment might only be able to stop or prolong the course of disease. Nevertheless it is worthwhile finding substances that inhibit further conversion of PrP^{C} and accumulation of PrP^{Sc}. Most strategies have the aim to prevent contact between PrP^{C} and PrP^{Sc} as this is known to be mandatory for conversion. It was shown that

PrP knockout mice were completely resistant to prion infections due to the lack of PrP^C (Bueler et al., 1993;Prusiner, 1998). A similar idea was taken into account when knocking down PrP^C using RNAi (Tilly et al., 2003).Other approaches used drugs influencing the cellular trafficking of PrP such as suramin. After treatment PrP^C accumulates in the Golgi and is degraded in lysosomes before reaching the cell membrane thus by passing the place of conversion (Gilch et al., 2001). The concept of over-stabilization is based on the idea that PrP^C exists in an equilibrium with a transition state named PrP^* which needs direct contact to PrP^{Sc} for its conversion into the disease related conformation (see also chapter 1.3.3). By over-stabilizing either PrP^C or PrP^{Sc}, e.g. by using chemical chaperons (Tatzelt et al., 1996) or congo red (Head et al., 2000), conversion into PrP^* and subsequently into PrP^{Sc} might be circumvented (Clarke et al., 2001;Cohen et al., 1994;Prusiner, 1998). Another way to prevent the contact between PrP^C and PrP^{Sc} are specific aptamers (Gilch et al., 2007;Proske et al., 2002;Weiss et al., 1997) or anti PrP antibodies (Enari et al., 2001;Gilch et al., 2003;Heppner et al., 2001b). Inhibition of factor X binding might be a successful strategy to prevent prion conversion (Head et al., 2000;Prusiner, 1998). This mechanism was discussed for a soluble PrP-dimer (Meier et al., 2003).

Effectiveness of only few drugs had been directly correlated to PrP^{Sc} based on increased clearance of the pathogenic protein. Both highly branched polyamides (Supattapone et al., 1999) and tyrosine kinase inhibitors were shown to be effective in prion therapy (Ertmer et al., 2004;Yun et al., 2007). A major obstacle in the treatment of central nervous system related diseases is the transfer of therapeutic agents via the blood brain barrier. Most drugs available to prevent or cure prion disease in cell culture models are retained, thus can only be effective locally in case of early treatment, e.g. in case of obvious accidental infection.

The most commonly method of broad protection against infection diseases ever since is active immunization. Indeed anti-PrP antibodies were shown to be very effective even in cell culture models (Enari et al., 2001;Peretz et al., 2001). Transgenic mice expressing PrP^C as well as a defined anti-PrP antibody revealed a radical decrease of infectivity in spleen (Heppner et al., 2001b). As PrP is expressed on nearly all cells of the body overcoming immunological tolerance presents the biggest challenge in obtaining a protective immune response.

Several different strategies were tried to reach the aim of an active immunisation. As antigen either full protein (Sigurdsson et al., 2002), peptides (Schwarz et al., 2003;Souan et al., 2001) or dimeric PrP were used (Polymenidou et al., 2004). Other strategies tried to overcome

tolerance by PrP-displaying retrovirus (Nikles et al., 2005). So far only one study showed protection against peripheral prion infection after a combination of recombinant PrP-dimer, Freund`s adjuvant and anti-OX40 antibody tolerance breaker although only in a few treated animals (Polymenidou et al., 2004). Interestingly none of any immunized animals showed any sign of autoimmune related side effects.

1.5 Aim of this work

Results of previous immunization using a recombinant tandem-PrP (tPrP) obtained very promising results. Sera of immunized mice showed to prevent *de novo* synthesis of prions in infected neuroblastoma cells (Gilch et al., 2003). In addition a combined active immunization strategy using tPrP with Freund's adjuvant together with a local tolerance breaker (anti-OX40 antibody) resulted in the protection of 2 of 8 mice after low dose i.p. prion inoculation without developing any sign of autoimmune side effect (Polymenidou et al., 2004).

Aim of this work was to get more insight into the properties of this promising antigen. Furthermore advanced immunization conditions should be found to receive the approach with a prophylaxis against TSEs. tPrP is believed to mimic either a conformation of a transition state of PrP such as PrP^{*} and by induction of specific antibodies might lead to effective immunization. Depending on refolding conditions solubility of tPrP varied and the protein differs in its immunogenicity. The same is true for interaction with CpG adjuvant. Hence structural characterisation of the antigen and the dependency of immune response in PrP wild type mice were examined. B-cell response was measured and some important features of induced antibodies should be characterised. Moreover response of T lymphocytes upon immunization was measured of all individual animals. Furthermore immune response should be enhanced by improved application of antigen. PLGA microspheres consist of biodegradable bubbles encapsulating antigen and/or adjuvant. Small bubbles can be phagocyted whereas bigger ones form antigen deposit slowly degrading. Thus PLGA microspheres have an immunological long term effect. DNA vaccination based on tPrP was performed by application of co-encapsulated DNA and CpG adjuvant. After detailed investigation in non infected mice some promising immunization strategies were applied to PrP wild type mice followed by intra peritoneal prion inoculation to prove their protective efficiency.

2 Material and Methods

2.1 Materials

2.1.1 Chemicals

Description	Company
β-Mercaptoethanol	Sigma, Munich, Germany
Agarose	Invitrogen, Karlsruhe, Germany
Ammoniumchloride	Sigma, Munich, Germany
Ammoniumpersulfate (APS)	Roth, Karslruhe, Germany
Ampicillin	Sigma, Munich, Germany
Bacto Tryptone	Becton Dickinson, Heidelberg, Germany
Bacto tryptone	Becton Dickinson, Heidelberg, Germany
Bacto yeast extract	Becton Dickinson, Heidelberg, Germany
Dimethyl sulfoxide (DMSO)	Sigma, Munich, Germany
EDTA	Roth, Karlsruhe, Germany
Ethidiumbromide	Roth, Karlsruhe, Germany
Glacial acetic acid	Roth, Karlsruhe, Germany
Kanamycin	Sigma, Munich, Germany
Lämmli-buffer 2x	Sigma, Munich, Germany
Methylene chloride	Merck, Germany
Optimem medium	Gibco/BRL Life Lab., Paisley, Scotland
Penicillin	Gibco/BRL Life Lab., Paisley, Scotland
Phosphate buffered saline (PBS)	Gibco/BRL Life Lab., Paisley, Scotland
PLG Resomer 502 50:50 with glycolide	Bohringer Ingelheim, Germany
Polyvinyl alcohol (Mowiol 40–88)	Sigma, Munich, Germany
Protogel - 30% (w/v) acrylamide: bisacrylamide (37.5:1)	National Diagnostics, Atlanta, USA
Sodiumdeoxycholate (DOC)	Roth, Karlsruhe, Germany
Sodiumdodecylsulfate (SDS)	Roth, Karlsruhe, Germany
Streptomycin	Gibco/BRL Life Lab., Paisley, Scotland
TEMED	Sigma, Munich, Germany
Tris	Roth, Karlsruhe, Germany
Triton X-100	Sigma, Munich, Germany
Trypsin-EDTA 0.25 %, 1mM EDTA	Gibco/BRL Life Lab., Paisley, Scotland
Tween-20	Roth, Karlsruhe, Germany
Urea	Sigma, Munich, Germany

All other chemicals were obtained from Invitrogen, Karlsruhe; Roth, Karlsruhe, Germany or Sigma, Munich, Germany.

2.1.2 Media and solutions

Bindingbuffer pH 7.8 (protein purification)	8 M Urea 20 mM Sodium-phosphate 500 mM NaCl
Cell culture medium	Optimem medium 100 IU/ml penicillin 0,1 mg streptomycin 10 %FCS (inactivated at 56°C for 30 min)
Coomassie staining solutions	25% (v/v) isopropanol 10% (v/v) acetic acid 0.05% (w/v) Coomassie Brilliant Blue
Coomassie de-staining solutions	45% (v/v) methanol 10% (v/v) acetic acid
DNA-Sample buffer	50 % (v/v) Glycerine 0.25 % (w/v) Bromphenoleblue 0.25 % Xylene-Cyanole FF
Elutionbuffer pH 6.3 (protein purification)	8 M Urea 20 mM Sodium-phosphate 500 mM NaCl 500 mM Imidazole
FACS-buffer	2.5 % (v/v) fetal calf serum (FCS) 0.05 % (w/v) Na-acide in PBS
Luri-Bertani-medium (LB)	10 g/l Bacto Trypton 5 g/l Bacto yeast extract 10 g/l NaCl
Lysisbuffer pH 7.8 (protein purification)	6 M GdnHCl 20 mM Sodium-phosphate 500 mM NaCl
Lysisbuffer (Westernblot)	100 mM NaCl 10 mM Tris-HCl pH 7.5 10 mM EDTA 0.5 % Triton X-100, 0.5 % DOC

Resolving gel (12.5 % acrylamide)	
	24.9 ml 30 % Protogel 15.4 ml resolving solution (4x) 20.3 ml ddH_2O 90 µl TEMED 192 µl 10 % (w/v) APS
Resolving solution (4x)	
	1.5 M Tris 0.4 % SDS; pH ad 8.8
SDS electrophoresis buffer (10x)	
	250 mM Tris 2.5 M Glycine 1 % SDS
SDS-sample buffer (3x)	
	6.7 % SDS 33 % Glycerol 16.6 % β-mercaptoethanol 0.0015% Bromphenolblue 83 mM Tris/HCl pH 6.8
SOC medium	
	2 % Bacto Tryptone 0,5 % Bacto yeast extract 10 mM NaCl, 2,5 mM KCl 10 mM $MgCl_2$, 10 mM $MgSO_4$ 20 mM Glucose
Stacking gel (5 % acrylamide)	
	2.8 ml Protogel 4.2 ml stacking solution (4x) 9.9 ml ddH_2O 30 µl TEMED 168. µl 10 % (w/v) APS
Stacking solution (4x)	
	0.5 M Tris 0.4 % SDS; pH ad 6.8
TAE-buffer	
	40 mM Tris 20 mM glacial acetic acid 1 mM EDTA
TBST	
	10 mM Tris/HCl pH 8.0 150 mM NaCl 0.05 % (v/v) Tween-20
TE-buffer	
	2 mM Tris/HCl pH 8.0 0.2 mM EDTA pH 8.0

TNE-buffer	
	50 mM Tris/HCl pH7.5 150 mM NaAc 5 mM EDTA
Washbuffer pH 6.3 (Protein purification)	
	8 M Urea 20 mM Sodium-phosphate 500 mM NaCl 80 mM Imidazole
Western blot transfer buffer	
	25 mM Tris 68 mM Glycin 20 % (v/v) Methanol

2.1.3 Antibodies

Name	Specificity	Origin	Company
4H11	prion protein	mouse	Kremmer (GSF)
A7	prion protein	rabbit (polyclonal)	Our laboratories
anti CD4-PE-Cy5	mouse CD4	rat	BD Pharmingen™
anti CD8-PE	mouse CD8	rat	BD Pharmingen™
anti IFNγ-FITC	mouse IFNγ	rat	BD Pharmingen™
anti-His	poly-His tag	mouse	Sigma
Fc Block	mouse CD16/CD32	rat	BD Pharmingen™
FITC-isotype control	rat IgG_1 isotype control	rat	BD Pharmingen™
OX86	CD134	mouse	ECACC
peroxidase-labeled anti IgG	mouse IgG	sheep	GE-Healthcare
peroxidase-labeled anti IgG	rabbit IgG	Donkey	GE-Healthcare

2.1.4 Sequences

2.1.4.1 pQE30-tPrP for recombinant tPrP expression

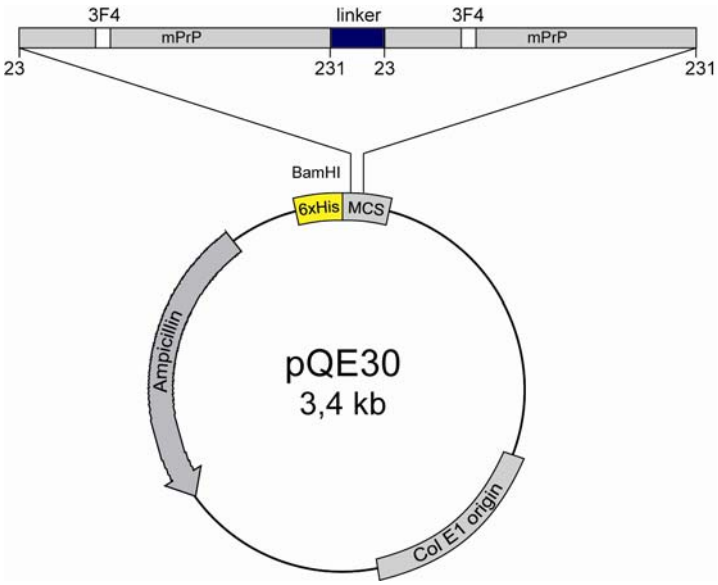

Figure 8
Expression vector pQE30-tPrP contains two mPrP sequences connected by a 7 amino acid linker. DNA insert was cloned into pQE30, containing a 6xHis tag near multiple cloning site.

```
1       ATGAGAGGATCGCATCACCATCACCATCACGGATCCTGCAAGAAGCGGCCAAAGCCTGGAGGGTGGAACACTGGC
1        M  R  G  S  H  H  H  H  H  H  G  S  C  K  K  R  P  K  P  G  G  W  N  T  G

76      GGAAGCCGATACCCTGGGCAGGGGAGCCCTGGAGGCAACCGTTACCCACCTCAGGGTGGCACCTGGGGGCAGCCC
26       G  S  R  Y  P  G  Q  G  S  P  G  G  N  R  Y  P  P  Q  G  G  T  W  G  Q  P

151     CACGGTGGTGGCTGGGGACAACCCCATGGGGGCAGCTGGGGACAACCTCATGGTGGTAGTTGGGGTCAGCCCCAT
51       H  G  G  G  W  G  Q  P  H  G  G  S  W  G  Q  P  H  G  G  S  W  G  Q  P  H

226     GGCGGTGGATGGGGCCAAGGAGGGGGTACCCACAATCAGTGGAACAAGCCCAGTAAGCCAAAAACCAACATGAAG
76       G  G  G  W  G  Q  G  G  G  T  H  N  Q  W  N  K  P  S  K  P  K  T  N  M  K

301     CACATGGCCGGCGCTGCTGCGGCAGGGGCCGTGGTGGGGGGCCTTGGTGGCTACATGCTGGGGAGTGCCATGAGC
101      H  M  A  G  A  A  A  A  G  A  V  V  G  G  L  G  G  Y  M  L  G  S  A  M  S

376     AGGCCCATGATCCATTTTGGCAACGACTGGGAGGACCGCTACTACCGTGAAAACATGTACCGCTACCCTAACCAA
126      R  P  M  I  H  F  G  N  D  W  E  D  R  Y  Y  R  E  N  M  Y  R  Y  P  N  Q

451     GTGTACTACAGGCCAGTGGATCAGTACAGCAACCAGAACAACTTCGTGCACGACTGCGTCAATATCACCATCAAG
151      V  Y  Y  R  P  V  D  Q  Y  S  N  Q  N  N  F  V  H  D  C  V  N  I  T  I  K

526     CAGCACACGGTCACCACCACCACCAAGGGGGAGAACTTCACCGAGACCGATGTGAAGATGATGGAGCGCGTGGTG
176      Q  H  T  V  T  T  T  T  K  G  E  N  F  T  E  T  D  V  K  M  M  E  R  V  V

601     GAGCAGATGTGCGTCACCCAGTACCAGAAGGAGTCCCAGGCCTATTACGACGGGAGAAGATCCAGCGCTGGAGCG
201      E  Q  M  C  V  T  Q  Y  Q  K  E  S  Q  A  Y  Y  D  G  R  R  S  S  A  G  A

676     ATCGGTGGAGCTAAAAAGCGGCCAAAGCCTGGAGGGTGGAACACTGGCGGAAGCCGATACCCTGGGCAGGGCAGC
226      I  G  G  A  K  K  R  P  K  P  G  G  W  N  T  G  G  S  R  Y  P  G  Q  G  S

751     CCTGGAGGCAACCGTTACCCACCTCAGGGTGGCACCTGGGGGCAGCCCCACGGTGGTGGCTGGGGACAACCCCAT
251      P  G  G  N  R  Y  P  P  Q  G  G  T  W  G  Q  P  H  G  G  G  W  G  Q  P  H

826     GGGGGCAGCTGGGGACAACCTCATGGTGGTAGTTGGGGTCAGCCCCATGGCGGTGGATGGGGCCAAGGAGGGGGT
276      G  G  S  W  G  Q  P  H  G  G  S  W  G  Q  P  H  G  G  G  W  G  Q  G  G  G

901     ACCCACAATCAGTGGAACAAGCCCAATAAGCCAAAAACCAACATGAAGCACATGGCCGGCGCTGCTGCGGCAGGG
301      T  H  N  Q  W  N  K  P  N  K  P  K  T  N  M  K  H  M  A  G  A  A  A  A  G

976     GCCGTGGTGGGGGGCCTTGGTGGCTACATGCTGGGGAGCGCCATGAGCAGGCCCATGATCCATTTTGGCAACGAC
326      A  V  V  G  G  L  G  G  Y  M  L  G  S  A  M  S  R  P  M  I  H  F  G  N  D

1051    TGGGAGGACCGCTACTACCGTGAAAACATGTACCGCTACCCTAACCAAGTGTACTACAGGCCAGTGGATCAGTAC
351      W  E  D  R  Y  Y  R  E  N  M  Y  R  Y  P  N  Q  V  Y  Y  R  P  V  D  Q  Y

1126    AGCAACCAGAACAACTTCGTGCACGACTGCGTCAATATCACCATCAAGCAGCACACGGTCACCACCACCACCAAG
376      S  N  Q  N  N  F  V  H  D  C  V  N  I  T  I  K  Q  H  T  V  T  T  T  T  K

1201    GGGGAGAACTTCACCGAGACCGATGTGAAGATGATGGAGCGCGTGGTGGAGCAGATGTGCGTCACCCAGTACCAG
401      G  E  N  F  T  E  T  D  V  K  M  M  E  R  V  V  E  Q  M  C  V  T  Q  Y  Q

1276    AAGGAGTCCCAGGCCTATTACGACGGGAGAAGATCCAGCAGCTAG
426      K  E  S  Q  A  Y  Y  D  G  R  R  S  S  S  *
```

Figure 9
tPrP DNA-sequence with in amino-acids translation from start to stop codon (bold); including poly-His-tag (yellow), Kräusslich linker (green) and 3F4-epitope tags (grey).

2.1.4.2 pVAX-mPrP and pVAX-tPrP for DNA vaccination

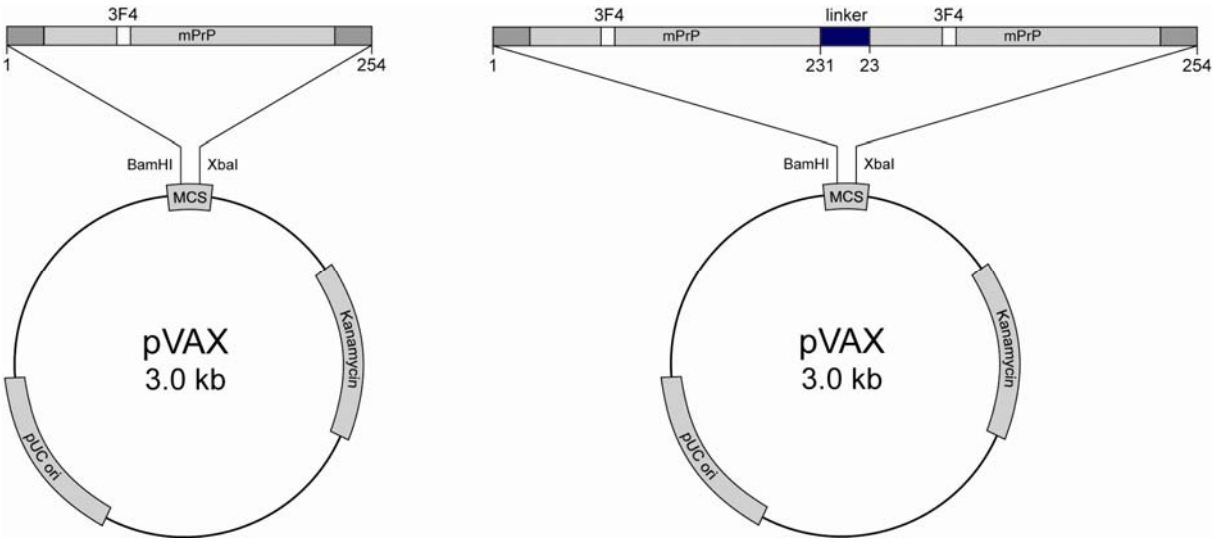

Figure 10
DNA vaccination vectors pVAX including mPrP and tPrP sequences bearing signal peptides at the flanking ends.

2.1.5 Animals

Female PrP wild-type (wt) mice were obtained from Janvier (Le Genest St. Isle, France). All animal experiments were in accordance with German animal experimentation regulations. NMRI mice are of *prnp*-A genotype as are e.g. CD1 and C57/Bl6 mice. All animal experiments were in accordance with German animal experimentation regulations.

2.2 Molecular Biological Methods

2.2.1 Agarose gel electrophoresis

Agarose was dissolved in TAE-buffer by boiling the mixture in a microwave. Thereby the percentage of agarose depended on the length of DNA fragments. The solution was cooled down to about 60°C and 1 µl ethidium bromide (1 mg/ml) was added per 50 ml gel solution before filling into the gel chamber. DNA samples were mixed with 5x DNA-Sample buffer prior to loading on the gel and run under constant 110 Volts with TAE-buffer. Ethidium bromide stained DNA was visualized with UV light and documented with an Eagle Eye. DNA fragments were isolated by cutting out the gel followed by GFX™ Purification Kit (GE-Healthcare, Freiburg, Germany) in accordance to the manufacturer instructions.

2.2.2 Preparation of chemically competent bacteria

XL1-Blue overnight culture was used to inoculate 100 ml fresh LB-medium and cultivated at 37°C under permanent shaking up to OD_{600} of 0.6-0.7. The culture was cooled on ice for 15 min. and centrifuged at 3000 g for 15 min. at 4°C. The pellet was suspended in 50 ml of pre-cooled sterile 100 mM $MgCl_2$ solution and incubated 30 min. on ice. After another centrifugation step bacteria were suspended in 50 ml ice-cold sterile 100 mM $CaCl_2$ solution and placed on ice for 30 min. followed by spinning down the cells again. Suspension in 2-5 ml 100 mM $CaCl_2$ solution followed by 24 h incubation at 4°C and addition of 2,5 ml ice-cold $CaCl_2$ solution and 0,5 ml glycerol. Bacteria were stored as 100 µl aliquots at -80°C.

2.2.3 Heat shock transformation

Heat shock DNA-transformations were done either with 50 µl BL21-Gold (DE3) pLysS competent bacteria (Stratagene, Amsterdam, Netherlands) or chemically competent *E.coli* XL1-Blue. Bacteria thawn on ice before plasmid DNA were added (0.5-1 µg) and incubated for 30 min. on ice. After 30-60 s heat shock at 42°C and 2 min. on ice 300 µl SOC-medium was added and incubated at 37°C stirring for 1 h. The bacteria were either transfered into 5 ml LB-medium and cultivated overnight at 37°C under permanent stirring or plated onto LB-agar plates each containing appropriate antibiotics.

2.2.4 DNA extraction and purification

Plasmid DNA in analytical amounts of 1-5 µg (e.g. sequencing) was isolated from 1 ml bacteria overnight culture with GFX Micro Plasmid Prep Kit (GE-Healthcare) according to the manufacturer instructions. Elution of DNA from the column matrix was done with 50-

100 µl sterile ddH_2O or TE-buffer. Higher DNA amounts (up to 15 mg) were isolated with Qiagen Maxi or Giga Prep Kits (Qiagen, Hilden, Germany) from 100-200 ml or 500-1000 ml bacteria culture respectively. Quantification was done by measuring OD_{260} values of eluted DNA. Thereby an OD_{260} value of 1 corresponds to a concentration of 50 µg/ml double stranded DNA. Evaluation of protein or RNA contamination was determined by the measurement of OD_{280}. An OD_{260}/OD_{280} ratio of around 1.8 indicated clean DNA preparations.

2.2.5 DNA digestion and ligation

Digestion of DNA was done with restriction enzymes from Roche and New England Biolabs with recommended buffers for 2-3 h at 37°C. Fragments were purified by agarose gel electrophoresis (2.2.1). Ligations were performed with Vector to insert ratios of 1:3 using the Quick Ligation Kit from Roche according to the manufacturer procedures.

2.2.6 DNA sequencing

DNA sequencings up to 800 bp were performed at GATC-Biotech, Freiburg, Germany from Plasmid DNA isolations in analytical scale with standard GATC primers or with individually designed primers obtained from Metabion, Martinsried, Germany.

2.3 Cell Biological Methods

2.3.1 Expression of recombinant protein

Murine PrP gene subunit for monomeric PrP was amplified by PCR as described before (Gilch et al., 2003). Tandem-PrP consists of two murine PrP sequences (aa 23-231), lacking the C- and N-terminal signal peptides, and covalently linked by a 7-amino acid linker (2.1.4.1). Each PrP moiety contains a 3F4 epitope tag. By cloning into bacterial expression vector pQE30 (Qiagen), an N-terminal poly-Histidine tag for purification was added. 50 µl BL21-Gold (DE3) pLysS competent bacteria were transformed with 0.35 µg pQE30-tPrP and 0.35 µg REP4 by heat shock (2.2.3) and cultivated overnight in Amp^+ Kan^+ LB-medium. Overnight pre-expression cultures were prepared by diluting either fresh transformation samples or earlier pre-cultures 1:500 with fresh LB Amp^+ Kan^+ LB-medium. Protein expression was done by 7-8 h cultivation at 37°C with 200 rpm of 1:20 diluted pre-culture in pre-warmed Amp^+ LB-medium (no addition of IPTG). After expression the cells were centrifuged 10 min. at 6000 g and stored either at -20°C overnight or -80°C for 2 h.

mPrP was expressed similar to tPrP supplemented by IPTG induction at OD_{600} value of 0.8 and decrease of cultivation time to 4-5 hours.

2.3.2 Cultivation of mammalian cells

Mammalian cells were cultivated in culture dishes (NUNC) in incubators with 90 % humidity, 5 % CO_2 and 37°C. Every two days Optimem medium was exchanged and not later than confluency cells were washed with PBS and Trypsin-EDTA was added to resolve cells from surface. After short incubation cells were suspended in fresh medium and passaged to new culture dish by adequate dilution.

2.4 Protein and Biochemical Methods

2.4.1 Recombinant PrP purification

For purification of 6xHis-tagged recombinant protein under denaturing conditions 3-4 ml of ProBond™ Nickel-Chelating Resin (Invitrogen) was prepared by washing twice with 10 ml ddH_2O and three times with Binding-Buffer by centrifugation for 2 min. at 900 rpm (Sigma centrifuge), subsequently removing supernatant. Bacteria pellet corresponding to 1 l expression culture was re-suspended in 15 ml of Lysis-Buffer and rotated in 50 ml Falcon tubes in a head-over-tail device at 4°C for 30-60 min. Supernatant was transferred to previously prepared resin after centrifugation at 6000 g for 30 min. 30 min. head-over-tail incubation at 4°C was followed by two washing steps with 10 ml Binding-Buffer and further 6 washings with 10 ml Washing-Buffer. Resin was transferred to empty columns and protein content in the supernatant was measured. When OD_{280} value turned below 0.06 compared to pure Washing-Buffer, Elution-Buffer was added and flow-through collected in 0.5-1 ml aliquots. Protein concentration was determined (2.4.3) and aliquots containing more than 0.5 mg/ml protein were pooled and stored at -20°C.

2.4.2 Refolding of recombinant proteins

Protein was refolded by dialysis against minimum of 1000 times volume of either ddH_2O or 10 mM NaAc buffer with varying pH values overnight at 4°C under permanent stirring with pre-cooled solutions. Dialyse-Cassettes of varying sizes (10.000 MWCO, Pierce, Rockfort, USA) were incubated for 1 min. in respective buffer prior to protein application.

2.4.3 Protein concentration measurement

Protein concentration was measured with the BCA-Kit (Pierce) according to the manufacturer instructions. 10 µl of sample was mixed with 200 µl of BCA-solution in a 96 well microtiter plate and incubated for 30 min. at 37°C before measuring OD_{405} in a Tecan-Reader. Protein concentrations were calculated in comparison to OD_{405} values of BSA standard curve (0.25-2 mg/ml) by Tecan-Software.

2.4.4 Solubility assay

Refolded protein samples were adjusted to final protein concentration of 1 mg/ml, mixed with respective CpG-ODN amounts, and analyzed by differential ultracentrifugation in a TL-100 ultracentrifuge (1 h at 100.000 g; TLA-45 rotor). Protein concentration of the supernatant was measured (2.4.3) and calculated in percentage of soluble control sample.

2.4.5 Preparation cell lysates

2.4.5.1 Bacteria lysates

Preparation of bacterial lysates for SDS-electrophoresis was done by 1 min. centrifugation of 1 ml culture followed by the addition of 2x Laemmli-buffer and incubation 5 min. at 95°C. Compensation of varying bacteria concentration was calculated with the formula:

$$X\ \mu l\ 2x\ SEB = OD_{600} \times 40$$

30 µl of the sample was used for acrylamide gels with Coomassie staining (2.4.8) and 10 µl for Western-Blot analysis (2.4.7).

2.4.5.2 Postnuclear lysates

Mammalian cells were washed with PBS twice before addition of 1 ml Lysisbuffer-WB. Incubation 10 min. at RT was followed by transfer of lysate into 1.5 ml Eppendorf tube and centrifugation of cell debris. Supernatant was pooled with 5 times volume of 100 % Methanol and protein precipitated by incubation at -20°C overnight. Samples were centrifuged 25 min. at 3500 rpm (Sigma), supernatant discarded and dried pellet suspended in TNE-buffer, volumes according to their size. Addition of appropriate 3x SDS-sample-buffer amounts and boiling at 95°C for 10 min. preceded loading to the gel.

2.4.5.3 Brain homogenate

1 ml of 10 % RML infected mouse brain homogenate (w/v) was centrifuged for 1 min. at full speed, the pellet suspended in 1 ml of Lysisbuffer WB followed by 10 min. of lysis at RT. Protein digestion was done for 30 min at 37°C after addition of 2 µl 1% Proteinase K (PK) to discriminate between PK sensitive PrP^{C} and partially resistant PrP^{Sc}. 40 µl PEFA Block solution (1%) was added to the supernatant after centrifugation for 1 min at full speed to block PK. The sample was mixed with 5 times volume of Methanol and further treated as described in 2.4.5.2.

2.4.6 SDS-Polyacrylamide Gel Electrophoresis (SDS-PAGE)

Denaturing SDS gels were made of a lower resolving and an upper stacking gel. After polymerization between glass plates the gels were connected to the electrophoresis chambers and filled with SDS electrophoresis buffer. Protein samples were added to respective pockets of the stacking gel. Proteins were separated according to their molecular weight by electrophoresis at 45 mA with constant voltage.

2.4.7 Western Blot

After separation with SDS-PAGE proteins were transferred to PVDF membrane (Hybond-P, GE-Healthcare) using semi-dry blotting. Three plies of Transfer-buffer soaked Whatman papers in the size of SDS gel were applied to the anode of blotting chamber followed by methanol activated and water equilibrated PVDF membrane. The gel was added and then covered by another layer of Whatman papers thereby preventing the formation of air bubbles between any of the layers. Blotting was performed with 2.5 mA/cm^2 for 45 min.. After blotting the membrane was incubated with 5 % (w/v) skim milk powder in TBST buffer for 30 min at RT under permanent shaking for saturation of unspecific binding sites. First antibody was diluted with TBST-buffer and incubated overnight at 4°C followed by washing 5 times for 5 min. each with TBST at RT. Horse-radish-peroxidase labeled secondary antibody was subsequently diluted in TBST and incubated for 45 min at RT followed by another washing. Documentation of specific protein-antibody complexes was done by incubating the membrane in ECL^+ Detection Reagent (GE-Healthcare) for 2 min., drying with Whatman paper and exposing to X-ray film (Kodak Optimax, GE-Healthcare) for suitable duration. Finally, films were developed with Typon Optimax X-Ray Filmdeveloper.

2.4.8 Coomassie staining

SDS-Polyacrylamide gels were incubated in Coomassie staining solution for 30-60 min. at RT under permanent shaking. Afterwards the gel was washed for several hours by permanent shaking and multiple exchanges of de-staining solution. Gels were dried with gel drier on Whatman paper for documentation.

2.4.9 Atomic force microscopy

Protein samples for atomic force microscopy (AFM) were refolded and diluted to a concentration of 0.1 mg/ml with respective dialysis buffer. Samples were mixed with CpG-ODN to a final concentration of 100 µM and immediately placed on freshly cleaved mica attached to AFM sample discs (Ted Pella, Redding, USA). After 3 min of adsorption at 25°C, the discs were washed 5 times with ddH_2O before allowing to air dry. Contact mode imaging was performed on a multimode scanning probe microscope (Veeco, Mannheim, Germany) by using silicon nitride probes (type DNP-S20, Veeco NanoProbe Tips; spring constant k=0.06 N/m). Measurements were done at the Institute of Biotechnology, Technical University of Munich with kind help of Simone Hess.

2.4.10 Fourier transformation infrared spectroscopy (FTIR)

tPrP was refolded either with 10 mM NaAc, pH 4.5, or ddH_2O overnight followed by desalting with G25 MicroSpin^{TM} devices (GE Healthcare, Munich, Germany) against Acetate Na/D_2O (pD 4.1) or D_2O, respectively. The protein concentrations were 6 mg/ml. FTIR spectra were recorded at the Unité de Virologie et Immunologie Moléculaires, Biologie Physico-chimique des Prions (BPCP), France with a Jasco 810 infrared spectrometer equipped with a thermostated cell-holder. Each spectrum was an overage of 20 scans with a 4 cm^{-1} resolution. The spectrum deconvolution was made using homemade software.

2.4.11 Size exclusion chromatography

Size exclusion chromatography (SEC) was done with Åkta FPLC chromatography equipment (GE-Healthcare) and a 7 mm x 600 mm gel filtration column TSK 4000SW (Interchim, Montlucon Cedex, France) at the Unité de Virologie et Immunologie Moléculaires, Biologie Physico-chimique des Prions (BPCP). Before use, the column was calibrated for molecular mass and Stokes radius with low and high molecular mass calibration kits (GE-Healthcare). Previously to each measurement, the column was equilibrated with a minimum of four column volumes of elution buffer. Flow rate was 1 ml/minute at 20°C; protein elution was monitored with UV-absorption at 280 nm.

2.5 Immunological Methods

2.5.1 Preparation of microspheres

Microspheres were prepared using solvent/evaporation technique (Lima et al., 2003). 200 mg of PLG-resomer was emulsified in 15 ml methylene chloride with 200 µl antigen/CpG-ODN solution (5-30mg of protein) at high speed using IKA homogenizer. This primary organic phase was then mixed with 50 ml of an aqueous phase containing 3% polyvinyl alcohol followed by stirring at RT for 4-5 h, allowing the methylene chloride to evaporate.

2.5.2 Preparation microspheres for DNA vaccination

Full-length murine PrP DNA sequence was obtained by subcloning from a vector construct using restriction enzymes XbaI and PstI. Tandem-PrP sequence bearing 3F4 tags and flanked by signal peptides (1-231-linker-23-254) was subcloned using BamHI and XbaI. Both constructs were ligated into the DNA vaccination vector pVAX (2.1.4.2) and 10-15 mg each with concentration of 15-20 mg/ml were purified with QIAGEN Plasmid Giga Kit before co-encapsulation with CpG-ODN into microspheres (2.5.1).

2.5.3 Antibody titers

96 well plates were coated with 150 µl sodium-carbonate buffer (0.1 M, pH 9.5) containing 1 µg of NaAc dialysed mPrP or tPrP and incubated overnight at room temperature. After washing 6 times with PBST (PBS, 1 % Tween), the plates were blocked for a minimum of 2 h with 150 µl PBST, 3 % bovine serum albumin, at 37°C. Sera of mice were diluted (as indicated) in PBST with 3 % serum albumin and 100 µl per well was incubated for 1 h at 37°C. After washing 6 times with PBST (300 µl in a Tecan plate washer), plates were incubated with 1:4.000 diluted horseradish peroxidase (HRP) labelled anti-mouse-IgG antibody (GE-Healthcare) for 1 h at 37°C. The plates were washed again and incubated with 100 µl ABTS solution (2,2'-Azino-bis(3-Ethylbenzthiazoline-6-Sulfonic Acid, Sigma). After 10 minutes at 25°C, the OD_{405} was measured (Tecan plate reader, Crailsheim, Germany). Cut-off was defined as three times the OD_{405} value of 1:100 diluted pre-immune serum of respective mice.

2.5.4 Antibody isotyping

Antibody isotyping was done with the same plate preparation as described for titer evaluation (2.5.3). Sera were diluted 1:100 and incubated with 1:4.000 dilution of biotin labeled secondary antibody for 45 minutes (IgG1, IgG2a, IgG2b, IgG3, IgA, IgM). After washing,

wells were incubated with HRP-labeled streptavidin with a 1:1.000 diluted for 30 minutes. The final wash was followed by 10 minute incubation with ABTS solution and measurement of OD_{405}.

2.5.5 FACS surface staining

Murine neuroblastoma cells overexpressing PrP (N2awt) were used for surface staining. The cells were singularized by 10 min. incubation with 10 ml PBS containing 1 mM EDTA per 10 cm plate at RT and 1 ml aliquots were transferred to FACS tubes. Equilibration of 15 min. with FACS buffer was followed by centrifugation (2 min. 1200 rpm; Sigma) and 45 min. incubation with 100 µl serum dilution (1:10 in FACS buffer). PrP control antibody 4H11 was diluted 1:100. Cells were washed 3 times with FACS buffer and then incubated with FITC-labeled anti mouse IgG secondary antibody for 45 min. After another washing step the stained cells were suspended in FACS buffer with addition of 7-AAD to exclude dead cells and measured with a flow cytometer.

2.5.6 Epitope mapping

For epitope mapping a peptide bank encompassing the mature full length murine PrP consisting of 20 residues with an overlap of 5 residues was used (PrP 23-231; depicted in Fig. 2C). Peptide 6 encompasses the 3F4 epitope, peptide 6b represents the corresponding wild-type murine sequence. The poly-histidine (MRG SHH HHH HGS CKK RPK PG) and linker region (DGR RSS AGA IGG AKK RPK P) of tPrP was used in addition. As full length protein control monomeric non-tagged PrP and tPrP were employed. Polyclonal antibody A7 was obtained by tPrP immunization in rabbit (Gilch et al., 2003). CovaLink NH microtiter plates (Nunc, Wiesbaden, Germany) were activated with the bifunctional linker DSS in carbonate buffer and incubated with peptide or recombinant protein, respectively, overnight at room temperature. The coated plates were blocked and incubated with pre-diluted sera, washed and incubated with corresponding HRP-labeled conjugate. Upon washing and incubation with ABTS solution, OD_{405} was measured and documented by scanning or digital photography.

2.5.7 Cytokine assay

Spleens of individual mice were harvested, isolated with a 100 µm cell strainer mesh (Becton Dickinson, Heidelberg, Germany), and individually analyzed. Lysis of erythrocytes was achieved by incubation with NH_4Cl (0.15 M, pH 7.4) for 7 minutes at 25°C followed by

filtration with 100 µm mesh. 2 x 10^7 cells in 2 ml RPMI medium, containing 5 % fetal calf serum and penicillin/streptomycin, were plated in 12 well plates and re-stimulated for 16 h either with 20 µg of freshly refolded tPrP or mock treated at 37°C. Control cells were treated with PMA/Ionomycin (25 ng/ml, 1 µg/ml respectively) for 6 h. 2 µl Golgi plug (BD) were added per 3 hours before addition of EMA solution (1 µl EMA, 10 µl anti-mouse CD16/CD32 (Fc-Block, BD) per ml wash-buffer (PBS with 2.5 % FCS)). Incubation on ice with strong light for 20 minutes was followed by transfer and separation into 96 well plates. After washing three times with 300 µl wash-buffer cells were surface stained with 1:100 dilution of PE-Cy5-CD4 and PE-CD8 antibodies (BD) in wash-buffer for 20 min. Washing was performed in accordance to the manufacturer's instructions. α-IFNγ-FITC or FITC labeled isotype antibody, were diluted 1:500 in Permwash-buffer and incubated 30 min before final washing. Samples were dissolved in PBS 1 % PFA. Samples were measured with a Beckman Coulter Epics XL flow cytometer (Beckman Coulter, Krefeld, Germany); resulting data were analyzed by EXPO 32 software.

2.6 Animal experiments

2.6.1 Immunization

NMRI mice were immunized with 100 µl containing 1 mg/ml freshly dialysed protein, CpG 1826 was added directly before administration to a final concentration of 100 µM. Injections were given in two or more portions subcutaneously (s.c.) into the dorsal region. Three boost injections were administered every three weeks. Blood samples and organs were taken 10-21 days after the final boost. For microsphere immunization, 5 mg of the respective PLGA-MS were diluted in PBS and injected subcutaneously into the tail base in 4 week intervals, a total of 4 injections. DNA-vaccination was performed by intramuscular (i.m.) application of PBS diluted PLGA-MS in two 50 µl portions.

2.6.2 Long term animal infection trial

Infection animal trial was performed in the laboratories of the Friedrich-Löffler-Institute on the Isle of Riems in cooperation with Prof. Martin Groschup and Fabienne Leidel. C57Bl/6 mice were immunized as described in 2.6.1 and additionally obtained several boost injections after i.p. inoculation with 100 µl 0.1 % RML infected mouse brain, corresponding to 10^4 LD_{50}. Figure 11 summarizes all injections in a timeline. Various vaccination groups with bare protein (Figure 11) and microsphere encapsulating antigen and/or CpG-ODN (Table 6) were prepared and partially supplemented by intra peritoneal application of 1 mg tolerance breaker antibody OX86 (200 µl; 0,5 mg/ml) in parallel to initial immunizations.

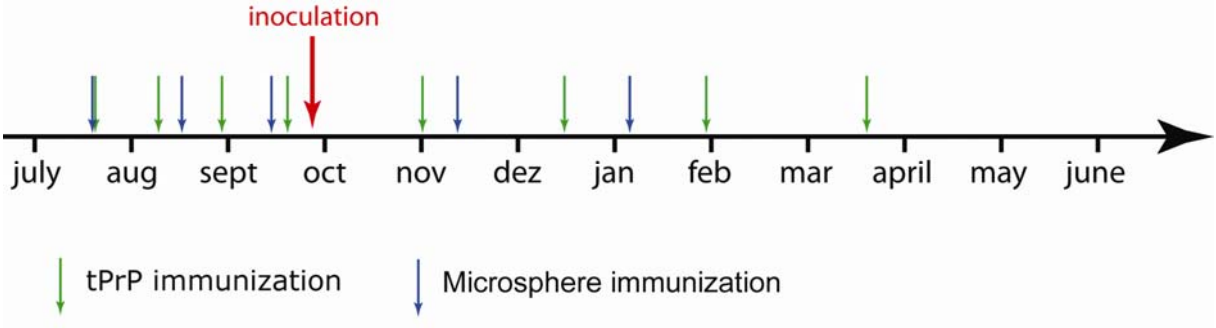

Figure 11
Timescale shows all immunizations and time of inoculation from animal infection trial. Protein immunizations are marked with green, MS applications with blue and prion inoculation by a red arrow.

Table 5
Protein based vaccination groups.

No. of animals	tPrP	CpG	tolerance breaker
40	+	+	+
10	+	+	∅
10	+	∅	+
10	∅	+	+

Table 6
Microsphere encapsulated antigen/adjuvant immunization groups.

No. of animals	Antigen	tolerance breaker
20	MS (tPrP+CpG)	+
10	MS (tPrP+CpG)	∅
10	MS (tPrP) + MS (CpG)	+
10	MS (tPrP) + MS (CpG)	∅
10	MS (tPrP)	+

2.7 Histological Methods

2.7.1 H&E staining

The brain, spleen, mesenterial lymph nodes, small and large intestine were explanted and immediately fixed in Roti-Histofix (Roth, Karlsruhe,Germany) and embedded in paraffin for histological examination. Three to five mm thick sections were cut and stained with haematoxylin and eosin (H&E). Histological samples were prepared and analysed at the Institute of Pathology at GSF-National Research Center for Environment and Health (Neuherberg, Germany) by Leticia Quintanilla-Martinez.

2.7.2 Electron microscopy

Kidney tissue was immediately fixed in 3 % glutaraldehyde for 2-5 h followed by dehydration by incubation with increasing ethanol concentration. The samples were embeded into Epon blocks and cuttet to 70-80 nm thick sliced using an Ultramicrotom. After contrasting with 0.5 % uranylacetat and 3 % Pb-citrate the tissue was examined by transmission electron microscope at the Institute of Pathology at GSF-National Research Center for Environment and Health (Neuherberg, Germany) with the help of Luise Jennen.

3 Results

3.1 Expression and purification of tPrP

3.1.1 Expression

Expression of tPrP was done with very robust *E.coli* strain BL21 (DE3) gold Lys to prevent losses in the rate of yield due to toxicity of the product. Furthermore several conditions of expression were tested to maximize protein production. Figure 12 shows examples of differences in the growth behavior and the state of tPrP after induction with IPTG or not. The growth curve clearly displays the inhibitory effect of IPTG on the growth of bacteria under these conditions. In addition the protein profile in poly-His-tag immunoblot revealed multiband pattern suggesting partial destruction of tPrP. In contrast non induced cells with Ampicillin only included in the expression medium showed an increase of growth up to 7 hours of cultivation without any detectable disintegration of protein product in the immunoblot. In the course of high yield tPrP production LB Amp^+ medium was used for expression without IPTG induction and a cultivation time of 6-8 hours.

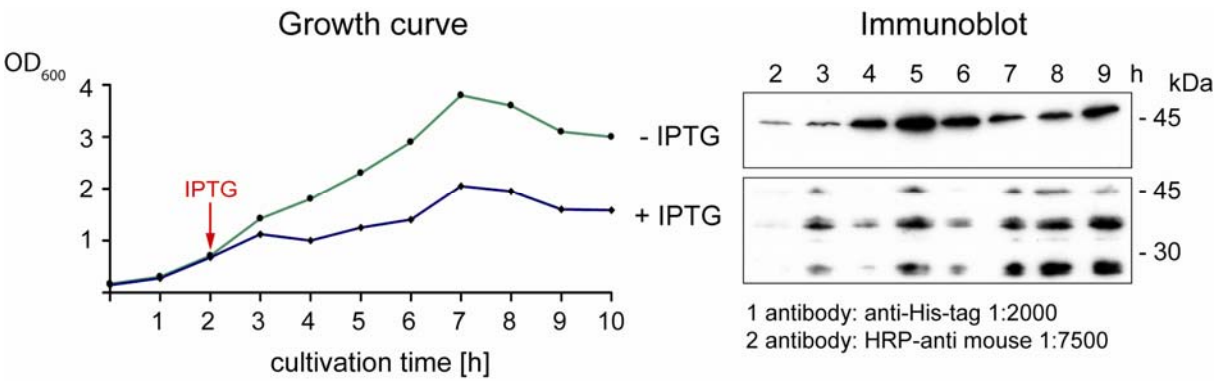

Figure 12
tPrP expression displayed by growth curves and anti-His Immunoblots. For WB analysis protein concentrations were normalized by including OD_{600} values.

3.1.2 Purification

Control and optimization of tPrP purification was done by collecting several samples during procedure and analyzed by Coomassie stained acrylamide gel and PrP specific Western-Blot analysis (Figure 13). The efficacy of cell lysis was demonstrated by the majority of tPrP found in the supernatant compared to much less recombinant protein in the pellet fraction of the lysate. Furthermore the decrease of the tPrP after Resin incubation indicated the efficient binding of 6xHis tagged protein to the Nickel Chelating Resin. Washing with Binding-Buffer removed unspecific proteins of the lysate exclusively, whereas Washing-Buffer, containing 80 mM imidazole, additionally rinsed some tPrP from the Resin also. Analysis of tPrP Elution showed a protein purity of approximately 98 %. The yield of recombinant tPrP was about 1-3 mg per litre expression medium.

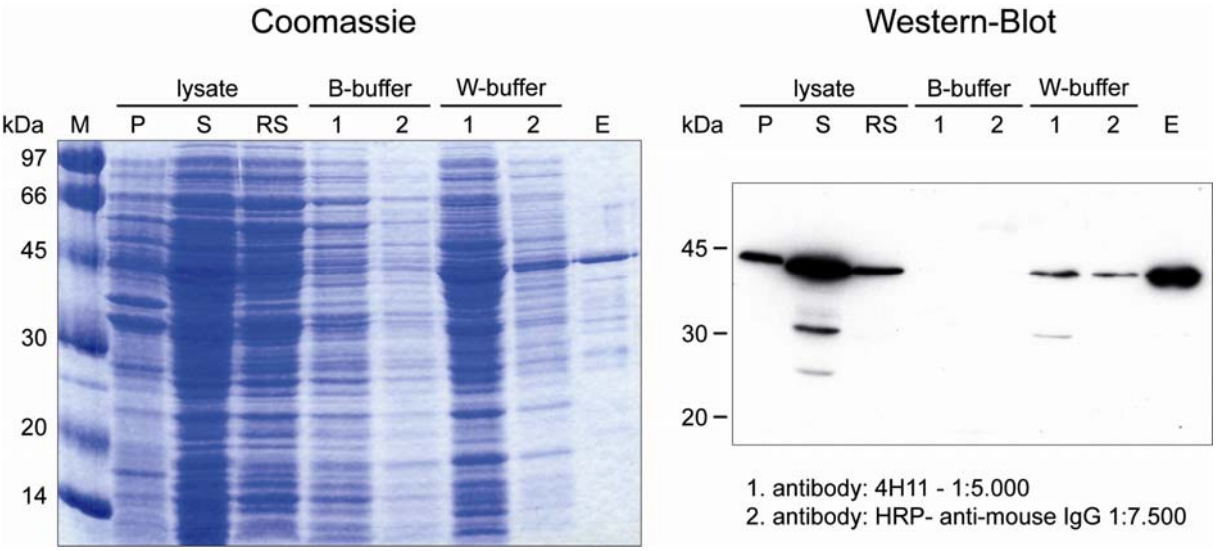

Figure 13
Analysis of tPrP purification samples by Coomassie stained acrylamid-gel and tPrP specific Western-Blot. (M-protein size standard; P-pellet after lysis; S-supernatant after lysis; RS-supernatant after resin incubation; E-elution)

3.2 Biochemical features of recombinant tPrP antigen

3.2.1 Solubility of tPrP

tPrP was expressed in *E.coli* and purified under denaturing conditions, thus refolding into a structured protein was required for further use as immunogen. tPrP solubility was tested by differential ultracentrifugation after dialysis in 10 mM NaAc buffers of varying pH-values (2.4.2). Both pellet and supernatant fractions were examined by Immunoblot using PrP specific antibody 4H11 (Figure 14). pH-values from 1-5 led to mainly soluble tPrP, indicated by strong bands in the supernatant, but not in the pellet fraction. In contrast, refolding in buffer with pH-values of 6-10 resulted in almost complete precipitation of proteins, at least with NaAc buffer if this concentration was used.

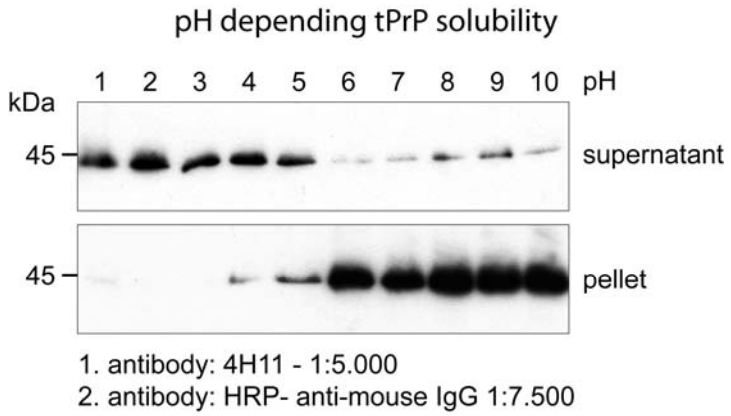

Figure 14
Western blot analysis of tPrP samples refolded in NaAc-buffer of varying pH-values. Solubility was examined by differential ultra-centrifugation followed by determine tPrP amounts contained in the supernatant and pellet fraction.

3.2.2 Structural features of recombinant PrP

Analysis of structural features was done by FTIR as also precipitated protein can be measured with this method. Figure 15 shows FTIR spectra from measurements of different proteins and preparations, including deconvolution. α-helical structure is characterized by a peak at 1651 cm^{-1} (in blue) and β-sheet content by a peak at 1619 cm^{-1} (in red); percentage rates are indicated in respective figures. Monomeric recombinant PrP, confirming previous CD measurements, contained mainly α-helical structure after refolding (α-helix: 41 %; β-sheet: 5 %). In contrast, tPrP showed the formation of mainly β-sheet structure with both

dialysis buffers. tPrP (NaAc) revealed a higher β-sheet content (α-helix: 15 %; β-sheet: 37 %) compared to tPrP (H_2O) (α-helix: 18 %; β-sheet: 25 %).

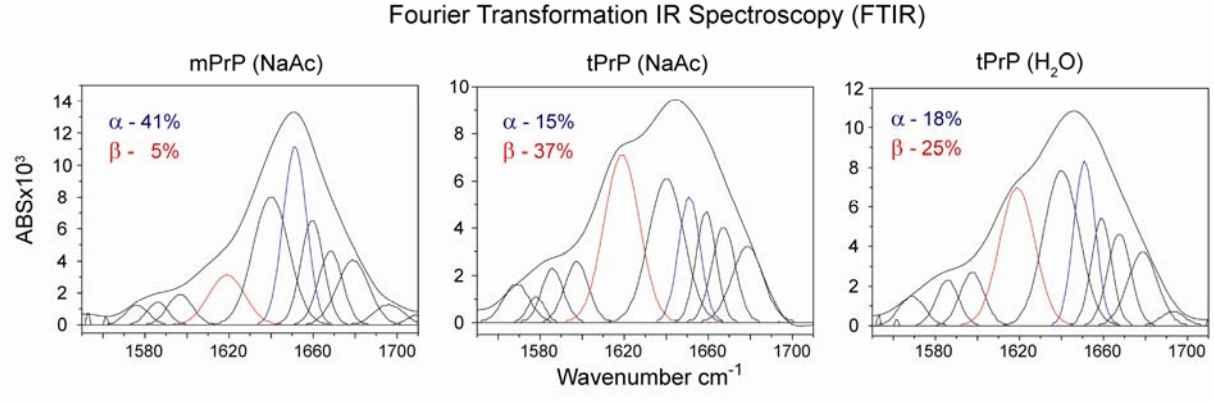

Figure 15
FTIR spectra, including deconvolution, revealed structural differences between the antigens, indicated by the percentages of α-helix (blue) and β-sheet (red) content. Monomeric recombinant PrP consisted mainly of α-helix after NaAc dialysis. In contrast, tPrP was mainly β-sheeted after both dialysis conditions.

3.2.3 Influence of ionic strength on aggregation state of tPrP

Size exclusion chromatography was used to study the aggregation state of tPrP depending on ionic strength. Under low ionic strength buffer conditions, comparable to our sodium acetate dialysis buffer, tPrP was found mainly in a monomeric state. In contrast, high ionic strength, corresponding to conditions after injection into mice, showed significant oligomerization.

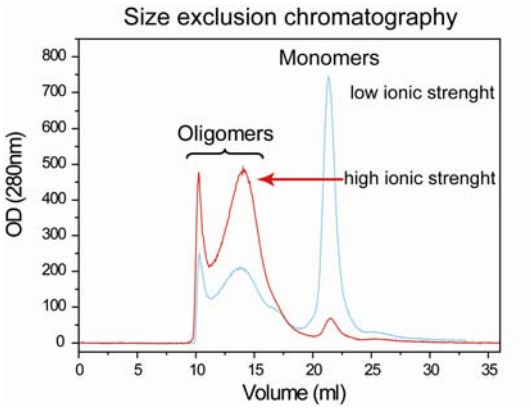

Figure 16
Overlay of size exclusion chromatography measurements with either low (blue) or high ionic strength (red) conditions at neutral pH.

3.2.4 Interaction with CpG

As expected from the solubility experiments, dialysis with 10 mM NaAc, pH 4.5 led to no visible precipitation. In contrast, refolding with pre-cooled ddH_2O resulted in a cloudy solution, indicating partial precipitation of the tPrP. Solubility of protein was therefore quantified by differential ultracentrifugation (2.4.4) combined with protein concentration measurements (2.4.3) of the supernatant and is shown as percentage of originally applied amount of protein (Figure 17). Under these conditions, tPrP (NaAc) was completely and tPrP (H_2O) ~70% soluble. Interestingly, mixing of refolded protein with adjuvant CpG-ODN led to very substantial and immediate precipitation. Virtually all tPrP (NaAc) precipitated after addition of 5 or 10 nmol CpG, whereas 28% and 23% tPrP (H_2O) remained soluble, respectively (Figure 17).

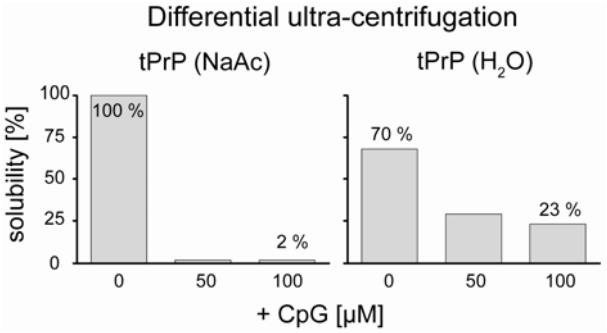

Figure 17
Solubility of tPrP after dialysis against ddH_2O or sodium acetate buffer, mixed with increasing amounts of CpG-ODN. The soluble tPrP fraction was determined by protein concentration measurement in the supernatant fraction after differential ultracentrifugation. Data are shown as percentage rate of original total tPrP amount (1 mg/ml).

To gain further insight into the aggregation behavior of tPrP in the presence or absence of CpG we applied atomic force microscopy (Figure 18). Without CpG, AFM revealed no obvious difference between tPrP (H_2O) and tPrP (NaAc) in structural appearance. Evenly widespread, unstructured proteins are visible in both preparations. In contrast, protein CpG mixtures showed the formation of two different types of aggregates. Canyon-like structures were of two-dimensional appearance and seemed to consist of smaller aggregates gathered in bigger groups. The second type of aggregate appeared as three-dimensional clumps in tPrP (NaAc) preparations, and smaller and less frequently in tPrP (H_2O) samples, indicating unstructured, oligomeric aggregates.

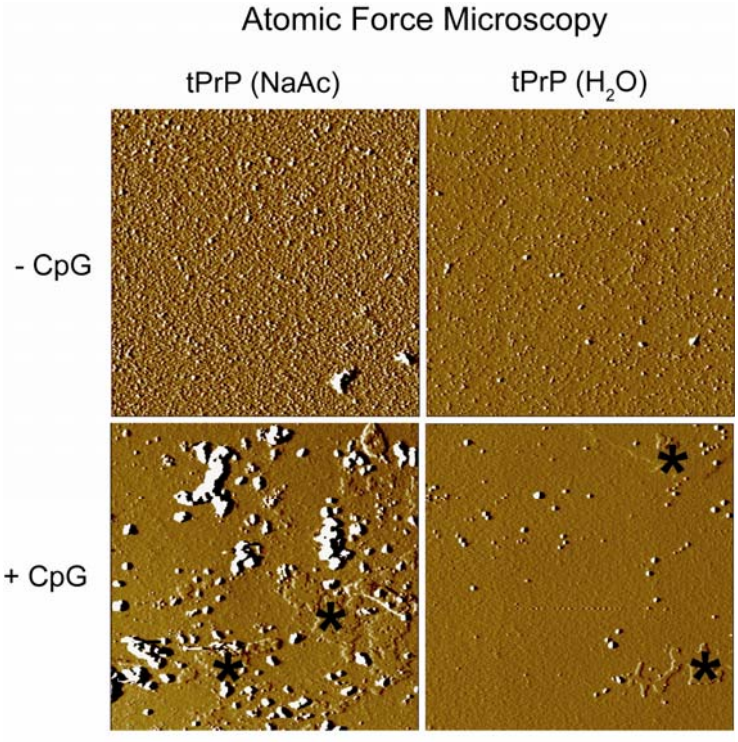

Figure 18
Atomic force microscopy images of differently refolded tPrP (0.1 mg/ml) in combination with or without 100 µM CpG-ODN (*-canyon like structures).

3.2.5 Aging of refolded tPrP

Refolded tPrP visually appeared to precipitate after storage of several months at +4°C. This aging effect was further quantified by monitoring the solubility of freshly dialysed and long term stored tPrP by differential ultracentrifugation and PrP specific immunoblot. As found before, tPrP freshly refolded in 10 mM NaAc pH 4.5 was found mainly in the supernatant fraction indicating its almost complete solubility. In contrast "aged" tPrP was found predominantly in the pellet fraction which suggests the change into insoluble protein. This feature is of fundamental importance concerning tPrP immunogenicity, as previous studies demonstrated the lack of immune response after immunization with aged tPrP.

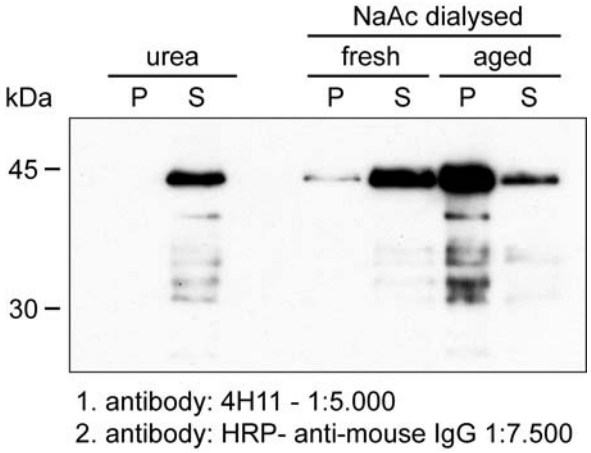

Figure 19
Solubility of tPrP after long term storage was monitored by presence in pellet and supernatant fractions after differential ultracentrifugation. Denatured protein in 8 M urea buffer was compared with freshly dialysed and aged tPrP.

Taken together, the biochemical characterization clearly shows the formation of mainly β-sheets for refolded tPrP, in contrast to high α-helical content in mPrP. Furthermore, solubility and conformation of recombinant tPrP is influenced by refolding conditions like the type of buffer, pH-value and storage after refolding. Ionic strength and interactions with CpG adjuvant can have great influence on the structure and thereby likely on the immunogenicity of tPrP antigen.

3.3 Immune responses after tPrP protein immunization

3.3.1 Humoral response (antibody titers)

Having found that various conditions significantly affected the biochemical properties of tPrP antigen, the next question was whether this is reflected by variations in humoral immune response *in vivo*. Therefore, PrP wild-type mice were immunized subcutaneously with NaAc or H_2O-dialysed recombinant tPrP and CpG-ODN four times in 21 day intervals. Blood was taken 10-21 days after final boost and antibody titers, specificity, isotypes and linear epitopes were measured. Final sera of immunized mice were examined in a recPrP-specific endpoint titration ELISA assay (2.5.3). Three times OD value of 1:100 diluted pre-immune sera of respective mice was defined as cut-off. Coating plates with either mPrP or tPrP revealed no considerable differences in OD values (data not shown). Figure 20 shows the endpoint titers of individual mice of three immunization groups. None of the CpG only treated mice displayed a titer, whereas 3 of 12 tPrP (NaAc) treated mice clearly showed auto-antibody titers. Of note, in the group of tPrP (H_2O) immunized mice 8 of 12 mice exhibited anti-PrP antibodies. However, the mean titer values between the 2 groups did not significantly differ.

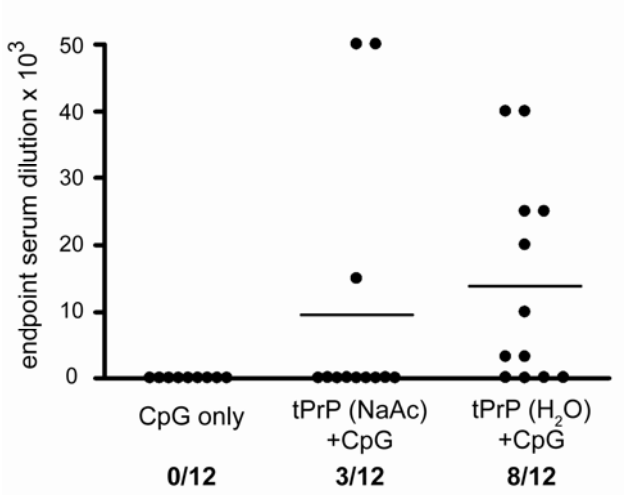

Figure 20
B cells respond to immunization with rec. tPrP and CpG-ODN depending on the refolding conditions. Endpoint dilution ELISA of final sera from individual mice are shown as dots, lines indicate the mean values. Plates were coated with tPrP; the cut-off was defined as 3 x OD_{405} value of a 1:100 dilution from pre-immune sera of respective mice

3.3.2 Linear epitope mapping

Differences in the quality of humoral response were analyzed by linear epitope mapping (2.5.5). The complete bank of covalently linked peptides is shown in Figure 21 A. A scheme of coating and digital images of selected epitope measurements including polyclonal tPrP control antibody A7 from rabbit are displayed in Figure 21 B. In mice antibodies are mainly reactive against epitope 10 and several N-terminal epitopes, confirming previous results (Gilch et al., 2003).

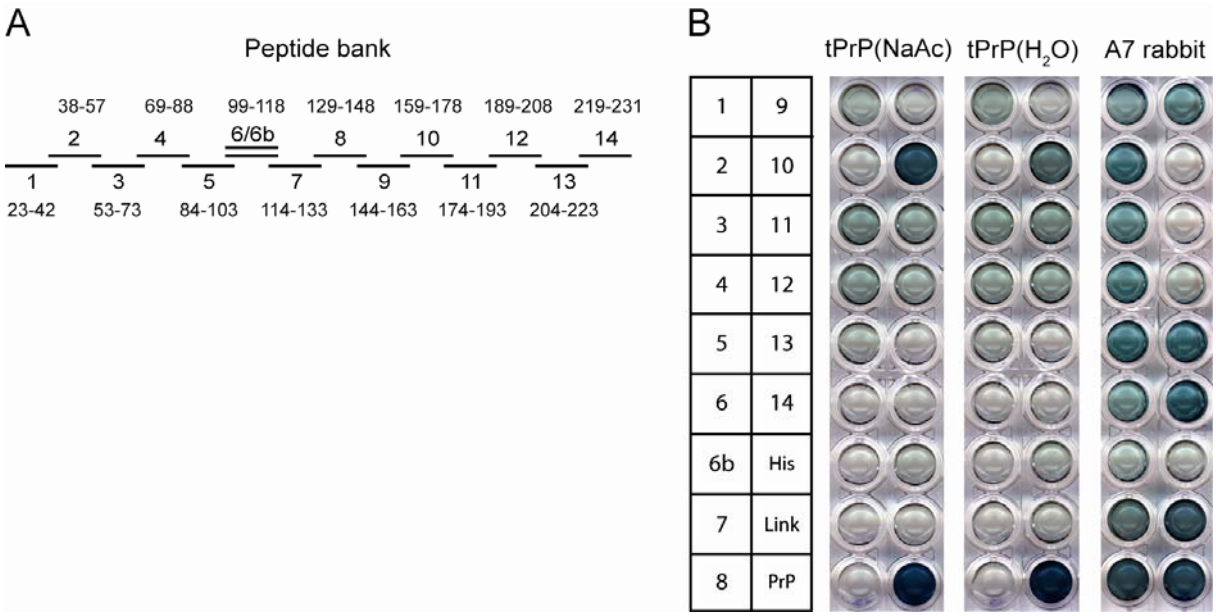

Figure 21
Linear epitope mapping of final titer positive sera showed no severe differences in antibody specificity to linear PrP epitopes between immunization groups. Peptides were covalently linked to CovaLink plates including a DSS linker. Peptide bank with respective numbering is shown **(A)**. Selected epitope measurements of each group and for rabbit control serum A7 are illustrated as digital images including a scheme of coated peptides **(B)**.

Epitopes were quantified by assembly of OD values displayed as mean values for both immunization groups and control antibody A7 (Figure 22). All titer positive sera were mapped, whereas tPrP (NaAc) samples (n=3) were measured as duplicates. Cut-off, indicated by a horizontal line at OD 0.2, was defined by three times OD value without incubation of first antibody. Control antibody A7 revealed signals to all epitopes except 10-12, including linker region. Within immunization groups, some weak N-terminal epitopes and the very prominent epitope 10 corresponding to amino acids 159-178 of PrP were found.

Neither reactivity against epitope 6 representing 3F4 epitope-tag sequence contained in tPrP used for immunization here, nor against the respective wild type epitope 6 was found. In

addition, no binding to potential His-tag or linker peptide epitopes was detected. We did not find any differences in signal intensity between microtiterplates coated with recombinant monomeric full length PrP without tags and tPrP controls. Here, full length protein control non-tagged monomeric recPrP (23-231) was used showing no differences in signal intensity compared to tPrP

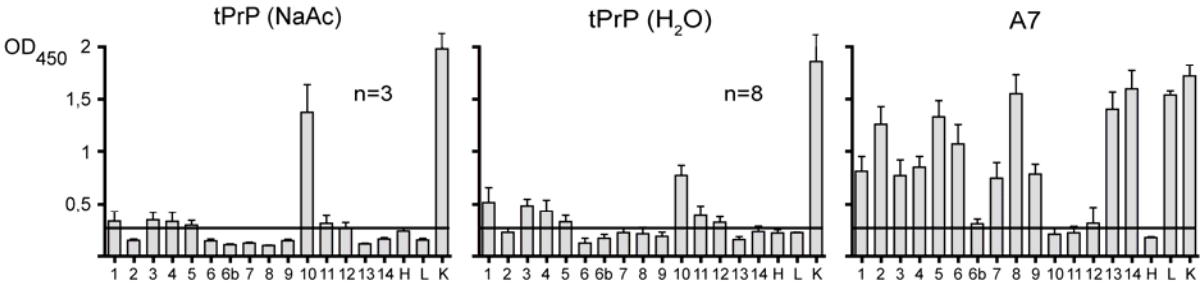

Figure 22
Quantification of epitope-mapping displayed as mean OD-values of both tPrP immunization groups and polyclonal rabbit serum A7.

3.3.3 Antibody specificity

As binding of antibodies to plastic coated proteins is critically discussed, the specificity of immune sera to PrP was further evaluated by Western-Stripe-Blot with N2a cell lysate (PrP^{C}) or proteinase K treated brain homogenate (PrP^{Sc}). Some of the examined sera indicated specific binding to PrP^{C} (Figure 23), whereas none of the sera showed binding to PrP^{Sc}, even under this denaturing condition.

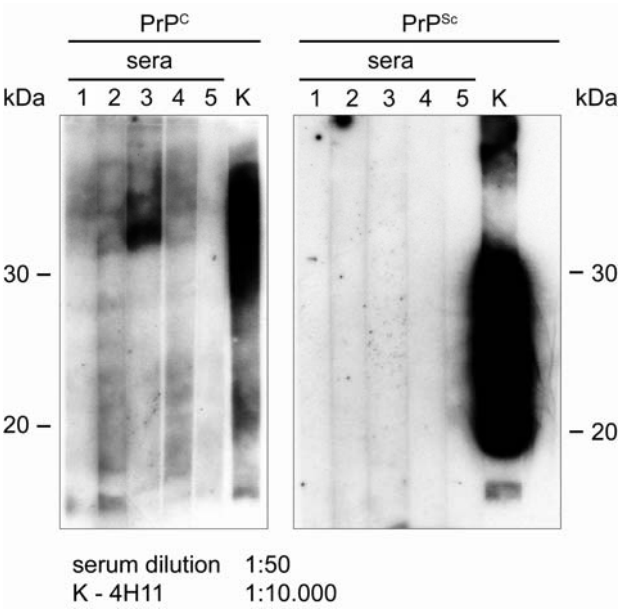

Figure 23

Western-Stripe-Blot with N2a lysate (PrP^{C}) or PK treated brain homogenate (PrP^{Sc}). Final Immune-sera were incubated in 1:50 dilutions, PrP specific antibody 4H11 was used 1:10.000.
In addition surface staining of PrP expressing N2a cells was performed to examine the ability of sera to bind native, structured PrP^{C}. Fluorescently labeled cells were analyzed by flow-cytometry and indicated specific binding by an increased fluorescence intensity of some sera compared to their respective pre-immune sera (Figure 24 A). A variety of control experiments was done which did not yield in clear-cut results supporting this assumption (Figure 24 B; PIPLC digestions, pre-incubation of sera with recombinant tPrP; data not shown).

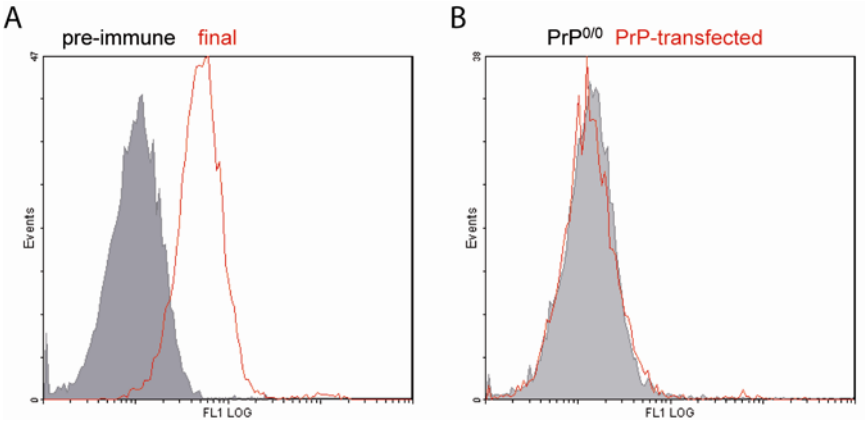

Figure 24
FACS histograms of surface stained N2a cell show an increase fluorescent intensity of final immune sera compared to respective pre-immune sera **(A)**. PrP-transfected $PrP^{0/0}$ did not show an increased fluorescent intensity after incubation with the same serum **(B)**.

3.3.4 Antibody isotyping

Isotyping experiments with all titer-positive sera showed no differences between the two protein preparation groups and revealed the presence of mainly IgG1, IgG2a and IgG2b, but not of IgG3, IgA or IgM antibodies (Figure 25).

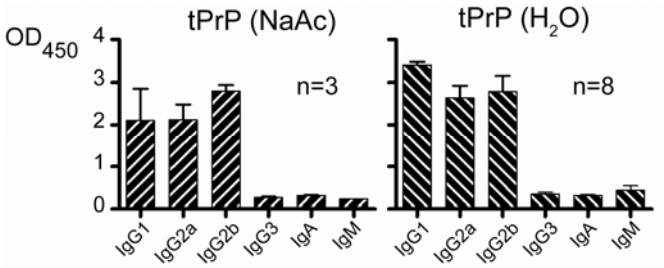

Figure 25
Antibody sub-typing was performed from individual titer positive sera. The mean OD_{450} values of the groups of 3 tPrP (NaAc) or 8 tPrP (H_2O) treated mice are shown.

3.3.5 T-cell responses

T-cell responses were analyzed upon immunization with tPrP + CpG-ODN and checked whether antigen preparation influences the response, similarly to the differences in B-cells. Therefore, spleen cells of individual mice were harvested and re-stimulated with tPrP or not. Cells were CD4 and CD8 surface labeled to distinguish T-cell subpopulations and stained for intracellular IFNγ. Figure 26 shows the percentage rates of IFNγ expressing $CD4^+$ splenocytes from all individual mice; horizontal lines indicate the mean values of groups. Two mice of the tPrP (NaAc) group responded with a well defined IFNγ expression, whereas the others showed only a weak increase.

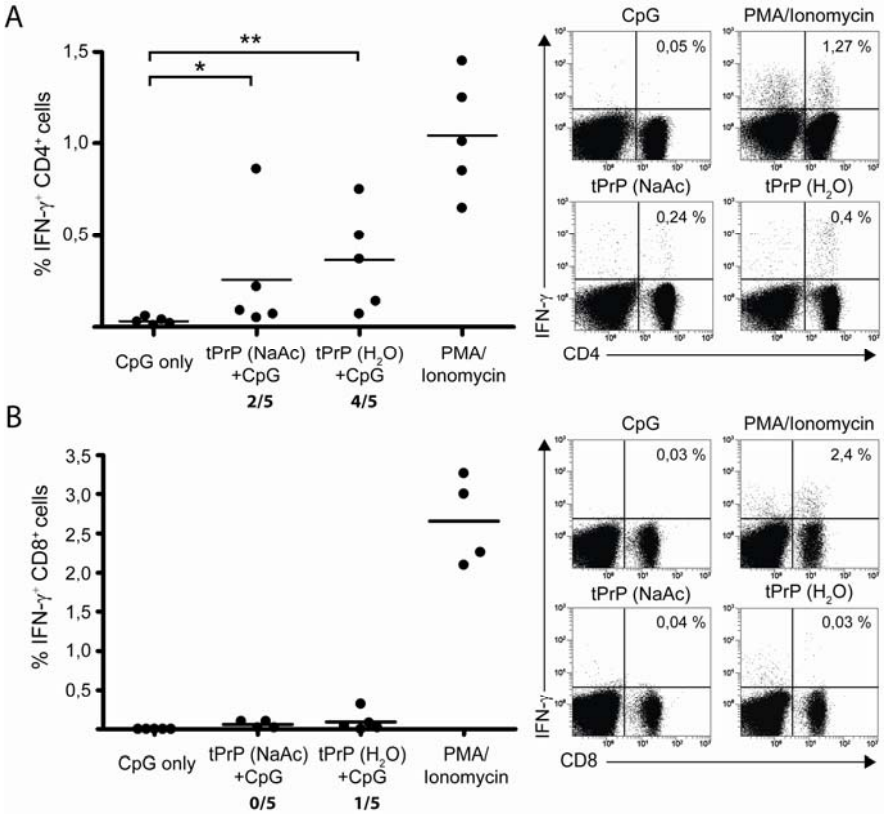

Figure 26
T-cell responses after immunization with tPrP and CpG-ODN determined by intracellular IFNγ staining of *in vitro* re-stimulated splenocytes. **(A)** The scatter blot illustrates the percentages of $CD4^+$ splenocytes expressing IFNγ, sorted by immunization groups. Each spot represents the result of an individual mouse; the mean values are displayed by horizontal lines. Exemplary dot blots from FACS measurements are shown for each group. **(B)** Same design as in (A), but with $CD8^+$surface staining.

Overall, the results were statistically significant compared to the CpG only control group (p=0.0159, Mann-Whitney-Test). Within the tPrP (H_2O) group, 4 of 5 animals clearly responded with even higher IFNγ mean values, thus leading to very significant increase compared to the control group (p=0.0079). From $CD8^+$ T-cell subpopulation only one mouse out of the tPrP (H_2O) group responded with a slightly increased IFNγ expression, not leading to significant mean value (Figure 26 B). Exemplary results of FACS measurements are shown as dot blot analysis of $CD4^+$ or $CD8^+$ T-cells (Figure 26 A, B; right panels).

Taken together, our data show that a significant T-cell response is induced upon immunization with both tPrP preparations. The intensity of response seems to depend on the preparation of antigen very slightly and to a lesser extend as compared to B-cell reactions.

3.4 Immune response after microsphere immunization

Encouraged by the promising T-cell responses found in some individual mice we tried to increase this effect by encapsulation of immunogens in PLGA-MS. We used two different PLGA-MS preparations for our immunization trials. PLGA-MS containing either tPrP or CpG-DNA exclusively were mixed together and applied to mice s.c. at the tail base. To the other PLGA-MS co-encapsulating both protein and CpG-DNA were used. T-cell responses of individual mice from both groups displayed partial IFNγ secretion upon *in vitro* re-stimulation of primed splenocytes (Figure 27).

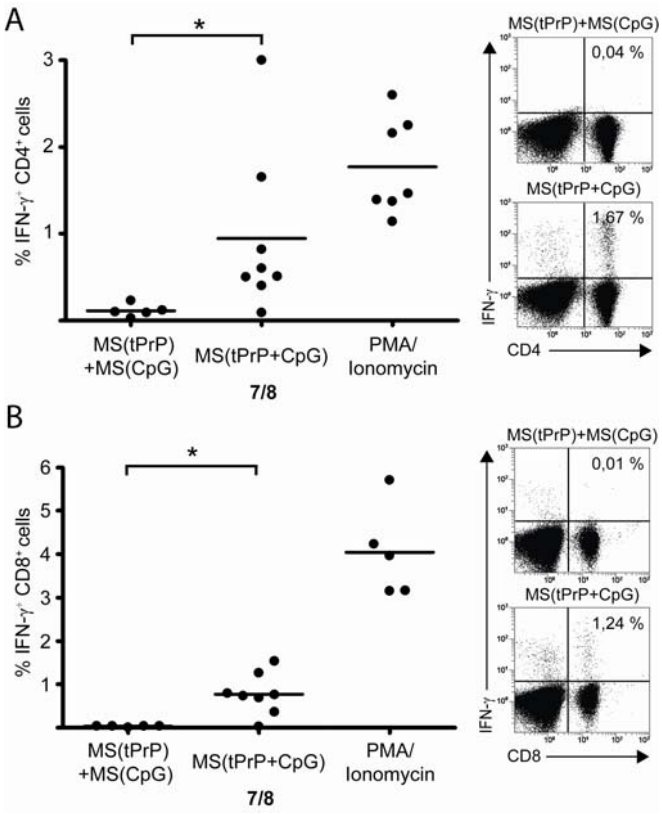

Figure 27
T cell response after vaccination with recombinant tPrP and CpG-ODN encapsulated with MS. Spleens of individual mice were re-stimulated *in vitro* by tPrP and expression of IFNγ determined by intracellular staining **(A)** Summary of $CD4^+$ splenocytes after immunization with either PLGA-MS containing tPrP and CpG-ODN in separate microspheres (MS(tPrP)+MS(CpG)) or both co-encapsulated in the same compartment (MS(tPrP+CpG)). Exemplary dot blot images of FACS measurements are shown for each immunization group. **(B)** Previous layout with $CD8^+$ surface staining.

The $CD4^+$ T-cells in the group of co-encapsulated PLGA-MS revealed a clear response in 7 of 8 animals, including two high responders (Figure 27 A). These results were statistically significant compared to the group of mixed PLGA-MS (p=0.0109; Mann-Whitney-Test),

therefore representing an ideal control group. Furthermore, $CD8^+$ T-cells of individual mice primed with co-encapsulated PLGA-MS showed a consistent IFNγ secretion (Figure 27 B), leading to a statistically significant difference compared to the control group ($p=0.0186$; Mann-Whitney-Test).

In summary, vaccination with PLGA-MS co-encapsulating tPrP plus CpG-ODN did not induce considerable B-cell response but causes a noticeable enhancement of $CD4^+$ and, to an even more extend, $CD8^+$ T-cell responses.

3.5 DNA vaccination with encapsulated PrP encoding vectors

DNA vaccines have been shown to be very efficient when applied encapsulated in microspheres (O'Hagan et al., 2004).Vaccination of wt mice with either pVAX (mPrP) or pVAX (tPrP) in combination with CpG, applied via microspheres i.m., resulted in very modest immune responses of only a few animals. Only 1 mouse out of 8 from the pVAX (tPrP) group showed an antibody titer in an endpoint titration ELISA not higher than 1:200. Two animals showed a slight expression of IFN γ in $CD4^+$ splenocytes in the same group. No activation of $CD8^+$ cells was seen (data not shown).

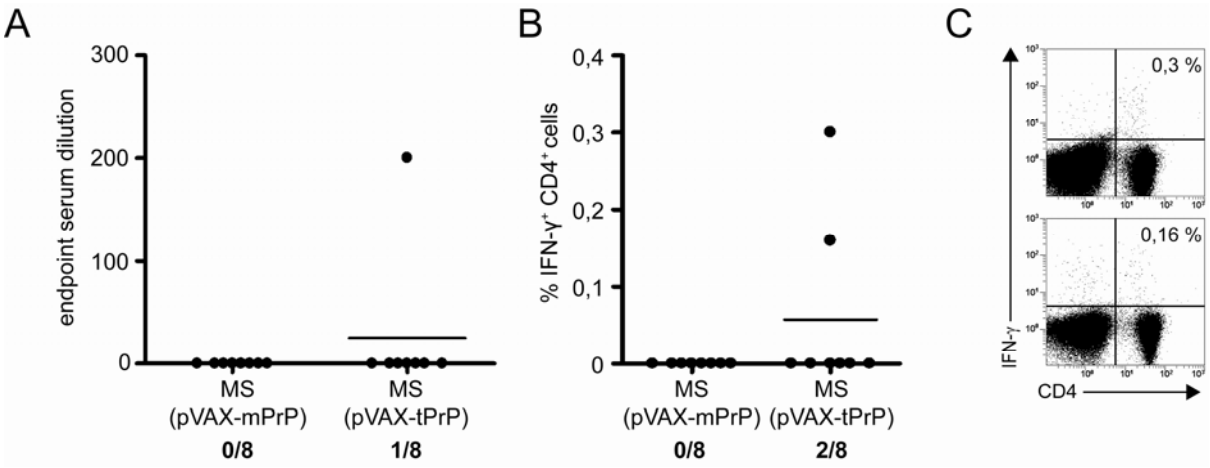

Figure 28
DNA vaccination with pVAX vectors encoding for monomeric PrP or tPrP, packed in PLGA-MS and injected i.m. **(A)** Endpoint dilution titer ELISA **(B)** Intracellular IFNγ expression of *in vitro* re-stimulated splenocytes of $CD4^+$ T-cells after pVAX tPrP immunization. **(C)** FACS dot blot examples of positive animals.

Taken together, only a marginal B and T-cell response is obtained in some animals when tPrP is used as micro-encapsulated DNA vaccine. No effect is found in this situation for DNA vaccination using monomeric PrP.

3.6 Examination of side effects

3.6.1 Histology of lymphatic organs

Histological examinations of representative lymphatic organs displayed no severe side effects in the auto-immunization situation described here. CpG-ODN only treated mice did not show severe changes in lymphatic organs, only minimal follicular hyperplasia in the lymph nodes and normal size peyer's patches (PP). Treatment with tPrP (NaAc) or tPrP (H_2O), both combined with CpG-ODN, did not reveal signs of severe changes in the lymphatic organs in any of the analyzed mice. In the gut lumen of ileum only small sized or no peyer's patches were visible after treatment with tPrP (H_2O); tPrP (NaAc) treated mice showed normal or middle sized peyer's patches without germinal centers. Animals immunized with separate microspheres (MS (tPrP)+MS (CpG)) showed the presence of peyer's patches without germinal centers and follicular and paracortical hyperplasia was observed in some lymph nodes. In contrast, animals receiving combined PLGA-MS (MS (tPrP+CpG)) showed major changes in the intestine and in lymph nodes. Some of the mice had very prominent peyer's patches with follicular hyperplasia including large germinal centers. In the lymph nodes all examined animals displayed paracortical T-cell hyperplasia, in addition to follicular hyperplasia with well developed germinal centers. Histological examination of both groups receiving DNA vaccination revealed very similar changes in the lymphatic organs. Peyer's patches in intestine were normal with little formation of germinal centers. The lymph nodes showed both follicular hyperplasia and paracortical hyperplasia or T-zone hyperplasia. The spleen looked normal. In addition, in two animals an acute/chronic inflammation was found in the muscle.

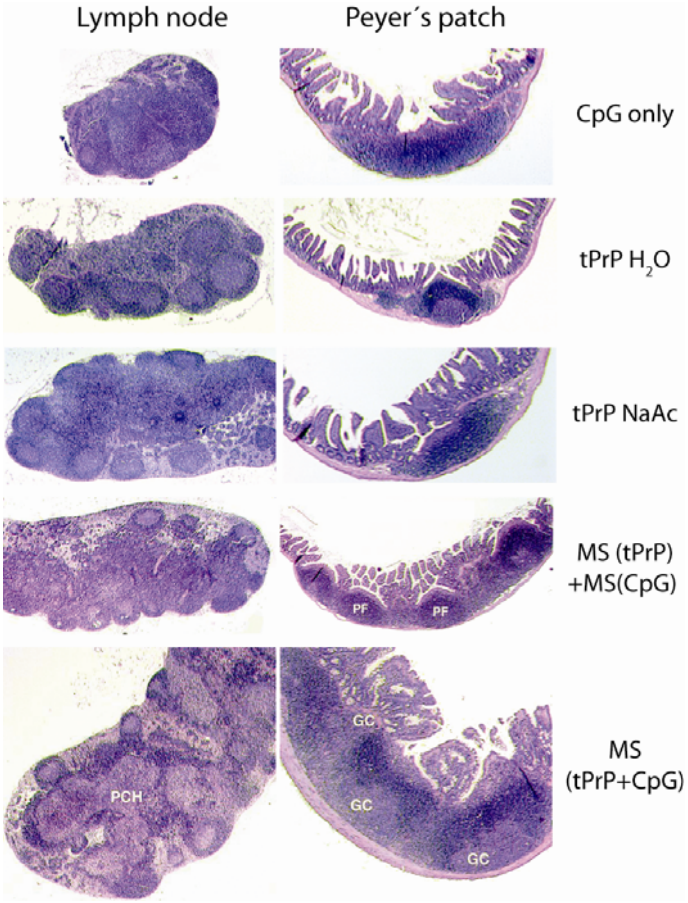

Figure 29
Histological appearance of lymphatic organs correlates with immune responses. Representative H&E stained samples of lymphnodes and peyer's patches in gut lumen of all immunization groups. (PF - primary follicles; GC - germinal centers; PCH - paracortical hyperplasia)

3.6.2 Histology of spleen after repeated CpG-ODN administration

The micro-architecture of spleen was examined to exclude the existence of previously reported deleterious effects after repeated administration of high CpG-ODN doses (Heikenwalder et al., 2004). None of the examined mice showed any destruction of spleen microstructure even after 4 times s.c. injections of 10 nmol in 3 weeks intervals.

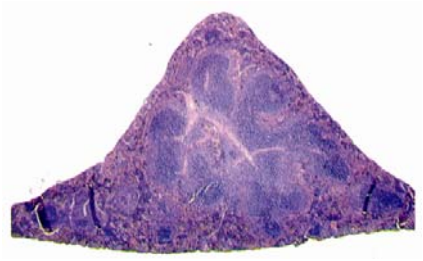

Figure 30
Histological samples of H&E stained spleen revealed intact microstructure after repeated CpG-ODN administration.

3.6.3 Histology of brain

Activation of auto-reactive T-cells bears the risk of side effects like meningoencephalitis in the brain of immunized individuals. Therefore, random histological samples of brains were examined in H&E staining and displayed no noticeable destructions or signs of inflammation after any of the used immunization protocols (Figure 31).

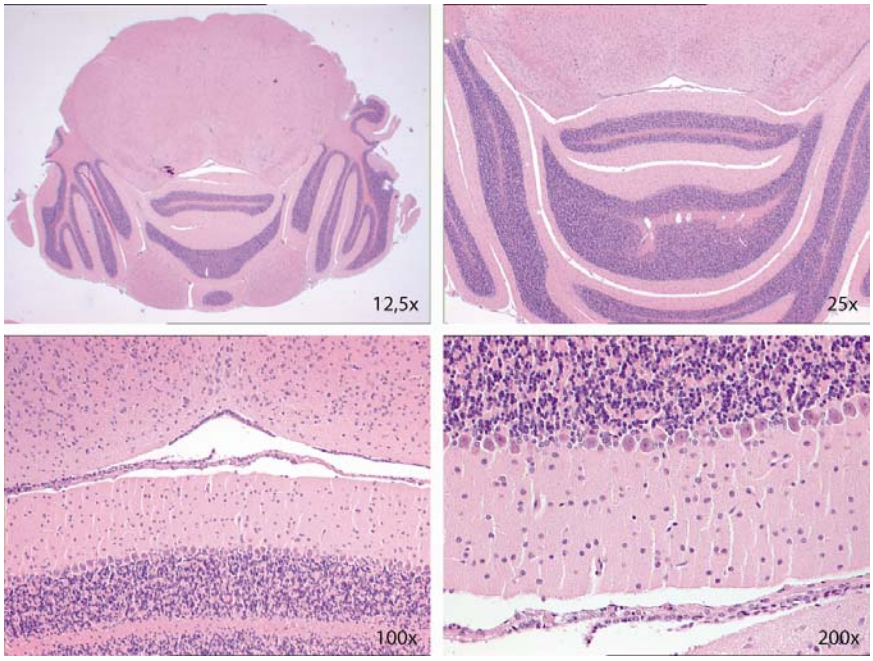

Figure 31
No detection of severe side effects in the brain of immunized mice. Histological examination of H&E stained brain sections of immunized mice did not show signs of inflammation indicative for meningoencephalitis.

3.6.4 Electron microscopy of kidneys

Kidneys of immunized mice were examined histologically in H&E staining for eye catching changes in their micro-structure. Conspicuous samples were then analyzed for electron dense deposits between the glomerular basement membrane and capillary endothelial cells in electron microscopy (Figure 32). Such aggregates are indicative for autoimmune reactions and consist of accumulated auto-antibodies with their respective self-target. None of the examined mice showed any subendothelial deposits underlining the absence of autoimmune diseases signs after immunization with tPrP antigen in combination with adjuvant CpG-ODN.

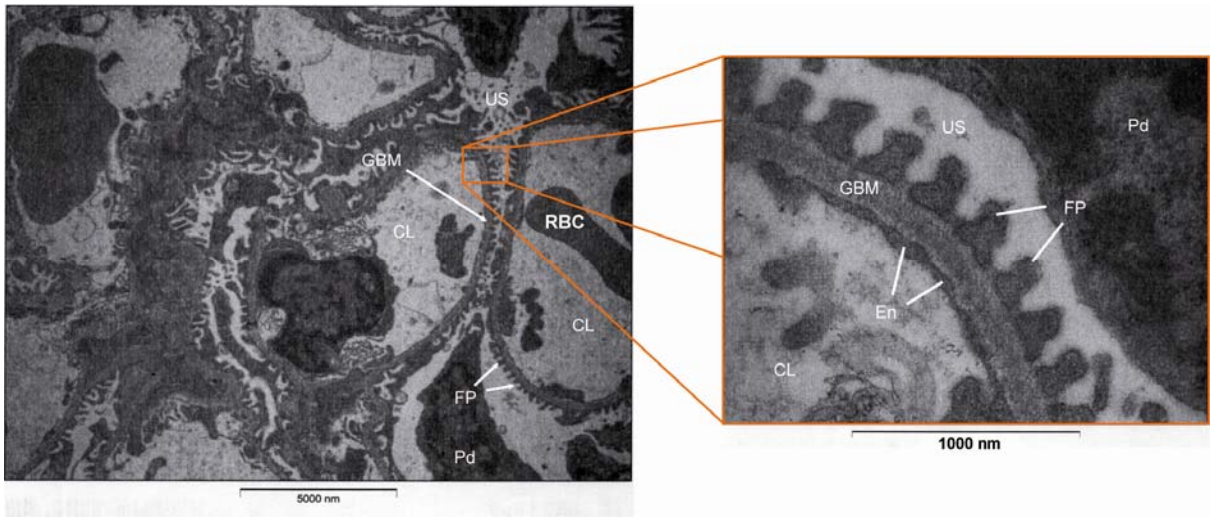

Figure 32
No detection of autoimmune particles in kidneys of immunized mice. (GBM: glomerular basement membrane, CL: capillary lumen, Pd: podocytes, FP: podocyte foot process, En: endothelial cells, US: urinal space)

Despite the obvious efficacy of the described auto-immunization regimen, neither signs of severe auto-immune reaction, acute inflammation in lymphatic organs, nor any CpG-ODN depending destruction in lymphatic organs were found. Of note, the histological appearance of lymphatic organs correlated with evoked immune responses. Signs of follicular hyperplasia were most prominent in animals receiving microspheres co-encapsulating tPrP antigen and CpG-ODN. Furthermore, immunized animals did not show changes in behavior upon treatment.

3.7 Long term animal infection study

Evaluation of vaccination efficacy can be displayed best by long term studies including prion inoculation. Therefore, an immunization trial with several mice was started in June 2006 including various group regimens (2.6.2). After three month of immunization animals were inoculated with 100 µl 0.1 % RML infected mouse brain intraperitoneal and boosted several times in the further course (Figure 11).

3.7.1 Immunization with bare antigen/adjuvant

Immunization with tPrP and CpG-ODN showed no noticeable prolongation of survival times compared to control groups neither with nor without application of tolerance breaker OX86 (Figure 33). All animals went down with clinical signs around day 215 ± 10.3 post inoculation with prions (Table 7). Interestingly one mouse immunized with tPrP and OX86 and lacking adjuvant CpG-ODN survived untill now (at present 278 days p.i.).

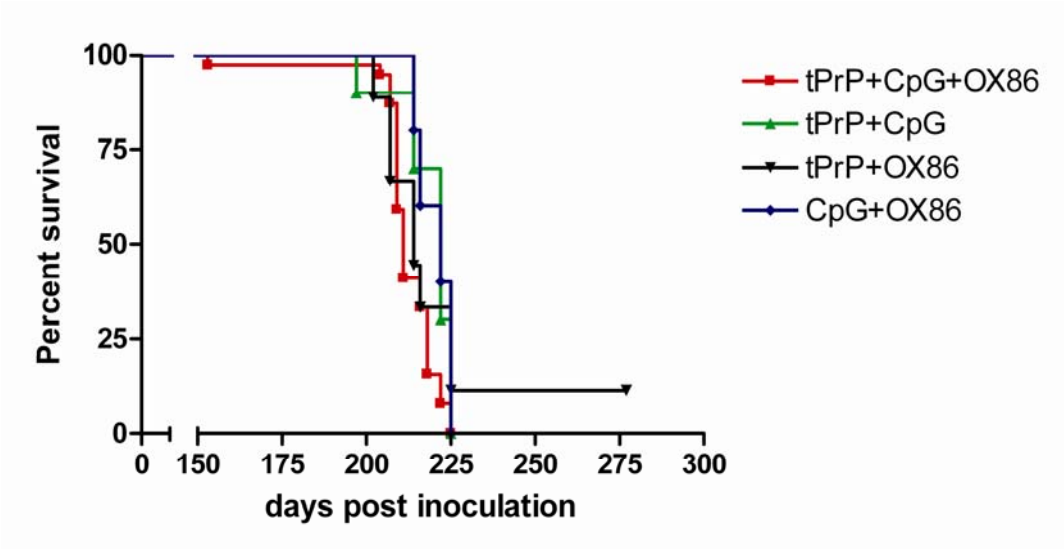

Figure 33
Survival curves summarizing animal survivals after protein immunization.

Table 7
Effect of protein based immunization on survival after prion inoculation.

Immunization	mean survival time ± SD[a]	No. of living/total animals
tPrP+CpG+OX86	212 ± 11.3 days	0/40
tPrP+CpG	219 ± 8.7 days	0/10
CpG+OX86	220 ± 4.8 days	0/10
tPrP+OX86	214 ± 8.4 days[b]	1/10[b]

[a] mice dying from non-scrapie causes were removed from the data sheet
[b] living animals are not included in mean survival times

3.7.2 Immunization with MS encapsulated antigen/adjuvant

Mice vaccinated with microspheres co-encapsulating tPrP+CpG-ODN and tolerance breaker OX86 displayed a minor prolongation of mean survival time of 10 days compared to the control group with seprately encapsulated antigen/adjuvant (Figure 34 and Table 8). Thereby two animals (10 % of group) of the first group survived untill present corresponding to >280 days p.i.. Comparison of co-encapsulated and separately encapsulated antigen/adjuvant groups lacking application of tolerance breaker OX86 did not reveal differences in mean survival time but one animal of 10 survived until present.

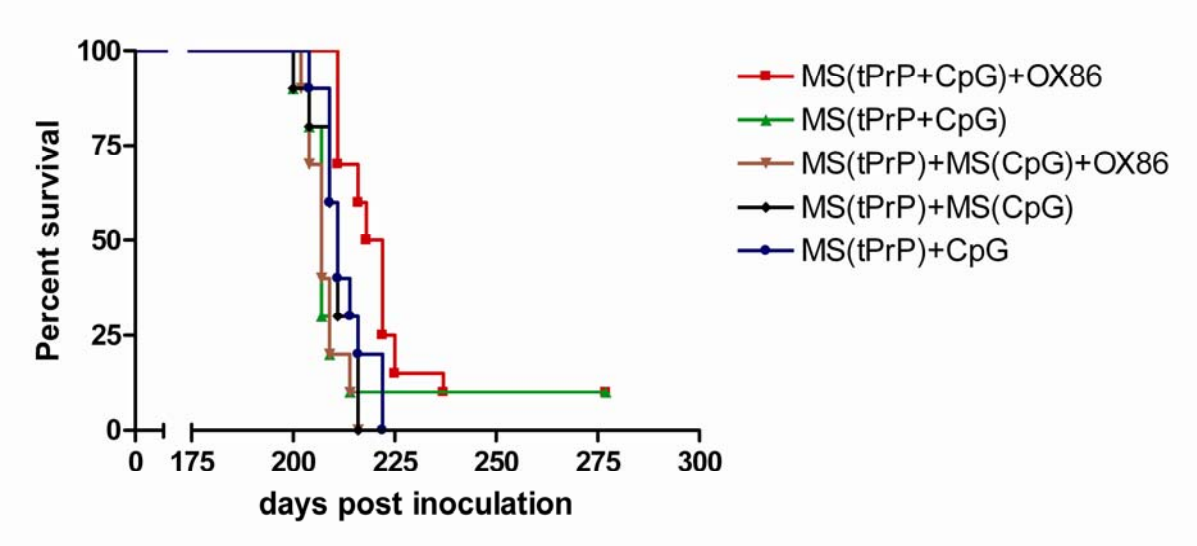

Figure 34
Overlay of survival curves from all animals receiving microsphere encapsulated antigen/adjuvant immunization.

Table 8
Effect of microsphere encapsulated antigen/adjuvant on the survival after prion inoculation.

Immunization	mean survival time ± SD[a]	No. of living/total animals
MS(tPrP+CpG)+OX86	218 ± 7.0 days[b]	2/20[b]
MS(tPrP+CpG)	207 ± 3.7 days[b]	1/10[b]
MS(tPrP)+MS(CpG)+OX86	208 ± 4.4 days	0/10
MS(tPrP)+MS(CpG)	210 ± 5.3 days	0/10
MS(tPrP)+CpG	213 ± 5.9 days	0/10

[a] mice dying from non-scrapie causes were removed from the data sheet
[b] living animals are not included in mean survival times

4 Discussion

The future spread of vCJD, initially caused by zoonotic trans-species transmission of BSE to humans, now also transmitted by human-to-human infection e.g. via blood products (secondary vCJD), remains elusive. As infection with prions is invariably lethal and no therapeutic or prophylactic regimens are available, there is an urgent need for developing protective anti-prion strategies. Prophylactic or therapeutic immunization may be an ideal strategy against a variety of infectious agents, but presumably is hampered in prion diseases by the pronounced self-tolerance against PrP. The aim of this work was the induction of PrP-specific humoral and T-cell immune responses in PrP-expressing wild-type mice by active immunization.

In previous studies in our lab (Gilch et al., 2003) and in others (Khalili-Shirazi et al., 2005;Koller et al., 2002;Polymenidou et al., 2004;Sigurdsson et al., 2002;Stoltze et al., 2003) it became obvious that antigen design and application may be major determinants in overcoming PrP self-tolerance. For example, the induction of comparable antibody titers and binding to the same linear epitopes was described after mPrP and tPrP immunization in wt mice (Gilch et al., 2003). From the fact that only tPrP induced sera led to an efficient blocking of the de novo PrP^{Sc} formation in prion-infected cell culture, the induction of antibodies with conformational epitopes was concluded, eventually specific to PrP^{Sc} or an accessible folding intermediate of prion conversion.

Here, some biochemical features of the tPrP antigen were analyzed in attempts to optimize conditions for improved immune responses. Examination of T cell responses that might help to trigger B cells producing conformational antibodies was done and it was tried to improve methods for antigen administration by using PLGA-MS and DNA vaccination approaches. An animal long term trial was performed to investigate the prophylactic effect of the above characterized immunization against prion infection.

4.1 Biochemical characterization of tPrP

4.1.1 Solubility

The conformation of recombinant PrPs has been extensively studied, mostly using N-terminally truncated mouse or hamster PrP encompassing residues 90-231 (Baskakov et al., 2002;Jackson et al., 1999a;Jackson et al., 1999b;Martins et al., 2006;Morillas et al., 2001). Overall, full length rPrP23-231 showed virtually identical biochemical properties compared to cellular PrP^C (Bocharova et al., 2005;Rezaei et al., 2005;Vendrely et al., 2005). Here it was shown, that in contrast to monomeric recombinant PrP with mainly α-helical structure, in both tPrP preparations β-sheet prevailed, leading to the conclusion, that the covalent linkage of two PrP monomers intrinsically forces the protein into β-sheet conformation. Interestingly, Jackson and colleagues described β-sheet rPrP to appear monomeric and soluble, a characteristic of proteins going from soluble monomer to aggregated amyloid (Jackson et al., 1999b). Indeed, tPrP (NaAc) was found monomeric and highly soluble, even at concentrations higher than 40 mg/ml. Moreover, refolding conditions are a critical factor in the formation of protein structure and level of solubility, and are influenced by several biochemical properties like protein concentration, temperature, salt concentration, and pH-value. In this context tPrP was found soluble only at pH values lower than 6 and physiological salt conditions caused the formation of distinct soluble oligomers, as also found by others (Rezaei et al., 2005;Vendrely et al., 2005). tPrP shares similarities to a possible transition state of prion conversion process, thus making it interesting as antigen for vaccination strategy against prion infection without the risk of inducing autoimmune side effects.

4.1.2 Interaction with CpG

Immunization needs the application of an immunogen to a living organism, thereby significantly changing the biochemical environment and eventually also the biochemical properties of the antigen. Addition of an adjuvant is a first step towards this direction. Interestingly, mixing of highly soluble tPrP (NaAc) with negatively charged adjuvant CpG-ODN resulted in an immediate and almost complete aggregation of proteins, indicated by the formation of canyon like structures as well as huge three dimensional clumps. In contrast, partially insoluble tPrP (H_2O) - most likely based on a salting-out effect while dialysis against ddH_2O - was less influenced by CpG-ODN contact without the induction of bigger clumps. It is known that recombinant mouse PrP has a high DNA binding capacity and can form

aggregates in the presence of high molecular weight DNA (Gabus et al., 2001;Nandi et al., 1999;Nandi et al., 2001). In contrast, contact to DNA oligonucleotides, as is basically CpG-ODN, resulted apparently in a dimerization of monomeric PrP (Cordeiro et al., 2001). As DNA binds to the structured C-terminal region of PrP, an influence on protein structure is likely (Lima et al., 2006) and tPrP might crosslink with CpG-ODN due to doubled binding sites compared to mPrP.

4.1.3 Aging of refolded tPrP

Prominence of the assumption that tPrP structure highly influences its immunogenic properties was emphasized by the discovery of tPrP aging. Long term storage of refolded recombinant tPrP resulted in the formation of insoluble protein thereby loosing its immogenicity. Moreover, it was described that tPrP formed ordered fibrils and lost its toxicity to primary neurons (Simoneau et al., 2007). Leffers and colleagues confirmed fibril formation for soluble β-sheeted recombinant and natural syrian hamster PrP 27-30 (Leffers et al., 2005). As a consequence all tPrP preparations were used here directly after refolding.

Although the biochemical properties of tPrP preparations could be partly characterized under defined *in vitro* conditions predictions after transfer into *in vivo* environment are difficult to make.

4.2 Immune response after tPrP vaccination

Antibodies directed against PrP^{C} or PrP^{Sc} are in principle able to inhibit *de novo* synthesis of PrP^{Sc} *in vivo* and *in vitro* (Enari et al., 2001;Gilch et al., 2003;Peretz et al., 2001;Sigurdsson et al., 2002;White et al., 2003). Here, previously demonstrated induction of PrP-specific antibodies in PrP wild-type mice was confirmed after immunization with tPrP in combination with CpG adjuvant (Gilch et al., 2003). Thereby, tPrP (NaAc) induced high antibody titers only in a few animals, whereas in immunizations with tPrP (H_2O) most mice developed titers with variations in individual endpoints.

No differences in linear antibody epitope reactivity could be detected between the groups. Linear epitope mapping with covalently linked peptides, including a DSS linker, measured individually for all ELISA titer positive sera showed weak reactivity near cut-off against some N-terminal epitopes, i.e. epitope #11 and #12, and one outstanding epitope #10. The induction of reactive antibodies against linear epitopes of foreign origin as contained in our protein sequence, like the 3F4 tag, the poly-Histidine tag or the linker region of tPrP could be

excluded. Control serum A7 obtained from tPrP immunized rabbit exhibited antibodies specific to the complete panel of linear epitopes, to a lesser extent to #10-12, thereby demonstrating the principle binding ability to all covalently linked peptides. In particular, the differentiation between epitope 6 and 6b, corresponding to 3F4 epitope tag or PrP wt sequence, respectively, was clearly demonstrated with this positive control experiment.

The quantity of humoral anti-PrP response as usually tested in ELISA-based formats is not an appropriate method to determine the efficacy of antibody binding to native, authentic PrP^{C} on living cells. So far it was not possible to conclusively show specific binding of auto-antibodies to authentic PrP^{C} or PrP^{Sc} in immunoprecipitation assays using brain homogenates or cell lysates, although we could measure some reactivity of final sera as compared to respective pre-immune sera in PrP surface FACS staining approaches. Specific binding of some sera to PrP^{C} was demonstrated by immuno stripe blot assays containing mouse brain homogenate and N2a cell lysate, even though under denaturing conditions.

On the other hand, the absence of detectable binding in this assays may not necessarily be interpreted as negative result, as the concentration of antibodies in blood might be below detection limit or antibodies might be able to interfere in prion conversion by other mechanisms, e.g. by reacting with putative folding intermediates. Such conformational epitopes are difficult to map, as the underlying structures are not known. In fact, the β-sheeted tandem version of PrP as used here is thought to mimic such putative folding intermediates. Importantly, sera of immunized wt mice have shown significant interference in the de novo PrP^{Sc} formation in cell culture, whereas monomeric PrP induced similar linear antibody reactivity, but mainly failed to prevent PrP^{Sc} formation (Gilch et al., 2003). An obvious explanation is the induction of conformational antibodies by specific binding of B cells to mainly soluble, beta-sheeted tPrP, followed by internalization, processing and presentation of linear tPrP epitopes via MHC II. Epitope specific $CD4^{+}$ T cells are then able to trigger B cells proliferation and antibody production. The induction of a tPrP specific T cell response in PrP wild-type mice using a syngenic recombinant full length PrP immunogen with only minor changes was demonstrated (e.g. two amino acids exchanged in the 3F4 tag). Significant IFNγ expression of $CD4^{+}$ splenocytes after re-stimulation with full tPrP protein together with the absence of Th2 specific IL4 and IL10 (data not shown) indicate the induction of a Th1 response at the final stage of immunization, presumably polarized by the adjuvant CpG-ODN (Wagner, 2002). The CpG-ODN-based general adjuvant effect may be further enhanced by

the strong binding between CpG and tPrP, as it is known for covalently linked CpG-proteins that promote a strong Th1 response via concomitant uptake of antigen and adjuvant (Heit et al., 2003;Maurer et al., 2002;Shirota et al., 2001). PrP-specific T-cell responses in wt mice in experimental vaccination scenarios and the protective effect of cellular-based immunity in prion infection are in part characterized (Gregoire et al., 2004;Gregoire et al., 2005;Rosset et al., 2004;Souan et al., 2001;Stoltze et al., 2003). Peptide immunizations with adjuvant CpG demonstrated two immunogenic PrP T cell epitopes (residues 143-172; 158-187) in wt mice (Rosset et al., 2004). Souan and colleagues successfully generated a T cell response in various mouse strains by designing peptides optimized to fit into the MHC class II binding groove of NOD mice (aa 131-150; 211-230) (Souan et al., 2001). β-sheet rich recombinant PrP, like the tPrP described here, is known to be partially proteinase K resistant, in contrast to easily degradable α-helical mPrP (Jackson et al., 1999b). Potentially, this biochemical characteristic of tPrP leads to changes in the lysosomal degradation in APCs and thereby leads to different MHC class II peptide loading, inducing T cells with possible 'foreign' PrP epitopes. At least in $PrP^{0/0}$ mice such variances in T cell response were found for α helical and β sheeted recombinant PrP (Khalili-Shirazi et al., 2005). Besides changes of wild type epitopes, xenogenic epitopes, in this case most likely against the two amino acid exchanges of the 3F4 tag in the tPrP antigen, might help to break tolerance and enhance T cell response, as it was demonstrated for shPrP immunized mice (Stoltze et al., 2003). This work focused on vaccination protocols able to improve the induction of T cell responses, since the auto-immune setting precludes strong responses. For T cell epitope mapping an effective protein immunization protocol is required, since peptides provoke a much lower T cell response compared to full protein re-stimulation (Stoltze et al., 2003). Since a strong CD4 response was demonstrated for tPrP in future approaches mapping of T cell epitopes by peptide re-stimulation and MHC-tetramer technology could be considered.

With the results of this work, it is now possible to give statements for the obvious lack of functional conformational antibodies in mPrP vaccinations seen in previous immunizations. The mainly α-helical folded monomer might present only conformational epitopes similar to PrP^{C}, thereby being recognized as 'self'. The explanation for differences between tPrP(H_2O) and tPrP (NaAc) immunization might follow similar mechanistic correlations. Both protein preparations share β-sheet conformation, whereas tPrP (H_2O) was partially soluble even after contact to adjuvant CpG. Antigen presentation of B cells is

essential for proper humoral response and the formation of huge aggregates in tPrP (NaAc) preparations might decrease or hinder the uptake and processing by B cells.
In summary, this data together with other reported data provide solid experimental evidence that an effective humoral anti-prion response can be evoked in certain experimental auto-immunization scenarios.

4.3 Microsphere immunization

Increasing $CD4^+$ T-cell help was tested by a vaccination protocol by co-encapsulation of tPrP and CpG-DNA in biodegradable microspheres (Heit et al., 2007;Lima et al., 2003). PLGA-based microspheres are taken up and digested mainly by macrophages and DCs after subcutaneous application *in vivo*, as observed in cells of mesenteric lymph nodes and spleen (Peyre et al., 2004). The efficacy of loaded PLGA-MS seems to be based on the enhanced concurrent uptake of proteinaceous antigen and the adjuvant into endosomes of DCs and macrophages (Singh et al., 2004). Exogenous antigens are classically internalized and processed by the MHC class II presenting pathway, resulting in APC activating CD4 T cell (T helper cells) response (Villadangos et al., 2000). In addition, DCs are able to direct exogenous antigen into the MHC class I presentation pathway via cross-presentation (Heath et al., 2004). Furthermore, immunostimulatory CpG-ODN motifs are known to specifically activate innate immune cells, including macrophages and DCs via targeting Toll-like receptor 9. Interaction between CpG-ODN and TLR9 takes place in late endosomal compartments (Ahmad-Nejad et al., 2002) and receptor-mediated endocytosis was reported to be essential for cross-priming (Heit et al., 2003). Via PLGA-MS immunization CpG-ODN and exogenous antigen are effectively co-translocated into endosomal compartments, thus enhancing TLR9 interaction with CpG-ODN and subsequent cross-presentation. This might explain the very pronounced increase in the response of $CD4^+$ cells, in the range of 1% and higher, and, interestingly, also of a $CD8^+$ T cell response. When PLGA-MS containing either tPrP or CpG-ODN alone are mixed, no detectable immune response at all is induced. One obvious explanation is that under these conditions no co-internalization of tPrP and CpG-ODN into the same APCs is taking place. The lack of antibody titers, despite the enhanced CD4 T-cell response, might be due to the encapsulation of antigen, thereby preventing direct contact to B cells. The potential lytic function of induced CD8 T-cells must be evaluated in future, because they might cause severe auto-immune responses like meningoencephalitis in brain.

4.4 DNA vaccination

Previous experiments demonstrated the potential of DNA based active immunization against prion disease either by fusing lysosomal targeting signal to PrP (Fernandez-Borges et al., 2006) or displaying full length PrP with a retroviral system (Nikles et al., 2005).In contrast, immunization studies dealing with fusion of tetanus toxin and PrP were not successful (Nitschke et al., 2007). In this studies DNA-vaccines encapsulated by microspheres failed to induce immune response, despite the potential of this method (O'Hagan et al., 2004). Several reasons are conceivable, most likely the lack or very little expression of recombinant PrP in mice, thus only moderate amounts can be taken up by immune cells. Furthermore mammalian features like GPI-anchor and glycosilation contained in the expressed PrPs might hinder the formation of immunogenic structures and availability to the immune system. Delayed expression of DNA-based vaccines moreover might prevent the concomitant presence of antigen and CpG-ODN thereby preventing adjuvant stimulating effects.

4.5 Examination of side effects

Inducing auto-immunity bears the obvious risk of induction of severe side effects. As was the case in anti-PrP immunization approaches reported by others (Fernandez-Borges et al., 2006;Gilch et al., 2003;Gregoire et al., 2005;Heppner et al., 2001b;Koller et al., 2002;Nikles et al., 2005;Polymenidou et al., 2004;Rosset et al., 2004;Schwarz et al., 2003;Sigurdsson et al., 2002), no such deleterious effects were found in this studies. In Alzheimer phase II vaccination studies in some cases meningoencephalitis appeared (Orgogozo et al., 2003). To exclude similar side effects in this immunization approach, brain sections of mice were examined for signs of inflammation. All examined brains appeared normal without any severe changes as indicative for meningoencephalitis. Besides histological examinations lack of sub-endothelial deposits in kidneys of immunized mice confirmed the absence of autoimmune reactions. The efficacy of CpG-ODN as adjuvant via stimulation of innate immunity was established by many groups (Wagner, 2002). Recently, it was reported that repeated daily administrations of high CpG-ODN doses have deleterious effects on the morphology and function of lymphoid organs (Heikenwalder et al., 2004). The micro-architecture of follicles in spleen and mesenteric lymph nodes was severely disturbed. Such dramatic side effects were excluded in this study, in which CpG-ODN was administered only at 3 weeks intervals

and as demonstrated by normal histological appearance of spleen, peyer's patches and mesenteric lymph nodes.

4.6 Animal infection trial study

The long term infection trial was performed to examine the prophylactic potential of tPrP using either direct administration or encapsulated into PLGA-MS.

None of the mice immunized with protein and CpG-ODN survived longer than control anmials. This is obiously due to a modest immune response not sufficient to prevent the spread of disease. Hence antibodies that were shown to be induced with this strategy (3.3.1) are either not able to specifically bind to native PrP^{C}, PrP^{Sc} or a conversion intermediate like PrP^{*} or the concentration of specific antibodies was too low to interfere with the progression of disease. In contrast to these disappointing results administration of co-encapsulated tPrP and CpG-ODN resulted in the survival of 3 animals. Even thought they only represent 10 % the the total group this result can be rated as a great success. Previous results showing survival of two tPrP treated animal in a group of 8 could thereby be fully confirmed even though using different administraion and adjuvant condition (Polymenidou et al., 2004). So far no other classical immunization approach resulted in the complete protection of PrP wild type animals (Griffin et al., 2005). As discussed (4.3) concomitant delivery of antigen and CpG-ODN is very important for induction of a pronounced immune response supported by finding a lack of protection in control animal receiving tPrP and CpG-ODN in seperate microspheres. The underlying mode of protection most probably is based on antibodies specific to an intermediate conformation of PrP^{C}. This assumption is not conflicting with finding only low titers after microsphere immunisations. Either measuring titers with recombinant protein might not be suitable to track these antibodies or only very small amounts of specific antibody might interfere with prion conversion when raised against the relatively rare intermediate state of PrP^{C}. If lytical function of T-cells also known to be induced might play a role in protection agains prions has to be tetermined.

Monoclonal anti-OX40 antibodies were administered with the aim of breaking self tolerance to PrP (Bansal-Pakala et al., 2001) but did not result in protection or prolongation of incubation times of mice immunized with tPrP antigen and CpG-ODN. Interestingly, one animal survived after administration of tPrP antigen and anti-OX40 antibody but lacking adjuvant CpG. In this special case tolerance might have been broken thus leading to a protection. In contrast, comparison of groups treated with microsphere co-encapsulating tPrP

and CpG-ODN resulted in a moderate prolongation of incubation time course in animals co-treated with anti-OX40. Thereby a moderate tolerance breaking efficiency was indicated. Apparently the relatively low efficacy of anti-OX40 antibody effect is based on the generation of anti-antibodies raised against the administered foreign monoclonal antibody. Hence with first or second administration of a monoclonal antibody obtained from rat immune system of mice effectively neutralized the potential pathogen therby anticipating with its tolerance breaking efficiency. Anti-OX40 antibodies might even have partially overcome tolerance in more animals but this did not manifest in the survival of mice. Generation of PrP^C specific antibodies might have failed to effectively protect due to their low concentration.

Experimental prion inoculation by intraperitoneal injection of relatively high amount of infectious particles might not reflect reality of an oral infection. Thus induction of a moderate immune response might be very well protective for lifelike scenarios.

Overall, with the induction of humoral and T-cell response upon tPrP immunisation and even few animals surviving prion inoculation the potential of prophylactic vaccination against TSE could be demonstated.

5 Reference list

Ahmad-Nejad, P., Hacker, H., Rutz, M., Bauer, S., Vabulas, R. M., and Wagner, H. (2002). Bacterial CpG-DNA and lipopolysaccharides activate Toll-like receptors at distinct cellular compartments. *Eur.J.Immunol.* **32**, 1958-1968.

Aldhous, P. (1990). BSE: spongiform encephalopathy found in cat. *Nature* **345**, 194.

Alper, T., Cramp, W. A., Haig, D. A., and Clarke, M. C. (1967). Does the agent of scrapie replicate without nucleic acid? *Nature* **214**, 764-766.

Alper, T., Haig, D. A., and Clarke, M. C. (1966). The exceptionally small size of the scrapie agent. *Biochem.Biophys.Res.Commun.* **22**, 278-284.

Alpers M. (1987). Epidemiological and clinical aspects of kuru. *In* "Prions: novel infectious pathogens causing scrapie and Creutzfeldt-Jakob disease" pp. 451-465. Academic Press, San Diego.

Anderson, R. M., Donnelly, C. A., Ferguson, N. M., Woolhouse, M. E., Watt, C. J., Udy, H. J., MaWhinney, S., Dunstan, S. P., Southwood, T. R., Wilesmith, J. W., Ryan, J. B., Hoinville, L. J., Hillerton, J. E., Austin, A. R., and Wells, G. A. (1996). Transmission dynamics and epidemiology of BSE in British cattle. *Nature* **382**, 779-788.

Anfinsen, C. B. (1973). Principles that govern the folding of protein chains. *Science* **181**, 223-230.

Arnold, J. E., Tipler, C., Laszlo, L., Hope, J., Landon, M., and Mayer, R. J. (1995). The abnormal isoform of the prion protein accumulates in late-endosome-like organelles in scrapie-infected mouse brain. *J.Pathol.* **176**, 403-411.

Bansal-Pakala, P., Jember, A. G., and Croft, M. (2001). Signaling through OX40 (CD134) breaks peripheral T-cell tolerance. *Nat.Med.* **7**, 907-912.

Baskakov, I. V., Legname, G., Baldwin, M. A., Prusiner, S. B., and Cohen, F. E. (2002). Pathway complexity of prion protein assembly into amyloid. *J.Biol.Chem.* **277**, 21140-21148.

Basler, K., Oesch, B., Scott, M., Westaway, D., Walchli, M., Groth, D. F., McKinley, M. P., Prusiner, S. B., and Weissmann, C. (1986). Scrapie and cellular PrP isoforms are encoded by the same chromosomal gene. *Cell* **46**, 417-428.

Beekes, M., Baldauf, E., and Diringer, H. (1996). Sequential appearance and accumulation of pathognomonic markers in the central nervous system of hamsters orally infected with scrapie. *J.Gen.Virol.* **77 (Pt 8)**, 1925-1934.

Beekes, M. and McBride, P. A. (2000). Early accumulation of pathological PrP in the enteric nervous system and gut-associated lymphoid tissue of hamsters orally infected with scrapie. *Neurosci.Lett.* **278**, 181-184.

Beringue, V., Demoy, M., Lasmezas, C. I., Gouritin, B., Weingarten, C., Deslys, J. P., Andreux, J. P., Couvreur, P., and Dormont, D. (2000). Role of spleen macrophages in the clearance of scrapie agent early in pathogenesis. *J.Pathol.* **190**, 495-502.

Bocharova, O. V., Breydo, L., Parfenov, A. S., Salnikov, V. V., and Baskakov, I. V. (2005). In vitro conversion of full-length mammalian prion protein produces amyloid form with physical properties of PrP(Sc). *J.Mol.Biol.* **346**, 645-659.

Bolton, D. C., Meyer, R. K., and Prusiner, S. B. (1985). Scrapie PrP 27-30 is a sialoglycoprotein. *J.Virol.* **53**, 596-606.

Borchelt, D. R., Koliatsos, V. E., Guarnieri, M., Pardo, C. A., Sisodia, S. S., and Price, D. L. (1994). Rapid anterograde axonal transport of the cellular prion glycoprotein in the peripheral and central nervous systems. *J.Biol.Chem.* **269**, 14711-14714.

Borchelt, D. R., Scott, M., Taraboulos, A., Stahl, N., and Prusiner, S. B. (1990). Scrapie and cellular prion proteins differ in their kinetics of synthesis and topology in cultured cells. *J.Cell Biol.* **110**, 743-752.

Brotherston, J. G., Renwick, C. C., Stamp, J. T., Zlotnik, I., and Pattison, I. H. (1968). Spread and scrapie by contact to goats and sheep. *J.Comp Pathol.* **78**, 9-17.

Brown, D. R. and Besinger, A. (1998). Prion protein expression and superoxide dismutase activity. *Biochem.J.* **334 (Pt 2)**, 423-429.

Brown, D. R., Qin, K., Herms, J. W., Madlung, A., Manson, J., Strome, R., Fraser, P. E., Kruck, T., von Bohlen, A., Schulz-Schaeffer, W., Giese, A., Westaway, D., and Kretzschmar, H. (1997). The cellular prion protein binds copper in vivo. *Nature* **390**, 684-687.

Brown, D. R., Wong, B. S., Hafiz, F., Clive, C., Haswell, S. J., and Jones, I. M. (1999). Normal prion protein has an activity like that of superoxide dismutase. *Biochem.J.* **344 Pt 1**, 1-5.

Brown, P., Liberski, P. P., Wolff, A., and GAJDUSEK, D. C. (1990). Resistance of scrapie infectivity to steam autoclaving after formaldehyde fixation and limited survival after ashing at 360 degrees C: practical and theoretical implications. *J.Infect.Dis.* **161**, 467-472.

Bruce, M., Chree, A., McConnell, I., Foster, J., Pearson, G., and Fraser, H. (1994). Transmission of bovine spongiform encephalopathy and scrapie to mice: strain variation and the species barrier. *Philos.Trans.R.Soc.Lond B Biol.Sci.* **343**, 405-411.

Bruce, M. E., Will, R. G., Ironside, J. W., McConnell, I., Drummond, D., Suttie, A., McCardle, L., Chree, A., Hope, J., Birkett, C., Cousens, S., Fraser, H., and Bostock, C. J. (1997). Transmissions to mice indicate that 'new variant' CJD is caused by the BSE agent. *Nature* **389**, 498-501.

Bueler, H., Aguzzi, A., Sailer, A., Greiner, R. A., Autenried, P., Aguet, M., and Weissmann, C. (1993). Mice devoid of PrP are resistant to scrapie. *Cell* **73**, 1339-1347.

Bueler, H., Fischer, M., Lang, Y., Bluethmann, H., Lipp, H. P., DeArmond, S. J., Prusiner, S. B., Aguet, M., and Weissmann, C. (1992). Normal development and behaviour of mice lacking the neuronal cell-surface PrP protein. *Nature* **356**, 577-582.

Carp, R. I. and Callahan, S. M. (1982). Effect of mouse peritoneal macrophages on scrapie infectivity during extended in vitro incubation. *Intervirology* **17**, 201-207.

Caughey, B., Kocisko, D. A., Raymond, G. J., and Lansbury, P. T., Jr. (1995). Aggregates of scrapie-associated prion protein induce the cell-free conversion of protease-sensitive prion protein to the protease-resistant state. *Chem.Biol.* **2**, 807-817.

Caughey, B. and Raymond, G. J. (1991). The scrapie-associated form of PrP is made from a cell surface precursor that is both protease- and phospholipase-sensitive. *J.Biol.Chem.* **266**, 18217-18223.

Chaplin, M. J., Aldrich, A. D., and Stack, M. J. (1998). Scrapie associated fibril detection from formaldehyde fixed brain tissue in natural cases of ovine scrapie. *Res.Vet.Sci.* **64**, 41-44.

Clarke, A. R., Jackson, G. S., and Collinge, J. (2001). The molecular biology of prion propagation. *Philos.Trans.R.Soc.Lond B Biol.Sci.* **356**, 185-195.

Clinton, J., Royston, M. C., Gentleman, S. M., and Roberts, G. W. (1992). Amyloid plaque: morphology, evolution, and etiology. *Mod.Pathol.* **5**, 439-443.

Cohen, F. E., Pan, K. M., Huang, Z., Baldwin, M., Fletterick, R. J., and Prusiner, S. B. (1994). Structural clues to prion replication. *Science* **264**, 530-531.

Collinge, J. (1997). Human prion diseases and bovine spongiform encephalopathy (BSE). *Hum.Mol.Genet.* **6**, 1699-1705.

Collinge, J. (2001). Prion diseases of humans and animals: their causes and molecular basis. *Annu.Rev.Neurosci.* **24**, 519-550.

Collinge, J., Palmer, M. S., and Dryden, A. J. (1991). Genetic predisposition to iatrogenic Creutzfeldt-Jakob disease. *Lancet* **337**, 1441-1442.

Collinge, J. and Rossor, M. (1996a). A new variant of prion disease. *Lancet* **347**, 916-917.

Collinge, J., Sidle, K. C., Meads, J., Ironside, J., and Hill, A. F. (1996b). Molecular analysis of prion strain variation and the aetiology of 'new variant' CJD. *Nature* **383**, 685-690.

Collinge, J., Whitfield, J., McKintosh, E., Beck, J., Mead, S., Thomas, D. J., and Alpers, M. P. (2006). Kuru in the 21st century--an acquired human prion disease with very long incubation periods. *Lancet* **367**, 2068-2074.

Collinge, J., Whittington, M. A., Sidle, K. C., Smith, C. J., Palmer, M. S., Clarke, A. R., and Jefferys, J. G. (1994). Prion protein is necessary for normal synaptic function. *Nature* **370**, 295-297.

Come, J. H., Fraser, P. E., and Lansbury, P. T., Jr. (1993). A kinetic model for amyloid formation in the prion diseases: importance of seeding. *Proc.Natl.Acad.Sci.U.S.A* **90**, 5959-5963.

Cordeiro, Y., Machado, F., Juliano, L., Juliano, M. A., Brentani, R. R., Foguel, D., and Silva, J. L. (2001). DNA converts cellular prion protein into the beta-sheet conformation and inhibits prion peptide aggregation. *J.Biol.Chem.* **276**, 49400-49409.

Creutzfeldt, H. G. (1920). Über eine eigenartige herdförmige Erkrankung des Zentralnervensystems. *Z.Ges.Neurol.Psychiatr.* **57**, 1-18.

Cuille, J. C. P. L. (1939). Experimental transmission of trembling to the goat. *ComptesRendus des Seances de l'Academie des Sciences* 1058-1160.

Dickinson, A. G., Stamp, J. T., and Renwick, C. C. (1974). Maternal and lateral transmission of scrapie in sheep. *J.Comp Pathol.* **84**, 19-25.

Dodelet, V. C. and Cashman, N. R. (1998). Prion protein expression in human leukocyte differentiation. *Blood* **91**, 1556-1561.

Donnelly, C. A., Ferguson, N. M., Ghani, A. C., and Anderson, R. M. (2002). Implications of BSE infection screening data for the scale of the British BSE epidemic and current European infection levels. *Proc.Biol.Sci.* **269**, 2179-2190.

Dorban, G., Defaweux, V., Demonceau, C., Flandroy, S., Van Lerberghe, P. B., Falisse-Poirrier, N., Piret, J., Heinen, E., and Antoine, N. (2007). Interaction between dendritic cells and nerve fibres in lymphoid organs after oral scrapie exposure. *Virchows Arch.* **451**, 1057-1065.

Edenhofer, F., Rieger, R., Famulok, M., Wendler, W., Weiss, S., and Winnacker, E. L. (1996). Prion protein PrPc interacts with molecular chaperones of the Hsp60 family. *J.Virol.* **70**, 4724-4728.

Enari, M., Flechsig, E., and Weissmann, C. (2001). Scrapie prion protein accumulation by scrapie-infected neuroblastoma cells abrogated by exposure to a prion protein antibody. *Proc.Natl.Acad.Sci.U.S.A* **98**, 9295-9299.

Ertmer, A., Gilch, S., Yun, S. W., Flechsig, E., Klebl, B., Stein-Gerlach, M., Klein, M. A., and Schatzl, H. M. (2004). The tyrosine kinase inhibitor STI571 induces cellular clearance of PrPSc in prion-infected cells. *J.Biol.Chem.* **279**, 41918-41927.

Farquhar, C. F., Dornan, J., Somerville, R. A., Tunstall, A. M., and Hope, J. (1994). Effect of Sinc genotype, agent isolate and route of infection on the accumulation of protease-resistant PrP in non-central nervous system tissues during the development of murine scrapie. *J.Gen.Virol.* **75 (Pt 3)**, 495-504.

Fernandez-Borges, N., Brun, A., Whitton, J. L., Parra, B., Diaz-San Segundo, F., Salguero, F. J., Torres, J. M., and Rodriguez, F. (2006). DNA vaccination can break immunological tolerance to PrP in wild-type mice and attenuates prion disease after intracerebral challenge. *J.Virol.* **80**, 9970-9976.

Foster, J. D., Parnham, D., Chong, A., Goldmann, W., and Hunter, N. (2001). Clinical signs, histopathology and genetics of experimental transmission of BSE and natural scrapie to sheep and goats. *Vet.Rec.* **148**, 165-171.

Fournier, J. G., Escaig-Haye, F., Billette, d., V, and Robain, O. (1995). Ultrastructural localization of cellular prion protein (PrPc) in synaptic boutons of normal hamster hippocampus. *C.R.Acad.Sci.III* **318**, 339-344.

Fraser, H. and Dickinson, A. G. (1978). Studies of the lymphoreticular system in the pathogenesis of scrapie: the role of spleen and thymus. *J.Comp Pathol.* **88**, 563-573.

Frigg, R., Klein, M. A., Hegyi, I., Zinkernagel, R. M., and Aguzzi, A. (1999). Scrapie pathogenesis in subclinically infected B-cell-deficient mice. *J.Virol.* **73**, 9584-9588.

Gabus, C., Auxilien, S., Pechoux, C., Dormont, D., Swietnicki, W., Morillas, M., Surewicz, W., Nandi, P., and Darlix, J. L. (2001). The prion protein has DNA strand transfer properties similar to retroviral nucleocapsid protein. *J.Mol.Biol.* **307**, 1011-1021.

GAJDUSEK, D. C., Gibbs, C. J., and Alpers, M. (1966). Experimental transmission of a Kuru-like syndrome to chimpanzees. *Nature* **209**, 794-796.

GAJDUSEK, D. C. and ZIGAS, V. (1957). Degenerative disease of the central nervous system in New Guinea; the endemic occurrence of kuru in the native population. *N.Engl.J.Med.* **257**, 974-978.

Gasset, M., Baldwin, M. A., Fletterick, R. J., and Prusiner, S. B. (1993). Perturbation of the secondary structure of the scrapie prion protein under conditions that alter infectivity. *Proc.Natl.Acad.Sci.U.S.A* **90**, 1-5.

Gauczynski, S., Peyrin, J. M., Haik, S., Leucht, C., Hundt, C., Rieger, R., Krasemann, S., Deslys, J. P., Dormont, D., Lasmezas, C. I., and Weiss, S. (2001). The 37-kDa/67-kDa laminin receptor acts as the cell-surface receptor for the cellular prion protein. *EMBO J.* **20**, 5863-5875.

Gerstmann, J. (1936). Über eine eigenartige hereditary-familiäre Erkrankung des Zentralnervensystem; zugleich ein Beitrag zur Frage des vorzeitigen lokalen Alterns. *Z.Ges.Neurol.Psychiatr.* **154**, 736-762.

Ghani, A. C., Donnelly, C. A., Ferguson, N. M., and Anderson, R. M. (2002). The transmission dynamics of BSE and vCJD. *C.R.Biol.* **325**, 37-47.

Gibbs, C. J., Jr., GAJDUSEK, D. C., Asher, D. M., Alpers, M. P., Beck, E., Daniel, P. M., and Matthews, W. B. (1968). Creutzfeldt-Jakob disease (spongiform encephalopathy): transmission to the chimpanzee. *Science* **161**, 388-389.

Gilch, S., Schmitz, F., Aguib, Y., Kehler, C., Bulow, S., Bauer, S., Kremmer, E., and Schatzl, H. M. (2007). CpG and LPS can interfere negatively with prion clearance in macrophage and microglial cells. *FEBS J.* **274**, 5834-5844.

Gilch, S., Winklhofer, K. F., Groschup, M. H., Nunziante, M., Lucassen, R., Spielhaupter, C., Muranyi, W., Riesner, D., Tatzelt, J., and Schatzl, H. M. (2001). Intracellular re-routing of prion protein prevents propagation of PrP(Sc) and delays onset of prion disease. *EMBO J.* **20**, 3957-3966.

Gilch, S., Wopfner, F., Renner-Muller, I., Kremmer, E., Bauer, C., Wolf, E., Brem, G., Groschup, M. H., and Schatzl, H. M. (2003). Polyclonal anti-PrP auto-antibodies induced with dimeric PrP interfere efficiently with PrPSc propagation in prion-infected cells. *J.Biol.Chem.* **278**, 18524-18531.

Gill, A. C., Ritchie, M. A., Hunt, L. G., Steane, S. E., Davies, K. G., Bocking, S. P., Rhie, A. G., Bennett, A. D., and Hope, J. (2000). Post-translational hydroxylation at the N-terminus of the prion protein reveals presence of PPII structure in vivo. *EMBO J.* **19**, 5324-5331.

Govaerts, C., Wille, H., Prusiner, S. B., and Cohen, F. E. (2004). Evidence for assembly of prions with left-handed beta-helices into trimers. *Proc.Natl.Acad.Sci.U.S.A* **101**, 8342-8347.

Gregoire, S., Bergot, A. S., Feraudet, C., Carnaud, C., Aucouturier, P., and Rosset, M. B. (2005). The murine B cell repertoire is severely selected against endogenous cellular prion protein. *J.Immunol.* **175**, 6443-6449.

Gregoire, S., Logre, C., Metharom, P., Loing, E., Chomilier, J., Rosset, M. B., Aucouturier, P., and Carnaud, C. (2004). Identification of two immunogenic domains of the prion protein--PrP--which activate class II-restricted T cells and elicit antibody responses against the native molecule. *J.Leukoc.Biol.* **76**, 125-134.

Griffin, J. K. and Cashman, N. R. (2005). Progress in prion vaccines and immunotherapies. *Expert.Opin.Biol.Ther.* **5**, 97-110.

Griffith, J. S. (1967). Self-replication and scrapie. *Nature* **215**, 1043-1044.

Harris, D. A., Lele, P., and Snider, W. D. (1993). Localization of the mRNA for a chicken prion protein by in situ hybridization. *Proc.Natl.Acad.Sci.U.S.A* **90**, 4309-4313.

Head, M. W. and Ironside, J. W. (2000). Inhibition of prion-protein conversion: a therapeutic tool? *Trends Microbiol.* **8**, 6-8.

Heath, W. R., Belz, G. T., Behrens, G. M., Smith, C. M., Forehan, S. P., Parish, I. A., Davey, G. M., Wilson, N. S., Carbone, F. R., and Villadangos, J. A. (2004). Cross-presentation, dendritic cell subsets, and the generation of immunity to cellular antigens. *Immunol.Rev.* **199**, 9-26.

Heggebo, R., Press, C. M., Gunnes, G., Lie, K. I., Tranulis, M. A., Ulvund, M., Groschup, M. H., and Landsverk, T. (2000). Distribution of prion protein in the ileal Peyer's patch of scrapie-free lambs and lambs naturally and experimentally exposed to the scrapie agent. *J.Gen.Virol.* **81**, 2327-2337.

Heikenwalder, M., Polymenidou, M., Junt, T., Sigurdson, C., Wagner, H., Akira, S., Zinkernagel, R., and Aguzzi, A. (2004). Lymphoid follicle destruction and immunosuppression after repeated CpG oligodeoxynucleotide administration. *Nat.Med.* **10**, 187-192.

Heit, A., Maurer, T., Hochrein, H., Bauer, S., Huster, K. M., Busch, D. H., and Wagner, H. (2003). Cutting edge: Toll-like receptor 9 expression is not required for CpG DNA-aided cross-presentation of DNA-conjugated antigens but essential for cross-priming of CD8 T cells. *J.Immunol.* **170**, 2802-2805.

Heit, A., Schmitz, F., Haas, T., Busch, D. H., and Wagner, H. (2007). Antigen co-encapsulated with adjuvants efficiently drive protective T-cell immunity. *Eur.J.Immunol.*

Heppner, F. L., Christ, A. D., Klein, M. A., Prinz, M., Fried, M., Kraehenbuhl, J. P., and Aguzzi, A. (2001a). Transepithelial prion transport by M cells. *Nat.Med.* **7**, 976-977.

Heppner, F. L., Musahl, C., Arrighi, I., Klein, M. A., Rulicke, T., Oesch, B., Zinkernagel, R. M., Kalinke, U., and Aguzzi, A. (2001b). Prevention of scrapie pathogenesis by transgenic expression of anti-prion protein antibodies. *Science* **294**, 178-182.

Herms, J., Tings, T., Gall, S., Madlung, A., Giese, A., Siebert, H., Schurmann, P., Windl, O., Brose, N., and Kretzschmar, H. (1999). Evidence of presynaptic location and function of the prion protein. *J.Neurosci.* **19**, 8866-8875.

Hill, A. F., Butterworth, R. J., Joiner, S., Jackson, G., Rossor, M. N., Thomas, D. J., Frosh, A., Tolley, N., Bell, J. E., Spencer, M., King, A., Al Sarraj, S., Ironside, J. W., Lantos, P. L., and Collinge, J. (1999). Investigation of variant Creutzfeldt-Jakob disease and other human prion diseases with tonsil biopsy samples. *Lancet* **353**, 183-189.

Hill, A. F., Desbruslais, M., Joiner, S., Sidle, K. C., Gowland, I., Collinge, J., Doey, L. J., and Lantos, P. (1997). The same prion strain causes vCJD and BSE. *Nature* **389**, 448-50, 526.

Hill, A. F., Joiner, S., Wadsworth, J. D., Sidle, K. C., Bell, J. E., Budka, H., Ironside, J. W., and Collinge, J. (2003). Molecular classification of sporadic Creutzfeldt-Jakob disease. *Brain* **126**, 1333-1346.

Hilmert, H. and Diringer, H. (1984). A rapid and efficient method to enrich SAF-protein from scrapie brains of hamsters. *Biosci.Rep.* **4**, 165-170.

Hope, J., Morton, L. J., Farquhar, C. F., Multhaup, G., Beyreuther, K., and Kimberlin, R. H. (1986). The major polypeptide of scrapie-associated fibrils (SAF) has the same size, charge distribution and N-terminal protein sequence as predicted for the normal brain protein (PrP). *EMBO J.* **5**, 2591-2597.

Horn, G. Review of the origin of BSE. 2001.
Ref Type: Report

Hornemann, S., Korth, C., Oesch, B., Riek, R., Wider, G., Wuthrich, K., and Glockshuber, R. (1997). Recombinant full-length murine prion protein, mPrP(23-231): purification and spectroscopic characterization. *FEBS Lett.* **413**, 277-281.

Hornshaw, M. P., McDermott, J. R., Candy, J. M., and Lakey, J. H. (1995). Copper binding to the N-terminal tandem repeat region of mammalian and avian prion protein: structural studies using synthetic peptides. *Biochem.Biophys.Res.Commun.* **214**, 993-999.

Hosszu, L. L., Baxter, N. J., Jackson, G. S., Power, A., Clarke, A. R., Waltho, J. P., Craven, C. J., and Collinge, J. (1999). Structural mobility of the human prion protein probed by backbone hydrogen exchange. *Nat.Struct.Biol.* **6**, 740-743.

Hsiao, K., Baker, H. F., Crow, T. J., Poulter, M., Owen, F., Terwilliger, J. D., Westaway, D., Ott, J., and Prusiner, S. B. (1989). Linkage of a prion protein missense variant to Gerstmann-Straussler syndrome. *Nature* **338**, 342-345.

Huang, F. P. and MacPherson, G. G. (2004). Dendritic cells and oral transmission of prion diseases. *Adv.Drug Deliv.Rev.* **56**, 901-913.

Jackson, G. S., Hill, A. F., Joseph, C., Hosszu, L., Power, A., Waltho, J. P., Clarke, A. R., and Collinge, J. (1999a). Multiple folding pathways for heterologously expressed human prion protein. *Biochim.Biophys.Acta* **1431**, 1-13.

Jackson, G. S., Hosszu, L. L., Power, A., Hill, A. F., Kenney, J., Saibil, H., Craven, C. J., Waltho, J. P., Clarke, A. R., and Collinge, J. (1999b). Reversible conversion of monomeric human prion protein between native and fibrilogenic conformations. *Science* **283**, 1935-1937.

Jackson, G. S., Murray, I., Hosszu, L. L., Gibbs, N., Waltho, J. P., Clarke, A. R., and Collinge, J. (2001). Location and properties of metal-binding sites on the human prion protein. *Proc.Natl.Acad.Sci.U.S.A* **98**, 8531-8535.

Jakob, A. M. (1921). Über eigenartige Erkrankungen des Zentralnervensystems mit bemerkenswertem anatomischen Befunden (Spastische Pseudosklerose - Encephalomyelopathie mit disseminierten Degenerationsherden). *Dtsch.Z.Nervenheilk.* 132-146.

James, T. L., Liu, H., Ulyanov, N. B., Farr-Jones, S., Zhang, H., Donne, D. G., Kaneko, K., Groth, D., Mehlhorn, I., Prusiner, S. B., and Cohen, F. E. (1997). Solution structure of a 142-residue recombinant prion protein corresponding to the infectious fragment of the scrapie isoform. *Proc.Natl.Acad.Sci.U.S.A* **94**, 10086-10091.

Jeffrey, M., McGovern, G., Goodsir, C. M., Brown, K. L., and Bruce, M. E. (2000). Sites of prion protein accumulation in scrapie-infected mouse spleen revealed by immuno-electron microscopy. *J.Pathol.* **191**, 323-332.

Kaneko, K., Zulianello, L., Scott, M., Cooper, C. M., Wallace, A. C., James, T. L., Cohen, F. E., and Prusiner, S. B. (1997). Evidence for protein X binding to a discontinuous epitope on the cellular prion protein during scrapie prion propagation. *Proc.Natl.Acad.Sci.U.S.A* **94**, 10069-10074.

Khalili-Shirazi, A., Quaratino, S., Londei, M., Summers, L., Tayebi, M., Clarke, A. R., Hawke, S. H., Jackson, G. S., and Collinge, J. (2005). Protein conformation significantly influences immune responses to prion protein. *J.Immunol.* **174**, 3256-3263.

Kimberlin, R. H. and Walker, C. A. (1979). Pathogenesis of mouse scrapie: dynamics of agent replication in spleen, spinal cord and brain after infection by different routes. *J.Comp Pathol.* **89**, 551-562.

Kimberlin, R. H. and Walker, C. A. (1989). Pathogenesis of scrapie in mice after intragastric infection. *Virus Res.* **12**, 213-220.

KLATZO, I., GAJDUSEK, D. C., and ZIGAS, V. (1959). Pathology of Kuru. *Lab Invest* **8**, 799-847.

Klein, M. A., Frigg, R., Flechsig, E., Raeber, A. J., Kalinke, U., Bluethmann, H., Bootz, F., Suter, M., Zinkernagel, R. M., and Aguzzi, A. (1997). A crucial role for B cells in neuroinvasive scrapie. *Nature* **390**, 687-690.

Klein, M. A., Frigg, R., Raeber, A. J., Flechsig, E., Hegyi, I., Zinkernagel, R. M., Weissmann, C., and Aguzzi, A. (1998). PrP expression in B lymphocytes is not required for prion neuroinvasion. *Nat.Med.* **4**, 1429-1433.

Kocisko, D. A., Come, J. H., Priola, S. A., Chesebro, B., Raymond, G. J., Lansbury, P. T., and Caughey, B. (1994). Cell-free formation of protease-resistant prion protein. *Nature* **370**, 471-474.

Koller, M. F., Grau, T., and Christen, P. (2002). Induction of antibodies against murine full-length prion protein in wild-type mice. *J.Neuroimmunol.* **132**, 113-116.

Kosco-Vilbois, M. H., Zentgraf, H., Gerdes, J., and Bonnefoy, J. Y. (1997). To 'B' or not to 'B' a germinal center? *Immunol.Today* **18**, 225-230.

Kretzschmar, H. A., Stowring, L. E., Westaway, D., Stubblebine, W. H., Prusiner, S. B., and DeArmond, S. J. (1986). Molecular cloning of a human prion protein cDNA. *DNA* **5**, 315-324.

Kurschner, C. and Morgan, J. I. (1996). Analysis of interaction sites in homo- and heteromeric complexes containing Bcl-2 family members and the cellular prion protein. *Brain Res.Mol.Brain Res.* **37**, 249-258.

Lasmezas, C. I., Deslys, J. P., Demaimay, R., Adjou, K. T., Lamoury, F., Dormont, D., Robain, O., Ironside, J., and Hauw, J. J. (1996). BSE transmission to macaques. *Nature* **381**, 743-744.

Leffers, K. W., Wille, H., Stohr, J., Junger, E., Prusiner, S. B., and Riesner, D. (2005). Assembly of natural and recombinant prion protein into fibrils. *Biol.Chem.* **386**, 569-580.

Legname, G., Baskakov, I. V., Nguyen, H. O., Riesner, D., Cohen, F. E., DeArmond, S. J., and Prusiner, S. B. (2004). Synthetic mammalian prions. *Science* **305**, 673-676.

Lima, K. M., Santos, S. A., Lima, V. M., Coelho-Castelo, A. A., Rodrigues, J. M., Jr., and Silva, C. L. (2003). Single dose of a vaccine based on DNA encoding mycobacterial hsp65 protein plus TDM-loaded PLGA microspheres protects mice against a virulent strain of Mycobacterium tuberculosis. *Gene Ther.* **10**, 678-685.

Lima, L. M., Cordeiro, Y., Tinoco, L. W., Marques, A. F., Oliveira, C. L., Sampath, S., Kodali, R., Choi, G., Foguel, D., Torriani, I., Caughey, B., and Silva, J. L. (2006). Structural insights into the interaction between prion protein and nucleic acid. *Biochemistry* **45**, 9180-9187.

Mabbott, N. A. and MacPherson, G. G. (2006). Prions and their lethal journey to the brain. *Nat.Rev.Microbiol.* **4**, 201-211.

Manuelidis, L. (1985). Creutzfeldt-Jakob disease prion proteins in human brains. *N.Engl.J.Med.* **312**, 1643-1645.

Marsh, R. F. and Hadlow, W. J. (1992). Transmissible mink encephalopathy. *Rev.Sci.Tech.* **11**, 539-550.

Martins, S. M., Frosoni, D. J., Martinez, A. M., De Felice, F. G., and Ferreira, S. T. (2006). Formation of soluble oligomers and amyloid fibrils with physical properties of the scrapie isoform of the prion protein from the C-terminal domain of recombinant murine prion protein mPrP-(121-231). *J.Biol.Chem.* **281**, 26121-26128.

Masters, C. L., GAJDUSEK, D. C., and Gibbs, C. J., Jr. (1981). Creutzfeldt-Jakob disease virus isolations from the Gerstmann-Straussler syndrome with an analysis of the various forms of amyloid plaque deposition in the virus-induced spongiform encephalopathies. *Brain* **104**, 559-588.

Maurer, T., Heit, A., Hochrein, H., Ampenberger, F., O'Keeffe, M., Bauer, S., Lipford, G. B., Vabulas, R. M., and Wagner, H. (2002). CpG-DNA aided cross-presentation of soluble antigens by dendritic cells. *Eur.J.Immunol.* **32**, 2356-2364.

McBride, P. A. and Beekes, M. (1999). Pathological PrP is abundant in sympathetic and sensory ganglia of hamsters fed with scrapie. *Neurosci.Lett.* **265**, 135-138.

McFarlin, D. E., Raff, M. C., Simpson, E., and Nehlsen, S. H. (1971). Scrapie in immunologically deficient mice. *Nature* **233**, 336.

McGowan, J. P. (1922). Scrapie in sheep. *Scottish J.Agric.* **5**, 365-375.

McKnight, S. and Tjian, R. (1986). Transcriptional selectivity of viral genes in mammalian cells. *Cell* **46**, 795-805.

Meier, P., Genoud, N., Prinz, M., Maissen, M., Rulicke, T., Zurbriggen, A., Raeber, A. J., and Aguzzi, A. (2003). Soluble dimeric prion protein binds PrP(Sc) in vivo and antagonizes prion disease. *Cell* **113**, 49-60.

Morillas, M., Vanik, D. L., and Surewicz, W. K. (2001). On the mechanism of alpha-helix to beta-sheet transition in the recombinant prion protein. *Biochemistry* **40**, 6982-6987.

Nandi, P. K. and Leclerc, E. (1999). Polymerization of murine recombinant prion protein in nucleic acid solution. *Arch.Virol.* **144**, 1751-1763.

Nandi, P. K. and Sizaret, P. Y. (2001). Murine recombinant prion protein induces ordered aggregation of linear nucleic acids to condensed globular structures. *Arch.Virol.* **146**, 327-345.

Neutra, M. R., Frey, A., and Kraehenbuhl, J. P. (1996). Epithelial M cells: gateways for mucosal infection and immunization. *Cell* **86**, 345-348.

Nikles, D., Bach, P., Boller, K., Merten, C. A., Montrasio, F., Heppner, F. L., Aguzzi, A., Cichutek, K., Kalinke, U., and Buchholz, C. J. (2005). Circumventing tolerance to the prion protein (PrP): vaccination with PrP-displaying retrovirus particles induces humoral immune responses against the native form of cellular PrP. *J.Virol.* **79**, 4033-4042.

Nitschke, C., Flechsig, E., van den, B. J., Lindner, N., Luhrs, T., Dittmer, U., and Klein, M. A. (2007). Immunisation strategies against prion diseases: Prime-boost immunisation with a PrP DNA vaccine containing foreign helper T-cell epitopes does not prevent mouse scrapie. *Vet.Microbiol.*

O'Hagan, D. T., Singh, M., and Ulmer, J. B. (2004). Microparticles for the delivery of DNA vaccines. *Immunol.Rev.* **199**, 191-200.

Oesch, B., Westaway, D., Walchli, M., McKinley, M. P., Kent, S. B., Aebersold, R., Barry, R. A., Tempst, P., Teplow, D. B., Hood, L. E., and . (1985). A cellular gene encodes scrapie PrP 27-30 protein. *Cell* **40**, 735-746.

Oidtmann, B., Simon, D., Holtkamp, N., Hoffmann, R., and Baier, M. (2003). Identification of cDNAs from Japanese pufferfish (Fugu rubripes) and Atlantic salmon (Salmo salar) coding for homologues to tetrapod prion proteins. *FEBS Lett.* **538**, 96-100.

Orgogozo, J. M., Gilman, S., Dartigues, J. F., Laurent, B., Puel, M., Kirby, L. C., Jouanny, P., Dubois, B., Eisner, L., Flitman, S., Michel, B. F., Boada, M., Frank, A., and Hock, C. (2003). Subacute meningoencephalitis in a subset of patients with AD after Abeta42 immunization. *Neurology* **61**, 46-54.

Owen, F., Poulter, M., Lofthouse, R., Collinge, J., Crow, T. J., Risby, D., Baker, H. F., Ridley, R. M., Hsiao, K., and Prusiner, S. B. (1989). Insertion in prion protein gene in familial Creutzfeldt-Jakob disease. *Lancet* **1**, 51-52.

Palmer, M. S., Dryden, A. J., Hughes, J. T., and Collinge, J. (1991). Homozygous prion protein genotype predisposes to sporadic Creutzfeldt-Jakob disease. *Nature* **352**, 340-342.

Pan, K. M., Baldwin, M., Nguyen, J., Gasset, M., Serban, A., Groth, D., Mehlhorn, I., Huang, Z., Fletterick, R. J., Cohen, F. E., and . (1993). Conversion of alpha-helices into beta-sheets features in the formation of the scrapie prion proteins. *Proc.Natl.Acad.Sci.U.S.A* **90**, 10962-10966.

Parchi, P., Castellani, R., Capellari, S., Ghetti, B., Young, K., Chen, S. G., Farlow, M., Dickson, D. W., Sima, A. A., Trojanowski, J. Q., Petersen, R. B., and Gambetti, P. (1996). Molecular basis of phenotypic variability in sporadic Creutzfeldt-Jakob disease. *Ann.Neurol.* **39**, 767-778.

Parchi, P., Giese, A., Capellari, S., Brown, P., Schulz-Schaeffer, W., Windl, O., Zerr, I., Budka, H., Kopp, N., Piccardo, P., Poser, S., Rojiani, A., Streichemberger, N., Julien, J., Vital, C., Ghetti, B., Gambetti, P., and Kretzschmar, H. (1999). Classification of sporadic Creutzfeldt-Jakob disease based on molecular and phenotypic analysis of 300 subjects. *Ann.Neurol.* **46**, 224-233.

Pattison, I. H. and Jones, K. M. (1968). Modification of a strain of mouse-adapted scrapie by passage through rats. *Res.Vet.Sci.* **9**, 408-410.

Pauly, P. C. and Harris, D. A. (1998). Copper stimulates endocytosis of the prion protein. *J.Biol.Chem.* **273**, 33107-33110.

Peretz, D., Williamson, R. A., Kaneko, K., Vergara, J., Leclerc, E., Schmitt-Ulms, G., Mehlhorn, I. R., Legname, G., Wormald, M. R., Rudd, P. M., Dwek, R. A., Burton, D. R., and Prusiner, S. B. (2001). Antibodies inhibit prion propagation and clear cell cultures of prion infectivity. *Nature* **412**, 739-743.

Pergami, P., Jaffe, H., and Safar, J. (1996). Semipreparative chromatographic method to purify the normal cellular isoform of the prion protein in nondenatured form. *Anal.Biochem.* **236**, 63-73.

Peyre, M., Fleck, R., Hockley, D., Gander, B., and Sesardic, D. (2004). In vivo uptake of an experimental microencapsulated diphtheria vaccine following sub-cutaneous immunisation. *Vaccine* **22**, 2430-2437.

Polymenidou, M., Heppner, F. L., Pellicioli, E. C., Urich, E., Miele, G., Braun, N., Wopfner, F., Schatzl, H. M., Becher, B., and Aguzzi, A. (2004). Humoral immune response to native eukaryotic prion protein correlates with anti-prion protection. *Proc.Natl.Acad.Sci.U.S.A* **101 Suppl 2**, 14670-14676.

Proske, D., Gilch, S., Wopfner, F., Schatzl, H. M., Winnacker, E. L., and Famulok, M. (2002). Prion-protein-specific aptamer reduces PrPSc formation. *Chembiochem.* **3**, 717-725.

Prusiner, S. B. (1982). Novel proteinaceous infectious particles cause scrapie. *Science* **216**, 136-144.

Prusiner, S. B. (1991). Molecular biology of prion diseases. *Science* **252**, 1515-1522.

Prusiner, S. B. (1997). Prion diseases and the BSE crisis. *Science* **278**, 245-251.

Prusiner, S. B. (1998). Prions. *Proc.Natl.Acad.Sci.U.S.A* **95**, 13363-13383.

Prusiner, S. B. (1999). "Prion Biology and Disease." Cold Spring Harbor Laboratory Press, New York.

Prusiner, S. B., Groth, D. F., Bolton, D. C., Kent, S. B., and Hood, L. E. (1984). Purification and structural studies of a major scrapie prion protein. *Cell* **38**, 127-134.

Prusiner, S. B., McKinley, M. P., Groth, D. F., Bowman, K. A., Mock, N. I., Cochran, S. P., and Masiarz, F. R. (1981). Scrapie agent contains a hydrophobic protein. *Proc.Natl.Acad.Sci.U.S.A* **78**, 6675-6679.

Prusiner, S. B., Scott, M., Foster, D., Pan, K. M., Groth, D., Mirenda, C., Torchia, M., Yang, S. L., Serban, D., Carlson, G. A., and . (1990). Transgenetic studies implicate interactions between homologous PrP isoforms in scrapie prion replication. *Cell* **63**, 673-686.

Raeber, A. J., Klein, M. A., Frigg, R., Flechsig, E., Aguzzi, A., and Weissmann, C. (1999). PrP-dependent association of prions with splenic but not circulating lymphocytes of scrapie-infected mice. *EMBO J.* **18**, 2702-2706.

Rezaei, H., Eghiaian, F., Perez, J., Doublet, B., Choiset, Y., Haertle, T., and Grosclaude, J. (2005). Sequential generation of two structurally distinct ovine prion protein soluble oligomers displaying different biochemical reactivities. *J.Mol.Biol.* **347**, 665-679.

Rieger, R., Edenhofer, F., Lasmezas, C. I., and Weiss, S. (1997). The human 37-kDa laminin receptor precursor interacts with the prion protein in eukaryotic cells. *Nat.Med.* **3**, 1383-1388.

Riek, R., Hornemann, S., Wider, G., Billeter, M., Glockshuber, R., and Wuthrich, K. (1996). NMR structure of the mouse prion protein domain PrP(121-321). *Nature* **382**, 180-182.

Riek, R., Hornemann, S., Wider, G., Glockshuber, R., and Wuthrich, K. (1997). NMR characterization of the full-length recombinant murine prion protein, mPrP(23-231). *FEBS Lett.* **413**, 282-288.

Robakis, N. K., Devine-Gage, E. A., Jenkins, E. C., Kascsak, R. J., Brown, W. T., Krawczun, M. S., and Silverman, W. P. (1986). Localization of a human gene homologous to the PrP gene on the p arm of

chromosome 20 and detection of PrP-related antigens in normal human brain. *Biochem.Biophys.Res.Commun.* **140**, 758-765.

Rosset, M. B., Ballerini, C., Gregoire, S., Metharom, P., Carnaud, C., and Aucouturier, P. (2004). Breaking immune tolerance to the prion protein using prion protein peptides plus oligodeoxynucleotide-CpG in mice. *J.Immunol.* **172**, 5168-5174.

Schatzl, H. M., Da Costa, M., Taylor, L., Cohen, F. E., and Prusiner, S. B. (1995). Prion protein gene variation among primates. *J.Mol.Biol.* **245**, 362-374.

Schwarz, A., Kratke, O., Burwinkel, M., Riemer, C., Schultz, J., Henklein, P., Bamme, T., and Baier, M. (2003). Immunisation with a synthetic prion protein-derived peptide prolongs survival times of mice orally exposed to the scrapie agent. *Neurosci.Lett.* **350**, 187-189.

Scott, M., Foster, D., Mirenda, C., Serban, D., Coufal, F., Walchli, M., Torchia, M., Groth, D., Carlson, G., DeArmond, S. J., and . (1989). Transgenic mice expressing hamster prion protein produce species-specific scrapie infectivity and amyloid plaques. *Cell* **59**, 847-857.

Shirota, H., Sano, K., Hirasawa, N., Terui, T., Ohuchi, K., Hattori, T., Shirato, K., and Tamura, G. (2001). Novel roles of CpG oligodeoxynucleotides as a leader for the sampling and presentation of CpG-tagged antigen by dendritic cells. *J.Immunol.* **167**, 66-74.

Sigurdson, B. (1954). Rida, a chronic encephalitis of sheep with general remarks of infections which develop slowly and some of their special characteristics. *Br.Vet.J.* 341-354.

Sigurdson, C. J., Williams, E. S., Miller, M. W., Spraker, T. R., O'Rourke, K. I., and Hoover, E. A. (1999). Oral transmission and early lymphoid tropism of chronic wasting disease PrPres in mule deer fawns (Odocoileus hemionus). *J.Gen.Virol.* **80 (Pt 10)**, 2757-2764.

Sigurdsson, E. M., Brown, D. R., Daniels, M., Kascsak, R. J., Kascsak, R., Carp, R., Meeker, H. C., Frangione, B., and Wisniewski, T. (2002). Immunization delays the onset of prion disease in mice. *Am.J.Pathol.* **161**, 13-17.

Simoneau, S., Rezaei, H., Sales, N., Kaiser-Schulz, G., Lefebvre-Roque, M., Vidal, C., Fournier, J. G., Comte, J., Wopfner, F., Grosclaude, J., Schatzl, H., and Lasmezas, C. I. (2007). In vitro and in vivo neurotoxicity of prion protein oligomers. *PLoS.Pathog.* **3**, e125.

Singh, M., Kazzaz, J., Ugozzoli, M., Chesko, J., and O'Hagan, D. T. (2004). Charged polylactide co-glycolide microparticles as antigen delivery systems. *Expert.Opin.Biol.Ther.* **4**, 483-491.

Souan, L., Tal, Y., Felling, Y., Cohen, I. R., Taraboulos, A., and Mor, F. (2001). Modulation of proteinase-K resistant prion protein by prion peptide immunization. *Eur.J.Immunol.* **31**, 2338-2346.

Sparkes, R. S., Simon, M., Cohn, V. H., Fournier, R. E., Lem, J., Klisak, I., Heinzmann, C., Blatt, C., Lucero, M., Mohandas, T., and . (1986). Assignment of the human and mouse prion protein genes to homologous chromosomes. *Proc.Natl.Acad.Sci.U.S.A* **83**, 7358-7362.

Spielhaupter, C. and Schatzl, H. M. (2001). PrPC directly interacts with proteins involved in signaling pathways. *J.Biol.Chem.* **276**, 44604-44612.

Stahl, N., Baldwin, M. A., Teplow, D. B., Hood, L., Gibson, B. W., Burlingame, A. L., and Prusiner, S. B. (1993). Structural studies of the scrapie prion protein using mass spectrometry and amino acid sequencing. *Biochemistry* **32**, 1991-2002.

Stahl, N., Borchelt, D. R., Hsiao, K., and Prusiner, S. B. (1987). Scrapie prion protein contains a phosphatidylinositol glycolipid. *Cell* **51**, 229-240.

Stoltze, L., Rezaei, H., Jung, G., Grosclaude, J., Debey, P., Schild, H., and Rammensee, H. G. (2003). CD4+ T cell-mediated immunity against prion proteins. *Cell Mol.Life Sci.* **60**, 629-638.

Strumbo, B., Ronchi, S., Bolis, L. C., and Simonic, T. (2001). Molecular cloning of the cDNA coding for Xenopus laevis prion protein. *FEBS Lett.* **508**, 170-174.

Supattapone, S., Nguyen, H. O., Cohen, F. E., Prusiner, S. B., and Scott, M. R. (1999). Elimination of prions by branched polyamines and implications for therapeutics. *Proc.Natl.Acad.Sci.U.S.A* **96**, 14529-14534.

Taraboulos, A., Raeber, A. J., Borchelt, D. R., Serban, D., and Prusiner, S. B. (1992). Synthesis and trafficking of prion proteins in cultured cells. *Mol.Biol.Cell* **3**, 851-863.

Taraboulos, A., Scott, M., Semenov, A., Avrahami, D., Laszlo, L., and Prusiner, S. B. (1995). Cholesterol depletion and modification of COOH-terminal targeting sequence of the prion protein inhibit formation of the scrapie isoform. *J.Cell Biol.* **129**, 121-132.

Taraboulos, A., Serban, D., and Prusiner, S. B. (1990). Scrapie prion proteins accumulate in the cytoplasm of persistently infected cultured cells. *J.Cell Biol.* **110**, 2117-2132.

Tateishi, J., Brown, P., Kitamoto, T., Hoque, Z. M., Roos, R., Wollman, R., Cervenakova, L., and GAJDUSEK, D. C. (1995). First experimental transmission of fatal familial insomnia. *Nature* **376**, 434-435.

Tatzelt, J., Prusiner, S. B., and Welch, W. J. (1996). Chemical chaperones interfere with the formation of scrapie prion protein. *EMBO J.* **15**, 6363-6373.

Telling, G. C., Parchi, P., DeArmond, S. J., Cortelli, P., Montagna, P., Gabizon, R., Mastrianni, J., Lugaresi, E., Gambetti, P., and Prusiner, S. B. (1996). Evidence for the conformation of the pathologic isoform of the prion protein enciphering and propagating prion diversity. *Science* **274**, 2079-2082.

Telling, G. C., Scott, M., Hsiao, K. K., Foster, D., Yang, S. L., Torchia, M., Sidle, K. C., Collinge, J., DeArmond, S. J., and Prusiner, S. B. (1994). Transmission of Creutzfeldt-Jakob disease from humans to transgenic mice expressing chimeric human-mouse prion protein. *Proc.Natl.Acad.Sci.U.S.A* **91**, 9936-9940.

Telling, G. C., Scott, M., Mastrianni, J., Gabizon, R., Torchia, M., Cohen, F. E., DeArmond, S. J., and Prusiner, S. B. (1995). Prion propagation in mice expressing human and chimeric PrP transgenes implicates the interaction of cellular PrP with another protein. *Cell* **83**, 79-90.

Tilly, G., Chapuis, J., Vilette, D., Laude, H., and Vilotte, J. L. (2003). Efficient and specific down-regulation of prion protein expression by RNAi. *Biochem.Biophys.Res.Commun.* **305**, 548-551.

Tobler, I., Gaus, S. E., Deboer, T., Achermann, P., Fischer, M., Rulicke, T., Moser, M., Oesch, B., McBride, P. A., and Manson, J. C. (1996). Altered circadian activity rhythms and sleep in mice devoid of prion protein. *Nature* **380**, 639-642.

van Keulen, L. J., Schreuder, B. E., Vromans, M. E., Langeveld, J. P., and Smits, M. A. (1999). Scrapie-associated prion protein in the gastrointestinal tract of sheep with natural scrapie. *J.Comp Pathol.* **121**, 55-63.

Vendrely, C., Valadie, H., Bednarova, L., Cardin, L., Pasdeloup, M., Cappadoro, J., Bednar, J., Rinaudo, M., and Jamin, M. (2005). Assembly of the full-length recombinant mouse prion protein I. Formation of soluble oligomers. *Biochim.Biophys.Acta* **1724**, 355-366.

Vey, M., Pilkuhn, S., Wille, H., Nixon, R., DeArmond, S. J., Smart, E. J., Anderson, R. G., Taraboulos, A., and Prusiner, S. B. (1996). Subcellular colocalization of the cellular and scrapie prion proteins in caveolae-like membranous domains. *Proc.Natl.Acad.Sci.U.S.A* **93**, 14945-14949.

Viles, J. H., Cohen, F. E., Prusiner, S. B., Goodin, D. B., Wright, P. E., and Dyson, H. J. (1999). Copper binding to the prion protein: structural implications of four identical cooperative binding sites. *Proc.Natl.Acad.Sci.U.S.A* **96**, 2042-2047.

Villadangos, J. A. and Ploegh, H. L. (2000). Proteolysis in MHC class II antigen presentation: who's in charge? *Immunity.* **12**, 233-239.

Wadsworth, J. D., Hill, A. F., Joiner, S., Jackson, G. S., Clarke, A. R., and Collinge, J. (1999). Strain-specific prion-protein conformation determined by metal ions. *Nat.Cell Biol.* **1**, 55-59.

Wagner, H. (2002). Interactions between bacterial CpG-DNA and TLR9 bridge innate and adaptive immunity. *Curr.Opin.Microbiol.* **5**, 62-69.

Weiss, S., Proske, D., Neumann, M., Groschup, M. H., Kretzschmar, H. A., Famulok, M., and Winnacker, E. L. (1997). RNA aptamers specifically interact with the prion protein PrP. *J.Virol.* **71**, 8790-8797.

Wells, G. A., Scott, A. C., Johnson, C. T., Gunning, R. F., Hancock, R. D., Jeffrey, M., Dawson, M., and Bradley, R. (1987). A novel progressive spongiform encephalopathy in cattle. *Vet.Rec.* **121**, 419-420.

White, A. R., Enever, P., Tayebi, M., Mushens, R., Linehan, J., Brandner, S., Anstee, D., Collinge, J., and Hawke, S. (2003). Monoclonal antibodies inhibit prion replication and delay the development of prion disease. *Nature* **422**, 80-83.

Whittal, R. M., Ball, H. L., Cohen, F. E., Burlingame, A. L., Prusiner, S. B., and Baldwin, M. A. (2000). Copper binding to octarepeat peptides of the prion protein monitored by mass spectrometry. *Protein Sci.* **9**, 332-343.

Wilesmith, J. W., Ryan, J. B., and Atkinson, M. J. (1991). Bovine spongiform encephalopathy: epidemiological studies on the origin. *Vet.Rec.* **128**, 199-203.

Wilesmith, J. W., Wells, G. A., Cranwell, M. P., and Ryan, J. B. (1988). Bovine spongiform encephalopathy: epidemiological studies. *Vet.Rec.* **123**, 638-644.

Will, R. G. (1998). New variant Creutzfeldt-Jakob disease. *Dev.Biol.Stand.* **93**, 79-84.

Will, R. G., Ironside, J. W., Zeidler, M., Cousens, S. N., Estibeiro, K., Alperovitch, A., Poser, S., Pocchiari, M., Hofman, A., and Smith, P. G. (1996). A new variant of Creutzfeldt-Jakob disease in the UK. *Lancet* **347**, 921-925.

Wille, H., Govaerts, C., Borovinskiy, A., Latawiec, D., Downing, K. H., Cohen, F. E., and Prusiner, S. B. (2007). Electron crystallography of the scrapie prion protein complexed with heavy metals. *Arch.Biochem.Biophys.* **467**, 239-248.

Wille, H., Michelitsch, M. D., Guenebaut, V., Supattapone, S., Serban, A., Cohen, F. E., Agard, D. A., and Prusiner, S. B. (2002). Structural studies of the scrapie prion protein by electron crystallography. *Proc.Natl.Acad.Sci.U.S.A* **99**, 3563-3568.

Williams, E. S. (2005). Chronic wasting disease. *Vet.Pathol.* **42**, 530-549.

Williams, E. S. and Young, S. (1980). Chronic wasting disease of captive mule deer: a spongiform encephalopathy. *J.Wildl.Dis.* **16**, 89-98.

Windl, O., Dempster, M., Estibeiro, P., and Lathe, R. (1995). A candidate marsupial PrP gene reveals two domains conserved in mammalian PrP proteins. *Gene* **159**, 181-186.

Wopfner, F., Weidenhofer, G., Schneider, R., von Brunn, A., Gilch, S., Schwarz, T. F., Werner, T., and Schatzl, H. M. (1999). Analysis of 27 mammalian and 9 avian PrPs reveals high conservation of flexible regions of the prion protein. *J.Mol.Biol.* **289**, 1163-1178.

Yun, S. W., Ertmer, A., Flechsig, E., Gilch, S., Riederer, P., Gerlach, M., Schatzl, H. M., and Klein, M. A. (2007). The tyrosine kinase inhibitor imatinib mesylate delays prion neuroinvasion by inhibiting prion propagation in the periphery. *J.Neurovirol.* **13**, 328-337.

ZIGAS, V. (1981). Letter to Gunther. In: Farquhar,J., from the collection of D. Calton Gajdusek. *Raven Press, New York.*

ZIGAS, V. and GAJDUSEK, D. C. (1957). Kuru: clinical study of a new syndrome resembling paralysis agitans in natives of the Eastern Highlands of Australian New Guinea. *Med.J.Aust.* **44**, 745-754.

6 Abbreviations

APS	ammonium-persulfate
B-cell	B lymphocyte
BSA	bovine serum albumin
BSE	bovine spongiform encephalopathy
CD	circular dichroism
CJD	Creutzfeldt-Jakob disease
CNS	central nervous system
CpG-ODN	CpG-Oligodeoxynucleotide
CWD	chronic wasting disease
DNA	deoxyribonucleic acid
DOC	Sodiumdeoxycholate
EDTA	ethylene-diamine-tetra-acetate
ER	endoplasmatic reticulum
FACS	Fluorescence activated cell sorter
FCS	fetal calf serum
FITC	Fluorescein Isothyocianate
FTIR	Fourier-transform infrared spectroscopy
GPI	glycosyl-phosphatidyl-inositol
i.p.	intraperitoneal
kDa	kilo Dalton
LB	Luri-Bertani Medium
OD	optical density
PLGA-MS	polylactide-co-glycolide microspheres
PrP	prion protein
PrP^{C}	cellular prion protein
PrP^{Sc}	pathogenic scrapie form of PrP
RT	room temperature
s.c.	subcutaneous
SDS	sodium dodecyl sulfate
T-cell	T lymphocyte
TEMED	N,N,N,N-tetramethylethylenediamine
TGN	trans golgi network
TSE	transmissible spongiform encephalopathy
wt mice	PrP wild type mice

7 Acknowledgements

I would like to express my gratitude to Prof. Dr. Hermann Schätzl for his encouragement, patience and supervision of my work.

I am grateful to Prof. Dr. Johann Bauer for his supervision of my doctoral thesis.

I thank Franziska Hammerschmidt for initiating the topic of this work.

I am very thankful to Dr. Antje Heit, Prof. Hermann Wagner, Dr. Frank Schmitz and Monika Hammel for their help with animal experiments and very fruitful discussions.

I thank all my co-operation partners Fabienne Leidel, Prof. Dr. Martin Groschup, Dr. Human Rezaei, Dr. Simone Hess, PD Dr. Leticia Quintanilla-Fend, Mrs. Moßbrugger, Mrs. Jennen and Dr. Elisabeth Kremmer for their great help.

I am also thankful to my colleagues at the Institute of Virology. It was a pleasure working with you.

Above all I thank my friends and familie for their continuous support and great patience.

8 Curriculum vitae

Persönliche Daten:

Name:	Kaiser-Schulz, geb. Schulz
Vorname:	Gunnar
Geburtstag:	5. Juni 1973
Geburtsort	Hamburg
Staatsangehörigkeit:	deutsch
Familienstand:	verheiratet, eine Tochter

Schulbildung

1979-1993	Schulen in Hamburg, Abschluss: Allgemeine Hochschulreife

Zivildienst

1993-1994	Zivildienst beim Diakonisches Werk, Hamburg

Studium

10.1995-02.2002	Studium der technischen Biologie an der Universität Stuttgart Abschluss: Diplom Biologie (technisch orientiert)
04.2001-02.2002	Diplomarbeit bei Prof. Rolf D. Schmid am Institut für technische Biochemie, Abteilung Analytische Biochemie, Universität Stuttgart
03.1999-10.1999	Studienarbeit bei Prof. Dieter F. Hülser am Biologischen Institut, Abteilung Biophysik, Universität Stuttgart
09.2002-05.2007	Promotion bei Prof. Schätzl am Institut für Virologie der Technischen Universität München, Betreuung durch Prof. Bauer am Lehrstuhl für Tierhygiene, WZW der Technischen Universität München

Erwerbstätigkeit

seit Juli 2007	GENEART AG in Regensburg

9 Publications

Gunnar Kaiser-Schulz, Antje Heit, Franziska Hammerschmidt, Letitia Quintanilla-Martinez, Simone Hess, Luise Jennen, Hermann Wagner, Hermann Schätzl *"PLGA microsphere co-encapsulated recombinant tandem PrP with CpG-ODN breaks self-tolerance to PrP in wt mice and induces CD4 and CD8 T cell responses"* J Immunol. 2007 Sep 1;179(5):2797-807

Steve Simoneau, Human Rezaei, Gunnar Kaiser-Schulz, Maxime Lefebvre-Roque, Jean-Guy Fournier, Julien Comet, Nicole Salès, Franziska Wopfner, Myriam Burel, Jeanne Grosclaude, Hermann Schätzl & Corinne Ida Lasmézas *"Identification of the neurotoxic form of the prion protein"*. PLoS Pathog. 2007 Aug 31;3(8):e125

Gunnar Kaiser-Schulz, Antje Heit, Franziska Hammerschmidt, Sabine Gilch, Hermann Wagner und Hermann Schätzl, *"Vakzinierungsstrategien gegen Prionenerkrankungen"*. Nova Acta Leopoldina NF 94, Nr.347, 265 (2006)

Czyz J, Irmer U, Schulz G, Mindermann A, Hülser DF: *"Gap-junctional coupling-measured by flow cytometry"*. Exp.Cell Res.2000, 255:40-4